

A scanning electron microscope study of rat sciatic nerve fiber regeneration  
through silicone rubber multiple-lumen nerve cuffs

by

Chih-Hui Chung

ISU  
1994  
C472  
c. 3

A Thesis Submitted to the  
Graduate Faculty in Partial Fulfillment of the  
Requirements for the Degree of  
MASTER OF SCIENCE

Interdepartmental Program: Biomedical Engineering  
Major: Biomedical Engineering

Signatures have been redacted for privacy

Iowa State University  
Ames, Iowa

**TABLE OF CONTENTS**

<b>1.</b>	<b>INTRODUCTION</b>	1
<b>2.</b>	<b>LITERATURE REVIEW</b>	4
<b>2.1.</b>	<b>Background</b>	4
2.1.1.	Organization of a peripheral nerve	4
2.1.2.	Nerve degeneration	6
2.1.3.	Nerve regeneration	8
<b>2.2.</b>	<b>Review of previous work in repair techniques</b>	10
2.2.1.	Present nerve repair techniques	10
2.2.2.	Summary of past research	11
<b>2.3.</b>	<b>Multiple-lumen nerve cuff</b>	16
2.3.1.	Organization of a multiple-lumen cuff	16
2.3.2.	Silicone rubber in a nerve cuff	16
<b>2.4.</b>	<b>Silver stain</b>	17
2.4.1.	The principle of silver stain	17
2.4.2.	The chemistry of a silver stain	18
<b>2.5.</b>	<b>Backscattered electron imaging for the silver stained axons</b>	19
<b>3.</b>	<b>MATERIALS AND METHODS</b>	21
<b>3.1.</b>	<b>Sample preparation</b>	21
<b>3.2.</b>	<b>Scanning electron microscope examination</b>	23
<b>3.3.</b>	<b>Quantitative evaluations</b>	23
<b>3.4.</b>	<b>Diameter frequency distribution</b>	25
<b>3.5.</b>	<b>Statistical methods</b>	26

<b>4. RESULTS</b>	28
<b>4.1. Microstructure</b>	28
4.1.1. Scanning electron microscope studies	28
4.1.2. Light microscope studies	40
<b>4.2. Fiber diameter frequency distribution</b>	40
4.2.1. 8 weeks post-implantation (animal #34)	41
4.2.2. 12 weeks post-implantation (animal #24)	41
4.2.3. 16 weeks post-implantation (animal #14)	42
4.2.4. 24 weeks post-implantation (animals #1, #2 and #3)	42
<b>4.3. Quantitative results</b>	43
<b>5. DISCUSSION</b>	79
<b>6. CONCLUSION</b>	82
<b>BIBLIOGRAPHY</b>	83
<b>ACKNOWLEDGMENTS</b>	90
<b>APPENDIX: FIBER DIAMETER HISTOGRAMS</b>	91

**LIST OF FIGURES**

Figure 2.1: Schematic representation of the structure of a typical mammalian peripheral nerve	5
Figure 2.2: Diagrams of the degeneration and regeneration of a single myelinated peripheral nerve fiber	7
Figure 4.1: Backscattered electron image of a cross section of the normal control right sciatic nerve (mid-thigh level)	30
Figure 4.2: Backscattered electron image of a cross section of a regenerated nerve from proximal, middle and distal sections of animal #3	32
Figure 4.3: Backscattered electron image of one nerve strand of the middle section of animal #2 and of one nerve strand of the middle section of animal #14	36
Figure 4.4: Backscattered electron image of one fascicle-like unit of the distal section of animal #2 and of the distal section of animal #14	38

**LIST OF TABLES**

Table 3.1: Sample list	22
Table 4.1: Area examined, total area, percentage of area examined to total area, axon counts for area examined, axon counts per unit area, mean axon diameter, and extrapolated counts based on total area in the proximal section observed by LM	47
Table 4.2: Area examined, total area, percentage of area examined to total area, axon counts for area examined, axon counts per unit area, mean axon diameter, and extrapolated counts based on total area in the middle section observed by LM	48
Table 4.3: Area examined, total area, percentage of area examined to total area, axon counts for area examined, axon counts per unit area, mean axon diameter, and extrapolated counts based on total area in the distal section observed by LM	50
Table 4.4: Area examined, total area, percentage of area examined to total area, axon counts for area examined, axon counts per unit area, mean axon diameter, and extrapolated counts based on total area in the proximal section observed by SEM	52
Table 4.5: Area examined, total area, percentage of area examined to total area, axon counts for area examined, axon counts per unit area, mean axon diameter, and extrapolated counts based on total area in the middle section observed by SEM	53
Table 4.6: Area examined, total area, percentage of area examined to total area, axon counts for area examined, axon counts per unit area, mean axon diameter, and extrapolated counts based on total area in the distal section observed by SEM	54
Table 4.7: Area examined, total area, percentage of area examined to total area, category I axon counts for area examined, category I axon counts per unit area, mean category I axon diameter, and extrapolated category I axon counts based on total area in the proximal section observed by SEM	55

Table 4.8: Area examined, total area, percentage of area examined to total area, category I axon counts for area examined, category I axon counts per unit area, mean category I axon diameter, and extrapolated category I axon counts based on total area in the middle section observed by SEM	56
Table 4.9: Area examined, total area, percentage of area examined to total area, category I axon counts for area examined, category I axon counts per unit area, mean category I axon diameter, and extrapolated category I axon counts based on total area in the distal section observed by SEM	57
Table 4.10: Area examined, total area, percentage of area examined to total area, category II axon counts for area examined, category II axon counts per unit area, mean category II axon diameter, and extrapolated category II axon counts based on total area in the proximal section observed by SEM	58
Table 4.11: Area examined, total area, percentage of area examined to total area, category II axon counts for area examined, category II axon counts per unit area, mean category II axon diameter, and extrapolated category II axon counts based on total area in the middle section observed by SEM	59
Table 4.12: Area examined, total area, percentage of area examined to total area, category II axon counts for area examined, category II axon counts per unit area, mean category II axon diameter, and extrapolated category II axon counts based on total area in the distal section observed by SEM	60
Table 4.13: Percentage of axons within $\pm 1 \mu\text{m}$ of the mean axon diameter (LM)	61
Table 4.14: Percentage of axons within $\pm 1 \mu\text{m}$ of the mean diameter for category I axons (SEM)	62
Table 4.15: Percentage of axons within $\pm 1 \mu\text{m}$ of the mean diameter for category II axons (SEM)	63
Table 4.16: Percentage of axons within $\pm 1 \mu\text{m}$ of the mean diameter for all the axons (Category I plus Category II; SEM)	64
Table 4.17: Diameter ratios and predicted differences of measurements for total axons (LM)	65

Table 4.18: Diameter ratios and predicted differences of measurements for category I axons (SEM)	66
Table 4.19: Diameter ratios and predicted differences of measurements for category II axons (SEM)	67
Table 4.20: Diameter ratios and predicted differences of measurements for total axons (SEM)	68
Table 4.21: Mean axon diameter comparisons between LM and SEM studies in the same nerve section	69
Table 4.22: Mean axon diameter comparisons between repaired nerve sections and normal control (LM)	70
Table 4.23: Mean axon diameter comparisons between nerve sections in the same animal (LM)	71
Table 4.24: Mean axon diameter comparisons between repaired nerve sections and normal control (SEM)	72
Table 4.25: Mean diameter comparisons of the same category axons between repaired nerve sections and normal control (SEM)	73
Table 4.26: Diameter comparisons between category I and category II stained axons in the same nerve section (SEM)	75
Table 4.27: Mean diameter comparisons of the same category of axons in different nerve sections (SEM)	76
Table 4.28: Mean diameter comparisons of total stained axons between nerve sections in the same animal (SEM)	78

## 1. INTRODUCTION

The choice of a peripheral nerve repair method depends on the type of nerve injury, severity of damage, and clinical considerations. End-to-end anastomosis, epineurial or perineurial (fascicular) suture repair is used to direct coaptation of the nerve stumps exhibiting small tissue loss or defects of the order of 1 cm or less. However, nerve grafting is usually considered if the gap is appreciable ( $\geq 1.5$  cm). The problem is that even though these repair techniques have been improved, they still do not provide completely satisfactory results.

Undesirable scar tissue or trauma caused by fascicular or epineurial surgical manipulations or by postoperative stretching which results in tension along the suture line frequently interferes with the growth from the proximal stump to the distal stump in end-to-end anastomosis repair. To date, biological materials have served as autografts, allografts, or heterografts to span such gaps between proximal and distal stumps of a severed nerve, but the primary requirements and the possibility of immunological unacceptance associated with a donor graft are difficult to predict. Therefore, the development of artificial biocompatible conduits to aid in reuniting the proximal and distal stumps of a severed nerve has been suggested as an alternative.

Until now, nerve conduits have been investigated with only single lumen cuff systems rather than multiple-lumen cuff systems, and tested with nondegradable polymers such as silicone rubber, Teflon<sup>®</sup>, cellulose acetate, Goretex<sup>®</sup>, and polyethylene terephthalate and erodible biomaterials such as polyglactin mesh, polyglycolic acid, polyester, and glycolide trimethylene carbonate. A wide variety of single lumen systems has been modified and improved by eliminating the roughness of the internal cuff surface, adjusting the permeability of the cuff materials (with a 50,000 dalton cutoff), or by changing the regeneration environment through the use of additives or stimulatives for cell growth (for example, saline



solution, laminin gel, collagen gel, or cultured Schwann cells). In addition, some single lumen nerve cuff studies showed that regenerating nerve cables become tapered toward the center of the gap region into which the material grows or exhibit branching during growth across a gap toward the distal stump of a severed nerve.

The first multiple-lumen nerve cuff system made of silicone rubber was developed by Daniel (1991). It was made of silicone rubber and was designed to bridge a 0.5 cm gap. Its purpose was to improve the alignment of regenerated nerve material across the gap and into the distal stump, to provide mechanical support, to eliminate or minimize scar tissue at the proximal stump, and to improve nerve axon organization as it regenerates across the gap to the distal stump. Light microscopy, electrophysiological evaluations and videotape observations were conducted to determine advantages in using such a cuff configuration. Like other silicone rubber nerve cuffs, the multiple-lumen nerve cuff system also provides an isolated regeneration environment to inhibit proliferation of fibroblasts and scar tissue that otherwise might come in from surrounding tissues. Also, it provides a way to maintain growth factors inside the cuff that can be released from the distal stumps.

As an extension of Daniel's study, the current work includes microstructural studies at a relatively higher level of magnification. This technique employs an electron backscattering signal from an electron beam interaction with the sample when using a scanning electron microscope system. The neurofilament proteins of axons have a high specific affinity for silver and can be stained using Bodian's method. Because the increase in backscattered electron signal production directly correlates with an increasing atomic number, high atomic number (high contrast) silver stained axons can be easily seen within a relatively low atomic number tissue matrix.

Following scanning electron microscope (SEM) observations, the characteristics of the regenerated axons, such as patterns, shapes, sizes, organization, and orientation, are determined for different implantation periods (8, 12, 16 and 24 weeks). Also, they are

compared with those measurements obtained for healthy control nerve fibers (as seen for samples obtained at the end of identical periods as those used for the experimental implants). The locations of penetration of the axons from the proximal stump which cross the gap and enter the distal stump are also characterized. Finally, fiber diameter frequency distributions are provided to show the regenerated axon diameter distributions in relation to the sampling location (proximal, middle, or distal). The middle samples represent all new regenerated material.

## 2. LITERATURE REVIEW

### 2.1. Background

#### 2.1.1. Organization of a peripheral nerve

The primary functional and structural unit of the nervous system is the neuron. The peripheral neuron is a specialized cell that serves two major functions: sensation and conduction. In the peripheral nervous system, a typical neuron is comprised of a cell body (soma or perikayon), an axon and a variable number of dendrites.

In the peripheral nervous system, nerve cells are classified as being either myelinated or unmyelinated based on the structural relationship between an axon and its satellite Schwann cells which are capable of forming myelin sheaths. In unmyelinated nerves, usually more than one nerve fiber may be enfolded by a Schwann cell and one layer of its plasma membrane. On the other hand, in myelinated nerves, a Schwann cell encompasses a single fiber by means of its lamellar wrapping sheath, or myelin (Figure 2.1). Along the length of myelinated axons, nodes of Ranvier appear as exposed junctions, where there is no myelin between consecutive Schwann cells.

Nerve fibers exhibit a range of possible diameters. There is a close proportional correlation between the thickness of a nerve fiber and the speed of electrical conduction. The absolute values vary according to the species and the site studied. The nerve fibers in human are arranged in three groups (Daniel and Terzis, 1977):

A -- diameter 2.5  $\mu\text{m}$  - 16  $\mu\text{m}$ , conduction velocities 15 m - 100 m per second;

B -- diameter about 3  $\mu\text{m}$ , conduction velocities 3 m - 15 m per second;

C -- diameter 0.2  $\mu\text{m}$  - 1.5  $\mu\text{m}$ , conduction velocities 0.3 m - 1.6 m per second.

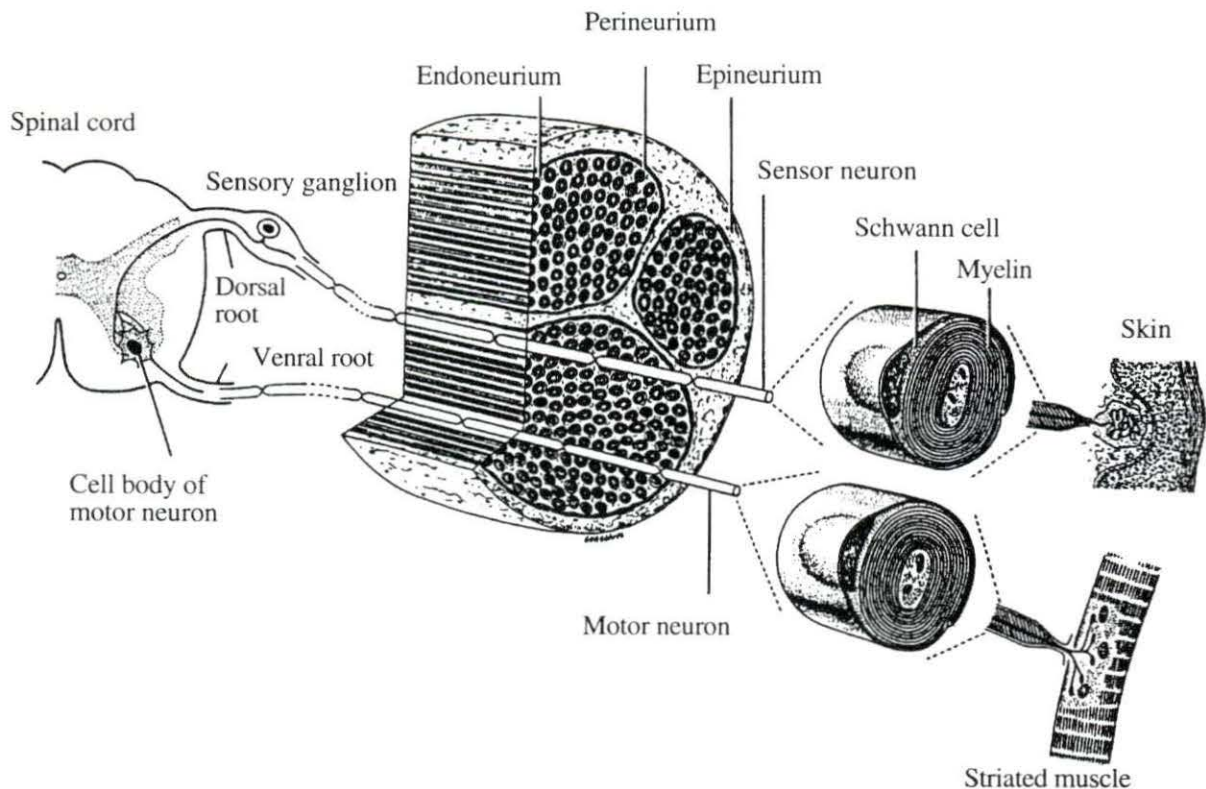


Figure 2.1. Schematic representation of the structure of a typical mammalian peripheral nerve (Junqueira et al., 1983; Fig. 9-28)

A slender connective tissue sheath, the endoneurium, encompasses each peripheral nerve fiber and associated Schwann cell (Figure. 2.1). The components of the endoneurium include fibroblasts, an occasional macrophage, and collagenous and reticular fibers. Nerve fibers collect into fascicles, enclosed entirely by a perineurium which is composed of compact cellular layers arranged concentrically. The inner layers are flattened epithelioid cells and the outer layers are connective tissue layers. The outer perimeter, the epineurium, possesses a thick areolar connective tissue sheath and is comprised of collagen fibers. The epineurium surrounds the entire nerve and blends with the connective tissue of the nearby parts (Gartner and Hiatt, 1987). The source of blood supply of a peripheral nerve is from regional arteries which enter

the epineurium, where the arteries can branch. After branching, the passage of the precapillary vessels through the perineurium becomes difficult to follow. The smaller endoneurial vascular plexus itself forms the endoneurial circulation in terms of a capillary network (Low, 1976).

### **2.1.2. Nerve degeneration**

When a peripheral nerve has been damaged or severed, degenerative processes spread into both nerve stumps along the axon from the zone of trauma. Then, these stumps retract from one another and start to swell. After persisting for about one week, this swelling slowly subsides. Because the proximal segment of an injured nerve still maintains continuity with the trophic center of the neuron, the proximal changes (called traumatic degeneration or ascending degeneration) extend no further than the second or third node of Ranvier from the point of severance (Figure 2.2B).

In contrast to proximal changes over a short distance, Wallerian degeneration occurs through the entire distal segment that is completely separated from the nerve cell body. This takes place with the involvement of Schwann cells and the loss of myelin and axons (Figure 2.2B). The severed axons located at the proximal end of the distal stump tend to detach and become isolated from the rest of the distal stump. Then the remaining portions of the distal axons break down more rapidly and become beaded. Accompanied by axonal retrogression, the myelin sheath retracts from the axon at the nodes of Ranvier, creating increased nodal gaps, and there is a loss of the laminated or layered organization. The sheath area becomes homogeneous. Later, it further breaks apart into ovoids and ellipsoids surrounding the axonal fragments. Neurofilaments and neurotubules, collectively termed as neurofibrils (in the axoplasm), disintegrate and disappear.

Fragments of the axon and the myelin sheath are absorbed by local phagocytes derived from vascular pericytes. However, the basal lamina of the Schwann cell still remains intact as a

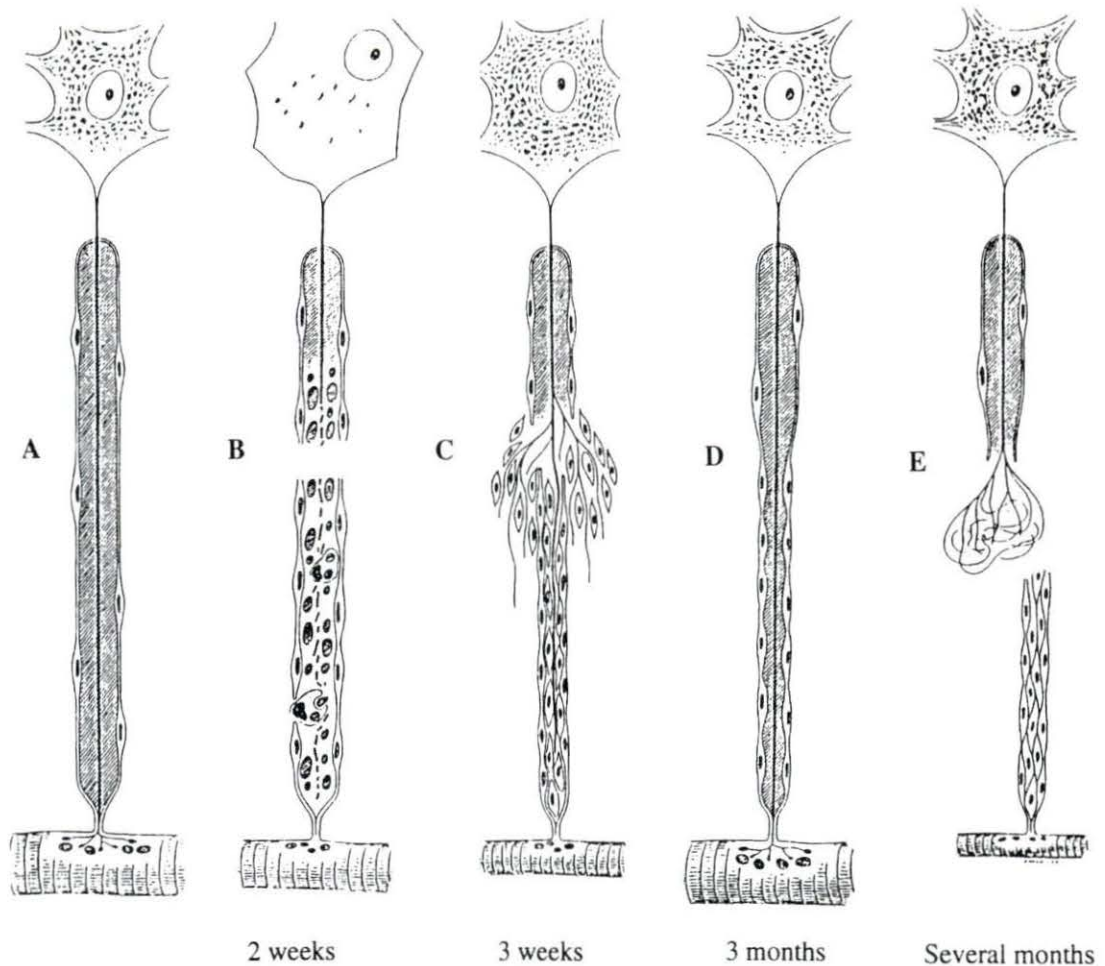


Figure 2.2. Diagrams of the degeneration and regeneration of a single myelinated peripheral nerve fiber. A: Normal nerve fiber, B: Changes during two weeks after transection. C: Three weeks after the transection. D: In this example, the nerve regeneration was successful. E: When the axon branches do not penetrate the connective tissue surrounding, its growth is not organized. (Junqueira et al., 1983; Fig. 9-18)

continuous tube all the way to the nerve terminal. In addition, Schwann cells are also involved in phagocytizing axonal and myelin debris and in protecting and remyelinating regenerating axons. While these regressive changes take place, Schwann cells proliferate within the remaining connective tissue sleeves leading to solid cellular columns. These rows of Schwann cells serve as guides to the sprouting axons formed during the repair phase.

### **2.1.3. Nerve regeneration**

Regeneration is the response of a peripheral nerve fiber to injury and its accompanying nerve degeneration. Regeneration initiates from the undegenerated proximal part of the neuron that is still connected to the trophic center cell body. Survival of neurons is inversely proportional to the distance from the cell body. Several factors influence the growth and development of the repairing nerve: location of the lesion; age of the individual; length of the impaired nerve; width of the destroyed nerve which leaves a gap; alignment of the cut surface of the nerve stumps; extent of the injury and amount of the hemorrhage in surrounding tissues (Swaim, 1987).

To complete a repair, the sequence of nerve regeneration requires the cell body to expend considerable energy. This process takes place similarly for both sensory and motor nerves. During chromatolysis and enlargement of the cell body, RNA and DNA synthesis activities increase within the cell. Simultaneously, this increases enzymatic activity and incorporation of amino acids within the cell body causing an increase in metabolic activity which leads to axonal regeneration. In addition, some peripheral nervous tissue releases substances, called nerve growth factors, to stimulate neuron growth. However, the cell body may die if the injury or severance gets too close to it, or if the metabolic capacity of the cell body does not satisfy the need of the amount of axon that must be regrown.

To meet the increased nutrient requirement and metabolic activity and to rebuild a fibrillar structure of regenerating axons, a complicated axonal transport system of five rate-components moves from the cell body down the regrowth axon. Each rate-component not only delivers a unique group of proteins synthesized in the cell body or polymerized from the parent axon stump but also carries axonal cytoplasm or organelles synthesized in the cell body. While traveling down the axon undergoing repair, a small portion of the slowly transported proteins migrates within the nerve membrane by microperistalsis and replaces enzymes catabolized in

the membrane. There is still a significant fraction that continues onto the terminal segments of the elongating axons (Swaim, 1987). Furthermore, when axons regenerate in response to severance of a nerve, the outgrowth rates of the axons are apparently limited by the supply of cytoskeleton associated with the delivery rate-components. Growth cone function (sprouting) is determined by microfilaments (polymers of actin). The asymmetry of the elongating axons is stabilized by microtubules (polymers of tubulin). The radial growth of an axon (maturation) is maintained by neurofilaments (polymers of triplet) (McQuarrie, 1983).

Nerve regeneration is influenced by the changes within the extracellular environment and the nerve stumps. Fibroblasts and circumferential cells infiltrate the injury site and migrate toward each other to establish a tissue bridge and capillary network between the proximal and distal stumps. Then axons initiate sprouting from the proximal stump. This is associated with the increased metabolic activity of the cell body. The axons elongate toward the distal stump along this newly built tissue pathway. Depending on the degree of the injury, axonal budding starts 1 to 3 cm proximal to the damage site (in cases of diffuse traumatic severance) or begins a few millimeters retrograde to the last node of Ranvier (in the case of a sharply localized injury).

As shown by light and electron microscopic studies, the proliferation of Schwann cells plays a key role in re-establishment of continuity between two stumps during axonal regeneration. Schwann tubes that were maintained by the basement membrane during degeneration begin to surround proliferating Schwann cells to form "bands of Bünger". Because regenerating axonal sprouts or branches have a natural affinity with Schwann cells (Figure 2.2C), called homotropism, regrowth of axons takes place alongside the band of Bünger between the basement membrane and the Schwann cells. The Schwann cells of the proximal stump slightly precede axonal growth cones; therefore, these longitudinally continuous bands provide a pathway to guide regenerating axons through the injury site and through the empty endoneurial tubes to their destinations (Allt, 1976; Lundborg et al., 1982a;



Williams et al., 1983; Williams and Varon, 1985). Subsequently, the Schwann cells enclose the regenerated axons by multiple concentric wrappings, that is, they remyelinate the regenerating axons.

Unmyelinated fibers regenerate more rapidly than myelinated axons (Allt, 1976; Williams et al., 1983; Williams and Varon, 1985). Axon branches push the Schwann cells of the tubule to the side while migrating into pre-existing endoneurial tubules in the distal stump.

However, if the axon branches do not enter the endoneurial tubules or are unable to penetrate the connective tissue surroundings, their regeneration is blocked (Figure 2.2E). Even though several axons may migrate into a tubule and develop, only one branch will become myelinated and fully mature once successful in contacting with a peripheral motor end plate or sensor receptor (Figure 2.2D).

## **2.2. Review of previous work in repair techniques**

### **2.2.1. Present nerve repair techniques**

Because mammalian peripheral nerve axons have a capability to regenerate following a transection, current repair techniques emphasize ways to re-establish the continuity of the impaired nervous tissue. Based on the extent of the injury and the length of the gap, suture and sutureless techniques have been applied to reunite whole nerves (epineurial repair) and components of nerves (perineurial, group perineurial, and interfascicular repair). If two stumps of a severed nerve with a gap of less than 1 cm can be placed in close approximation, suture repair (end-to-end anastomosis) is the most common clinical choice. Epineurial suture repair is utilized to bridge the outmost epineurial layer of the nerve sheath. To obtain a precise alignment, fascicles or small groups of fascicles are joined by fascicular (perineurial) or grouped fascicular suture repair techniques.

Scar tissue or trauma in the perineurium, intrafascicular tissue or perineurium can be caused by fascicular or perineurial surgical manipulations. This scar tissue frequently interferes with the growth of axons from the proximal stump into the distal nerve stump and after repair, some fascicles still can override, gap, buckle, or straddle the aligned components. In addition, if the injury is extensive or if the gap between the nerve stumps is longer than 1.5 cm, these nerve stumps cannot be brought together satisfactorily. A nerve graft or a nerve tube (sutureless repair technique) provides an alternative to bridge this condition. To separate a fibrous healing from axonal regeneration until the perineurium re-establishes continuity, a cellular approach using a fascicular tube or a nerve coupler as an artificial perineurium was introduced by Rosen et al. (1979, 1983) and by Marshall et al. (1989). To deal with problems of central tapering and gapping, Daniel (1991) developed the first multiple-lumen cuff system. It was made of silicone rubber. These preliminary studies were performed to bridge 0.5 cm gaps in the sciatic nerves of rats. They demonstrated the feasibility of using a multiple lumen cuff for support, guidance and orientation of axon growth from proximal to distal stumps.

### **2.2.2. Summary of past research**

Various natural materials and synthetic materials were investigated because of their suitability for sutureless repair. Biological materials such as autografts, allografts, or heterografts have served as nerve grafts to guide peripheral nerve regeneration across gaps. Autografts (e.g., autogenous veins) can undergo revascularization. This helps to preserve Schwann cells which aid in the regeneration process (Chiu et al., 1982, 1988; Suematsu et al., 1988). Sometimes, allografts and heterografts are used as alternatives. However, Kline (1988) pointed out that, with time, such vein grafts collapse and fibrosis results constricting the regenerating neuron fibers that regenerate across the site of the injury. Also, in order to obtain the vein for use, a new vein lesion may need to be introduced. However, there might be a

problem of finding a vein with the appropriate dimensions. Even though an allograft or a heterograft has a potential to serve as a nerve bridge, immune rejection might introduce problems.

Biocompatible materials have provided an alternative to serve as a nerve cuff when an autograft is unavailable. Many types of materials have been employed. Nonpermeable, or slightly permeable, and nonbiodegradable materials have been investigated such as silicone rubber (Daniel, 1991; Fields and Ellisman, 1986a, 1986b; Gibson and Daniloff, 1989; Jenq and Coggeshall, 1985; Le Beau et al., 1988b; Lundborg et al., 1982a; Müller et al., 1987; Politis et al., 1982; Satou et al., 1986; Williams et al., 1983, 1984, 1987; Williams and Varon, 1985; Yannas et al., 1989), Teflon<sup>®</sup> (Cuadros and Granatir, 1987), cellulose acetate (Bassett et al., 1959), Goretex<sup>®</sup> (Young et al., 1984), and polyethylene terephthalate (Yoshii et al., 1987). Bioresorbable or biodegradable materials have been introduced to reduce the confinement of newly formed epineurial sheaths or to eliminate compression of the regenerating nerves. Examples include polyglactin mesh (Molander et al., 1983), polyglycolic acid (Mathur et al., 1983; Rosen, et al., 1983, 1989), polyester (Henry et al., 1985) and glycolide trimethylene carbonate (Rosen et al., 1992). In addition to providing axon guidance, certain nerve cuffs may influence the regeneration process by modulating solute exchange between regenerating and extra-channel environments. The use of semipermeable materials such as polysulfone with a range of molecular weight cutoffs (Aebischer et al., 1989a, 1988), hemodialysis-type acrylic copolymer with a 50,000 dalton cutoff (Uzman and Villegas, 1983a, 1983b) and polyvinylchloride acrylic copolymer with a 50,000 dalton cutoff (Valentini et al., 1987) permits selected intra- and extra-channel factors to provide nutrition.

The gap length separating a proximal and distal rat sciatic nerve stumps must be less than 1 cm for a successful regeneration of nerves in empty silicone chambers (Lundborg et al., 1982a; Madison et al., 1985; Seckel et al., 1984; Williams, et al., 1984). However, if the silicone chambers are modified by prefilling with phosphate-buffered saline, a successful

regeneration can be promoted to span 2 cm interstump gap lengths (Williams et al., 1987). Williams and Varon (1985) demonstrated that an increase in the chamber volume (11, 25, and 75  $\mu$ l) through an increase in the chamber diameter (1.2, 1.8, and 3.1 mm inner diameter) adversely affects the natural matrix formation and results in a significant retardation of regeneration in chambers that were empty when implanted.

Prefilling selected chambers with dialyzed plasma results in a 3.5 fold increase in the endoneurial area of regeneration and in axon counts (Williams et al., 1987). On the other hand, Le Beau et al. (1988b) and Fields and Ellisman (1986b) suspected that a constrictive effect was present during nerve regeneration in silicone rubber nerve cuffs. Ducker and Hayes (1968) pointed out that the growth of axons regenerating through silicone tubes has been shown to be stunted by the constricting and ischemic effects of the tube itself. The problem is accentuated as the length of the gap increases and vascularization is further restricted. The authors suggested that the optimum cross-sectional area of the cuff for maximum fiber growth might be 2.5 to 3 times that of the nerve.

The importance of the distal nerve as a source of target-derived neurotrophic factors necessary for successful regeneration of the proximal nerve has been recognized by several investigators (Lundborg et al., 1981; Lundborg et al., 1982a, 1982b; Madison et al., 1985; Politis et al., 1982; Seckel et al., 1984; Williams et al., 1984). The distal stump influences axonal regeneration over a limited distance of the order of 1 cm.

Rapid proliferation and migration of Schwann cells follow a nerve transection (Williams et al., 1983; Williams and Varon, 1985). Cultured Schwann cells have been transplanted into peripheral nerves. The Schwann cells can ensheath and remyelinate axons (Aguayo et al., 1979 and Shine et al., 1985). Fluid conditioned by cells participating in nerve regeneration promotes Schwann cell adhesion, migration and proliferation in vitro (Le Beau et al., 1988a). However, there are conflicting investigation reports. If Schwann cells are killed by repeated freezing and thawing, but their basement membranes are kept intact, sprouting axons

still can follow the basal lamina tubes (Kumagai et al., 1990; Tohyama and Kumagai, 1992). The dead Schwann cells killed by repeated freezing are phagocytosed by macrophages. The basal laminae of the Schwann cells remain as tubular scaffolds and the regenerating axons can grow through such scaffolds from the proximal stump (Ide et al., 1983).

To improve the environment of regeneration in the chambers, humoral or substrate-bound chamber components such as laminin gel (Madison et al., 1985, 1987; Yoshii et al., 1987), collagen (Rosen, et al., 1989; Satou et al., 1986), collagen-glycosaminoglycan (Yannas, et al., 1989), collagen and cultured dorsal root ganglia cells (Shine et al., 1985), collagen and laminin gels (Madison et al., 1988; Valentini et al., 1987), basic fibroblast growth factor (b-FGF) or b-FGF and  $\alpha$ 1-glycoprotein ( $\alpha$ 1-GP) (Aebischer et al., 1989b), dialyzed plasma (Williams et al., 1987), or saline (Gibson and Daniloff, 1989; Williams et al., 1987; Williams and Varon, 1985) have been evaluated. The observations suggest that growth or trophic factors which are secreted by reactive cells or introduced by prefilling materials diffuse into the regenerative environment. They contribute to allow nerve regeneration even in the case of a presence of long gap lengths (greater than 1 cm, and up to 2 cm) or the use of blind-ended or empty distal nerve chambers.

The ultrastructural and morphometric characteristics of regenerated nerves (i.e., axon diameter, fiber diameter, myelin thickness, myelinated and unmyelinated axon counts, and organization) correlate with nerve physiological function recovery. Even after long implantation times, regenerated nerves are smaller than comparable normal adult nerves of a rat. Fiber diameter histograms display a bimodal diameter distribution with a much broader diameter range in control rats compared with similar aged animals used in nerve regeneration studies. For normal Sprague-Dawley rat sciatic nerves (Fields and Ellisman, 1986b), myelinated axons show a bimodal diameter distribution with peaks at 3.5 and 5 micrometers. In addition, there are larger axons of up to 9  $\mu$ m diameter. By comparison, even after a 302 day implantation

period, the regenerated axon diameter range only extends to about 6  $\mu\text{m}$  and the diameter distribution is skewed below the peak 3.5  $\mu\text{m}$  diameter (Rosen et al., 1983, 1992).

This decrease in average diameters seen for regenerated axons also agrees with the observations of Espejo and Alvarez (1986), Henry et al. (1985), Le Beau et al. (1988b), and Rosen et al. (1989). Le Beau et al. (1988b) found the rat sciatic mean fiber diameter at 435 days implantation to be  $2.39 \pm 0.10 \mu\text{m}$ . This is significantly smaller than that of normal rat,  $5.13 \pm 0.13 \mu\text{m}$ . In addition, the myelin sheath thickness is also significantly reduced in the regenerated myelinated fibers compared to those of the normal control animals. Sheath thickness becomes thicker with the increase in recovery time after the surgery (Espejo and Alvarez, 1986; Le Beau et al., 1988b).

Regressive changes in axon morphology are also apparent in older regenerated fibers. The two-zone reorganization seen by Daniel (1991) for both single and multiple lumen cuff systems is also seen in the single-lumen nerve cuff system (Jenq and Coggeshall, 1986; Lundborg et al., 1982a; Madison et al., 1988; Seckel et al., 1984; Williams and Varon, 1985; Williams et al., 1983, 1984). The peripheral zone contains dispersed blood capillaries and collagenous connective tissues (epineurial, perineurial and perineurial-like cells). The collagenous connective tissue matrix in a regenerated nerve is significantly wider than that seen in a normal control animal. In addition, there is some fluid-filled space between these two zones. The central zone is filled with myelinated and unmyelinated axons, an endoneurial connective tissue matrix, and an invading perineurium. Compared to highly packed axons in a normal nerve, regenerated axons are surrounded by relatively wider areas of invading perineurium. Some regenerated axons are grouped and separated further by invading perineurium. There are referred to as mini-fascicles or small regenerated units. Numerous prominent blood vessels appear in this zone (Jenq and Coggeshall, 1986; Seckel et al., 1984).

## **2.3. Multiple-lumen nerve cuff**

### **2.3.1. Organization of a multiple-lumen cuff**

The first multiple-lumen nerve cuff system was developed by Daniel (1991). The multiple-lumen tubular component that fills a 0.5 cm gap between proximal and distal nerve stumps is positioned coaxially within a single-lumen Silastic<sup>®</sup> medical-grade tube (single lumen: catalog number 602-265, Dow Corning Corp., Midland, Michigan) which is 11 mm in length. There is a 3 mm opening on each end of single lumen tube for inserting and anchoring the stumps. The outer diameter of this single lumen tube is 2.41 mm (0.095 inch). The inner diameter of this single lumen tube is 1.57 mm (0.062 inch). The rat sciatic nerves used in the study were approximately 1.2 mm in diameter. The 7-lumen cuff consists of one central lumen (0.38 mm in diameter). Six lumens (each 0.38 mm in diameter) are spaced 0.3 mm from the central lumen (wall-to-wall distance) in a circular pattern.

### **2.3.2. Silicone rubber in a nerve cuff**

Silicone rubber is predominantly built up utilizing the dimethyl-siloxane unit. The medium and hard grades are made from polydimethylsiloxane copolymerized with very small amounts of methylvinyl siloxane whose methylvinyl portion makes for a more efficient vulcanization. On the other hand, a small fraction of phenyl methyl siloxane contributes to the softness for the soft medical grade silicone rubber variety.

To turn the polymers into the three dimensional network structure, a medical-grade of silicone rubber is processed by heat-vulcanizing or room-temperature-vulcanizing (RTV). The heat vulcanization process is initiated by a catalyst, dichlorobenzoyl peroxide. Furthermore, the RTV silicone rubber is subclassified into the two component RTV and the one component RTV (Braley, 1970). For one-component silicone rubber, the cross-linking agent--methyl

triacetoxysilane--is activated by absorption of water from the air. For the two-component system, stannous octoate is added as a catalyst.

Very pure, finely divided particles of about 30 $\mu$ m in diameter serve as fillers in two component RTV silicone rubber to enhance its mechanical properties. In general, the more fillers used, the higher the density of the rubber (Park, 1984). Other varieties of silicone rubber utilized silica particles of the order of 120 $\text{\AA}$  in diameter (heat vulcanizing varieties).

Silastic<sup>®</sup> elastomer Q7-4750 was used for the central 7-lumen component of the cuff. This two-part enhanced tear resistant heat setting elastomer consists of dimethyl and methylvinyl siloxane copolymers and reinforcing silica particles. It is graded as being medium hard. The elastomer is cured with a platinum catalyst for 10 minutes at 240°F. It is then post-cured for 1-hour at 350°F.

## **2.4. Silver stain**

### **2.4.1. The principle of silver stain**

Bodian's silver stain has a specific affinity for neurofilaments of nerve fibers (Katz and Watson, 1985; Phillips et al., 1983). It is suggested that the neurofilaments contain an amino acid sequence or some secondary modification which binds directly with the silver.

The cytoskeleton of a neuron has three major components: neurofilaments, microtubules, and actin filaments. Actin filaments form a cortical network just under the membrane surface. Neurofilaments and microtubules are concentrated in axons and dendrites. They are oriented longitudinally and are connected by cross links. They are less abundant in the actin-rich cortex. In large mammalian axons, the number of neurofilaments is correlated with the size of axon cross sectional areas. Axons establish their diameters in relation to the radial extent of the network of cross linked neurofilaments that they contain (Vale et al., 1992). The



silver impregnation method stains the areas of axonal fibers according to the content and density of neurofilaments and, thus, highlights individual axons.

Schlaepfer and Micko (1978a) showed the selective disappearance of 69,000, 150,000, and 200,000 dalton neurofilament proteins in transected peripheral nerves. The same proteins have been identified in isolates of intact neurofilaments from a rat peripheral nerve and spinal cord (Schlaepfer and Freeman, 1978b). This suggests that the organization of neurofilament proteins is broken down during Wallerian axonal disintegration. Subsequently, axonal regeneration, particularly during the maturation phase (which emphasizes the radial growth of the axon), involves the laying down of neurofilaments (McQuarrie, 1983). Newly-formed (immature axons), contain relatively few neurofilaments and fine cell processes. The standard Bodian method does not stain them (Katz and Watson, 1985). In addition, if an amino acid sequence which has been proposed to bind directly with the silver greatly decreases in the regenerated axon, the cross section of this regenerated axon would display a non-uniform stain. Therefore, the intensification procedure needs to be followed in order to enhance and define more clearly the fine cytoskeletal structures normally stained by the Bodian silver stain.

#### **2.4.2. The chemistry of a silver stain**

A silver stain technique has three common features (Kiernan, 1981):

1. impregnating fixed tissue in a solution containing silver ions ( $10^{-5}$  M to 1.0 M concentration).
2. subsequently treating the specimen with a reducing agent to initiate the reaction:  $\text{Ag}^+ + \text{e}^- = \text{Ag}$ .
3. depositing opaque dark material consisting mainly or entirely of metallic silver in the argyrophilic axons.

Silver is taken up in two ways in the first step of the staining procedure. During impregnation, most of the silver is bound chemically by proteins throughout the tissue. This chemically bound silver is not specifically related to any axons. A much smaller fraction of the silver is reduced at sites in the argyrophilic axons and is precipitated as small silver nuclei (about 2-6 atoms). Then the tissue sections are transferred to a solution similar to an alkaline photographic developer containing sodium sulphite and hydroquinone. First, the sulphite initially removes the chemically bound silver from the proteins and simultaneously stabilizes the spontaneous reduction of  $\text{Ag}^+$  by introducing  $[\text{Ag}(\text{SO}_3)_2]^{3-}$  ions into the solution. Second, the hydroquinone then reduces this complex ion to metallic silver on the surfaces of the previously formed nuclei associated with the argyrophilic axons. The metallic silver nuclei present in the axons thus enlarge and coalesce. The axons will appear black or brown in reflected light.

To overcome an inadequate light microscopy contrast for axons impregnated with silver, the contrast can be enhanced by toning the silver-stained tissue sections in gold chloride. After gold toning, provided that this still does not produce adequate improvement in contrast, it is necessary to add a further reduction stage to the procedure by using oxalic acid. Substantial deposits of gold precipitate around each original particle of silver. Finally, the specimens are immersed in aqueous sodium thiosulphate to remove residual silver salts and to stop the silver impregnation (Kiernan, 1981).

## **2.5. Backscattered electron imaging for the silver stained axons**

When the primary electrons of a beam from a scanning electron microscope interact with the specimen, several scattering events occur. These interactions can be generally divided into two groups. One interaction group comprises elastic events which occur whenever a primary beam electron comes into proximity with a specimen atom nucleus or outer shell

electron and the electron rebounds with negligible energy loss. This leads to the production of backscattered electrons. The other interaction group comprises inelastic collisions which happen whenever a primary beam collides with an electron of the specimen atom. The beam provides substantial energy to that atom, resulting in the generation of secondary electrons, Auger electrons, characteristic X-rays and continuum (Bremsstrahlung) X-rays, long wavelength electron magnetic radiation, electron-hole pairs, lattice vibrations (photons), and electron oscillations (plasmons).

Backscattered electrons can escape from a relatively large depth within the sample (approximately 1 to 2  $\mu\text{m}$  for a low atomic number matrix containing a high atomic number feature). Backscattered electron production shows a strong correlation with increasing atomic number. As the atomic number of a region of the specimen increases, a backscattered electron image results in increased image contrast for a feature. For this reason, based on the mean atomic number differences between features of a sample, several phases may be distinguished in the backscattered electron image. Thus, stained neuron fibers can be recognized easily due to higher contrast provided by electrons backscattering from the silver (atomic number  $Z=47$ ) precipitated in the fibers compared to the low atomic number of the myelin and connective tissue components surrounding the nerve fiber ( primarily, nitrogen ( $Z=7$ ), oxygen ( $Z=8$ ) and carbon ( $Z=6$ )).

### **3. MATERIALS AND METHODS**

#### **3.1. Sample preparation**

As an extension of the evaluation of the multiple-lumen cuff (Daniel, 1991), the present study utilizes several of the thin sections from that study (Table 3.1). The nerve thin section specimens were stained with Bodian's silver stain for light microscopy studies. They were also suitable for an electron backscattered imaging study of axons. Three sections, about 2-3 mm long, had been removed from the proximal section (4.5 mm proximal to the center of the cuff), the middle section (the center of the nerve cuff) and the distal section (4.5 mm distal to the center of the cuff) of experimental animals that had received a multiple-lumen cuff (8, 12, 16, or 24 week implantation periods). A 5 mm section of the sciatic nerve corresponding to the repair area of experimental animals was removed at the end of each implantation period for control animals. The male Sprague-Dawley rats used in this study were adults.

For the light microscope microstructural study, the specimens were processed with 10% neutral buffered formalin and then dehydrated in ascending concentrations of ethanol (from 70%, 80%, 90%, up to 100%). The samples were embedded (JB-4<sup>®</sup> embedding kit, Polyscience Inc., Warrington, PA) and then the 2-3 mm nerve blocks were sectioned (1.5  $\mu$ m to 2.5  $\mu$ m thickness sections). After the plastic matrix was removed by etching in a 10% solution of sodium hydroxide in 100% ethanol, and following a wash using a few drops of 100% ethanol, the tissue sections were mounted on glass slides and the thin sections were stained by using the Bodian's silver stain method and by using gold toning to enhance contrast. All of these processes were performed in the histo-pathology laboratory in the Department of Veterinary Pathology, Iowa State University.

Table 3.1. Sample list

Group	Control <sup>a</sup>		Experiment		
Time	16 week	8 week implantation	12 week implantation	16 week implantation	24 week implantation
Animal number	19	24	14	34	1, 2, & 3
Specimen number <sup>b</sup>	91R729	91R637A 91R637C 91R637B	91R724A 91R724C 91R724B	91R626A 91R626C 91R626B	91R712A 91R712C 91R712B 91R713A 91R713C 91R713B 91R714A 91R714C 91R714B

a Control animal (no surgery during the 16 week period) was sacrificed for comparisons of normal nerve with that of nerve samples from the multiple lumen experiments.

b Specimen number A, C, or B represents a proximal, middle or distal section, respectively (A = proximal, B = distal, and C = middle). The control animal has only one site and can be compared with sections from the proximal, middle, and distal locations from retrieved multiple lumen experimental cases.

To generate the electron backscattered image of the surface of the thin sections directly, the glass cover slip had to be removed from the light microscope slides. The slides were immersed in xylene until the cover slip detached from the sample slide (within 4 to 5 days). The mounting medium that had been used to adhere the cover slip onto the thin section of the slide was acrytol (a mixture composed of methyl methacrylate, residual monomers, toluene, dibutyl phthalate, and 2,6-di-tert-butyl-p-cresol).

The dry specimen surfaces were then coated with a 100Å thin film of gold applied using a sputter coating device (SEM Coating Unit E5100, Polaron Instruments Inc.) operated at 2.2 kV ion potential with an ion current of 20 mA for one minute. The sample was then ready for mounting on the scanning electron microscope specimen stage for electron backscatter imaging.

### **3.2. Scanning electron microscope examination**

An adhesive (a mixture of colloidal graphite and isopropanol; Energy Beam Sciences, MA) is applied to the base of the slide and the top of the sample holder to hold the slide mount to the SEM stage. To reduce sample charging in the SEM, the four edges of the glass slide are also covered by the conductive adhesive (Von Langsdorff et al., 1990). The specimens are examined in a JEOL JSM-840 scanning electron microscope equipped with a backscattered electron detector. Secondary emission imaging (SE) is done using an accelerating voltage of 15 kV, probe current of 0.05 to 0.5 nA, aperture size of 70  $\mu\text{m}$  or 110  $\mu\text{m}$ , and a working distance of 37 to 39 mm. The backscattered electron image (BSE) is then obtained using the same accelerating voltage, probe current, aperture size, but a shorter working distance of 6 mm to 15 mm in order to collect sufficient backscattered electron signals for optimal contrast. The image is collected using a digital imaging system that averages multiple scans in order to decrease noise in an image. Final photographic recording utilizes Polaroid Type 55 film.

The same specimen is also examined at 160x or 400x magnification (16x or 40x by 10x Optivar) using a light microscope (Dialux 20, Leitz). Photographic images are recorded using the accessory camera (2.5x Optivar) with Kodak technical pan film (TP135-36).

### **3.3. Quantitative evaluations**

Morphometric parameters for the repaired peripheral nerve include axon core diameters, axon counts, total regenerated axon area, axon cross sectional area of the regenerated strand or fascicle-like unit, and axon counts per unit area. These are evaluated for the proximal, middle, and distal cross sections. Light microscope (LM) and scanning electron microscope (SEM) techniques are used. These analyses are performed on backscattered electron images (1000X

micrographs) and enlarged light microscope photographs (400X or 1000X). The results are then compared.

Measurements were performed using the method of Vejsada et al. (1985) in which the **axon core diameter** is obtained by measuring the longest dimension of the axon (major axis) and the longest axon dimension perpendicular to this (minor axis), and averaging the two measurements. The measurements are scaled by a machinist ruler with the smallest scale being markings 1/64 inch apart. Measurements of the current study are reported to  $\pm 0.2 \mu\text{m}$  on the 1000X basis [ $1/128 \text{ inch} \times 25.4 \text{ mm}/\text{inch} \times 10^3 \mu\text{m}/\text{mm} \div 10^3$  (magnification)]. After these measurements, every axon feature is first classified according to its staining uniformity characteristics, and then grouped into diameter classes for frequency-size distribution plots. Axon features smaller than  $0.75 \mu\text{m}$  are excluded from measurement (less than 0.1% of the features measured).

The diameter ratio of major axis to minor axis is calculated to investigate the shape of regenerated axons. For comparison between Daniel's measurement method (an equivalent circle diameter method) done by automated image analysis and that of the current study (an equalized ellipse method, Vejsada et al., 1985), the differences in axon diameters are calculated and the differences are reported as percent.

The cross sectional area containing the regenerated axons measured is defined as the **area examined**. The area is examined with a micrometer disc (Bauch & Lomb) covering the specimen. The related position between the border of the area with the smallest square grid of the micrometer disc (0.2 mm one side) is drawn on grid paper. The smallest square grid on the micrometer disc is further divided by 25 small grids. One side of the small grid on the grid paper corresponds to 0.04 mm. The axon cross sectional area of the proximal section, that of the strand examined in the middle section, and that of the fascicle-like units examined in the distal section is termed as **total area**. These measurements are estimated to 1/6 of area of the small grid on the grid paper [ $1/6 \times (0.04 \text{ mm})^2 \times 10^6 \mu\text{m}^2/\text{mm}^2 = 266 \mu\text{m}^2$ ] but are reported to

$\pm 500 \mu\text{m}^2$  to include uncertainty from drawing. The **area examined relative to total area** is obtained by multiplying 100 times the ratio of the area examined divided by total area.

The **axon counts** are obtained from the area examined. The **extrapolated axon counts for the total area** are calculated by dividing the axon counts in the area examined by the percentage of the area examined to the total area. However, there are several nerve strands in the middle section and fascicle-like units in the distal section. To investigate variances for axon counts among different strands which bridge the gap, the **number of strands in the middle section**, the **axon counts per strand**, and the **number of fascicle-like units in the distal section**, and **axon counts per fascicle-like unit** are evaluated. The **axon counts per unit area (axons/ $\mu\text{m}^2$ )** represent the axon counts divided by the area examined in which axons were counted and measured. For comparisons of the two observation methods, the identical strand or the fascicle-like unit is examined by both LM and SEM and is identified by the **same series number** in both measurement cases.

### 3.4. Diameter frequency distribution

When nerve regenerates through the repair site, axon cones may branch into empty endoneurial tubes distal to the repair site. With an increasing demand on the proximal axons during this branching process, the average size of the distal axon fibers diminishes. For this reason, there is an uncertainty in knowing the percentage of connected axons for comparisons of the counts of axons proximal and distal to the repair nerve site. To eliminate this factor of uncertainty, axon fiber diameter frequency distributions (FDH) are introduced to measure the numbers and the sizes of the regenerated axons in proportion to their maturation and conduction velocity. Also, the reduction of axonal fiber size due to branching is reflected in an FDH.



The diameter histogram is obtained from the sum of the axon counts ranked in each diameter range based on the same staining uniformity feature characteristic. Each diameter rank contains a diameter range of 0.5  $\mu\text{m}$  (within plus 0.24  $\mu\text{m}$  and minus 0.25  $\mu\text{m}$ ). For example, the 1- $\mu\text{m}$  diameter rank includes diameters between 0.75  $\mu\text{m}$  and 1.24  $\mu\text{m}$ . The diameter histogram is plotted as percent versus the diameter ranks. The percent in a size range is calculated by 100 times the ratio of sum of the axons found in the diameter rank divided by the total number of axons examined. Diameter frequency distributions for the proximal, middle and distal sections of each animal are then compared. To further examine the grouping characteristic, the sum of the percent in a size range of 2  $\mu\text{m}$  (with plus and minus 1  $\mu\text{m}$  of diameter rank in which the mean axon diameter is located) is also characterized.

### **3.5. Statistical methods**

The Tukey method of multiple comparisons is applied. If all factor level sample sizes are the same, the Tukey method is exact. On the other hand, a modified Tukey-Kramer method is suitable for unequal sample sizes. This was used in this study. Variable names are set for comparison. These include evaluation methods (SEM and LM), animal groups (experimental and the normal control), implant periods (8, 12, 16 and 24 weeks), animal number, locations of the sections (proximal, middle and distal sections) and stain uniformity characteristics (category I, uniformly stained, and category II, nonuniformly stained). These tests are based on the assumption that there is no significant difference between the means obtained from pairs of factor levels such as SEM versus LM. The analysis is generated at the 0.05 level of significance ( $\alpha = 0.05$ ). Pairs of mean differences between section levels of experimental animals and the single control animal are tested under each evaluation method factor level. Further analysis tables of variance are determined by testing the relative repaired location level for each animal of each evaluation method, by comparing the location level based on the same

stain uniformity characteristic and by calculating the mean diameters among different stain uniformity characteristics for each section. All statistical tests are run with Statistical Analysis System (SAS), (Release 6.06, SAS Institute, Cary, NC).

## **4. RESULTS**

### **4.1. Microstructure**

#### **4.1.1. Scanning electron microscope studies**

The BSE image emphasizes the composition contrast. Because Bodian's silver stain is specific to axons and silver has a relatively high atomic number atom, contrast for silver is relatively high in BSE imaging of regenerated axons compared with that for the low atomic number atoms of the surrounding tissue matrix. According to their appearance, regenerated axon features can be divided into two categories. Category I axons display uniform staining for axon features. Category II axons appear nonuniform in their staining for axon features.

An example of normal adult rat axons is shown in Figure 4.1. These axons have a clearly defined cross section surrounded by a myelin sheath. Blood capillaries are present in the perineurium connective tissue matrix. Only a few blood capillaries are inside the fascicles. The shape of every fascicle appears as a flattened oval. After the nerve is transected and is then repaired utilizing a multiple lumen cuff, these general normal nerve structural characteristics are absent. Examples from multiple lumen experiments of sections from the proximal, middle, and distal sections are shown in Figures 4.2A, B, and C for animal 3.

##### **4.1.1.1. Proximal section**

The structure of the proximal section for all four implant periods appears to be the most organized among those of the three section locations. The collagenous endoneurial connective tissue matrix among axons in this section is much more extensive than that seen in normal axon sections. Category I and II axonal features are present in this section (Figure 4.2A). Blood

capillaries appear inside the endoneurial connective tissue matrix and among the outer perineurium connective tissue matrix. With time, more perineurium invades the endoneurial connective tissue matrix to form fascicles of nerve; however, the mean diameter of axons is still smaller than that of normal axons of the control.

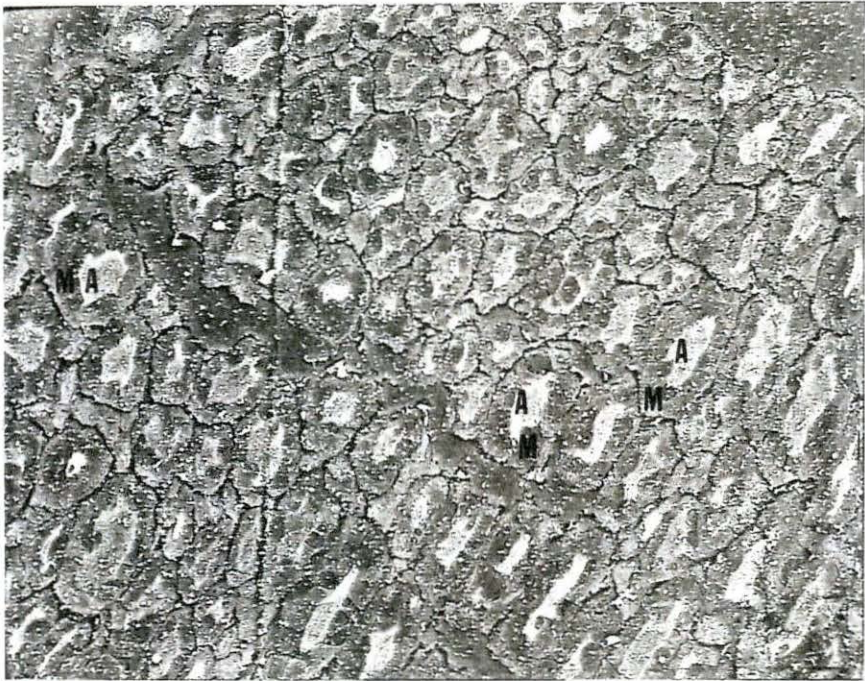
#### **4.1.1.2. Middle section**

Because of the seven lumen multiple lumen nerve cuff design, one to seven strands of nerve bundles are seen for a repair. The round shape of a strand is different from the flattened oval shape of the normal fascicles. If nerve cuffs are implanted and filled with saline solution at the time of implantation, the regenerated nerve strand number appear to be higher compared with multiple lumen cuffs used with empty lumens at the time of implantation. There are 5, 6, or 7 regenerated strands in nerve cuffs implanted and prefilled with saline solution (at 16 weeks post-implantation) compared to 2, 5, or 6 regenerated strands of multiple lumen cuffs implanted empty (at 24 weeks post-implantation).

A regenerated strand has two prominent zones (shown in Figure 4.2B). The central zone is mainly filled by category I axons, category II axons, blood capillaries, endoneurial connective tissue matrix, and invading perineurial cells. These neural elements form a fascicular regeneration unit. The peripheral zone primarily contains numerous dispersed blood capillaries and collagenous connective tissue (epineurial, perineurial, or perineurial-like cells). It is organized into concentric layers. Squamous cell layers line the periphery, occupying a large fraction of the total strand cross section. This zone contains more collagen matrix between each layer than the control.

There are numerous blood vessels which are larger in middle sections of the multiple lumen cuffs implanted with saline in the lumens compared with those cuffs implanted with empty lumens. Also, the cuffs implanted with a saline prefill appear to exhibit better

Figure 4.1 Backscattered electron image of a cross section of the normal control right sciatic nerve (mid-thigh level). The normal axons are highly organized. Each neuron axon (A) has a clearly defined fiber area containing a myelin sheath (M), stained gray, and the bright white axon. Normal control animal #19. Mean diameter=  $4.2 \pm 1.9 \mu\text{m}$ , Bodian stain. Scale bar =  $10 \mu\text{m}$




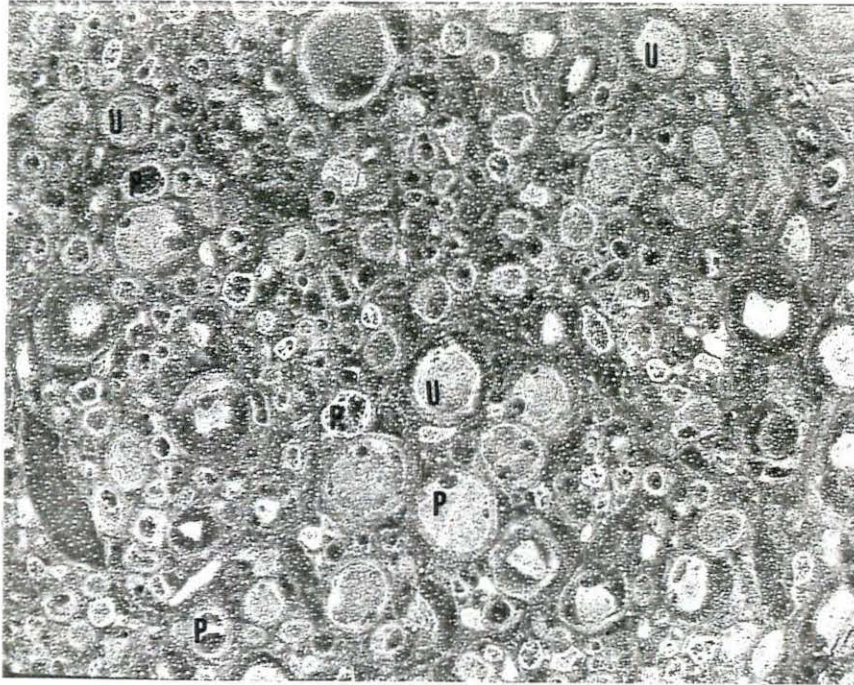
10  $\mu\text{m}$  

Figure 4.2 Backscattered electron images of a cross section of a regenerated nerve from the proximal, middle and distal sections of animal #3. 24 weeks post-implantation. (2A) Proximal, (2B) middle, and (2C) distal sections. Bodian stain. Scale bar = 10  $\mu\text{m}$

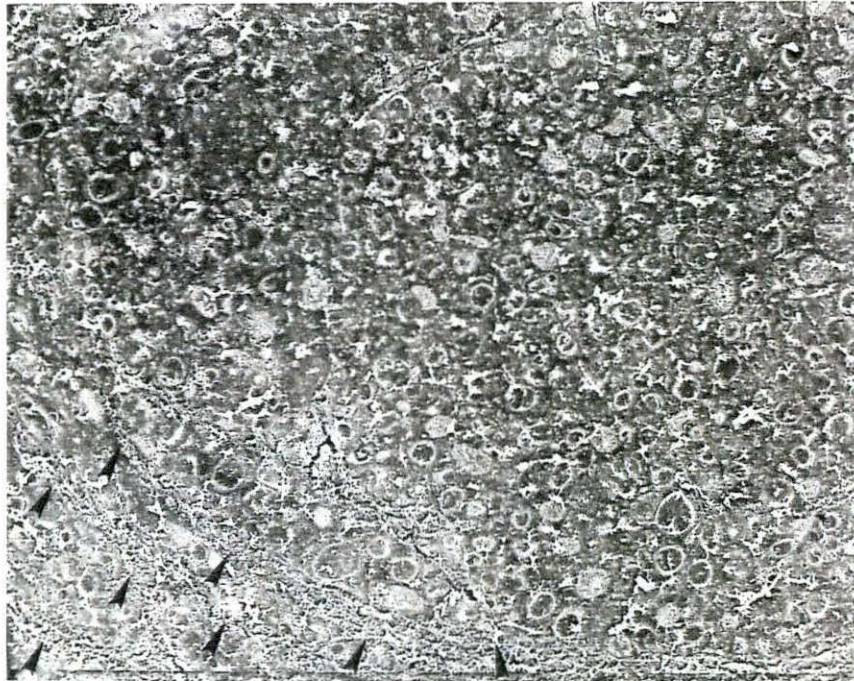
A) Category I, uniformly stained axon features (U), and category II, non-uniformly stained axon feature (P). Mean diameter =  $3.4 \pm 1.9 \mu\text{m}$

B) The central zone of the regenerated nerve strand. Category I and II axon features, blood capillaries, endoneural connective tissue matrix, and invading perineurial cells are confined by layers of perineurium (arrow heads) among the peripheral zone.



A

10 μm



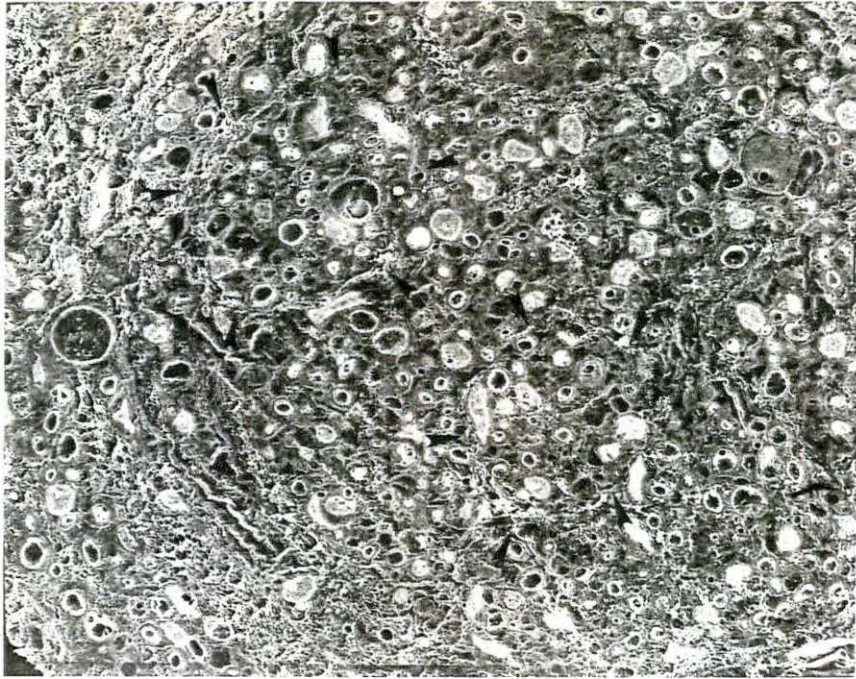
B

10 μm



Figure 4.2: continued

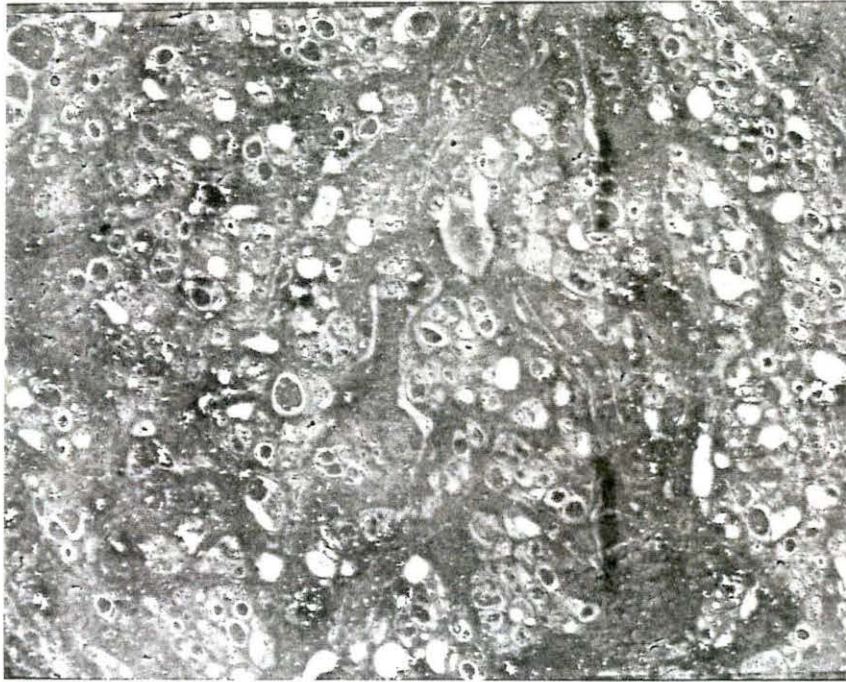
- C) The distal section still maintained the two-zone pattern seen in the middle section: a central zone and a peripheral zone. Neural elements grouped into units (arrow heads) in the distal section.




C

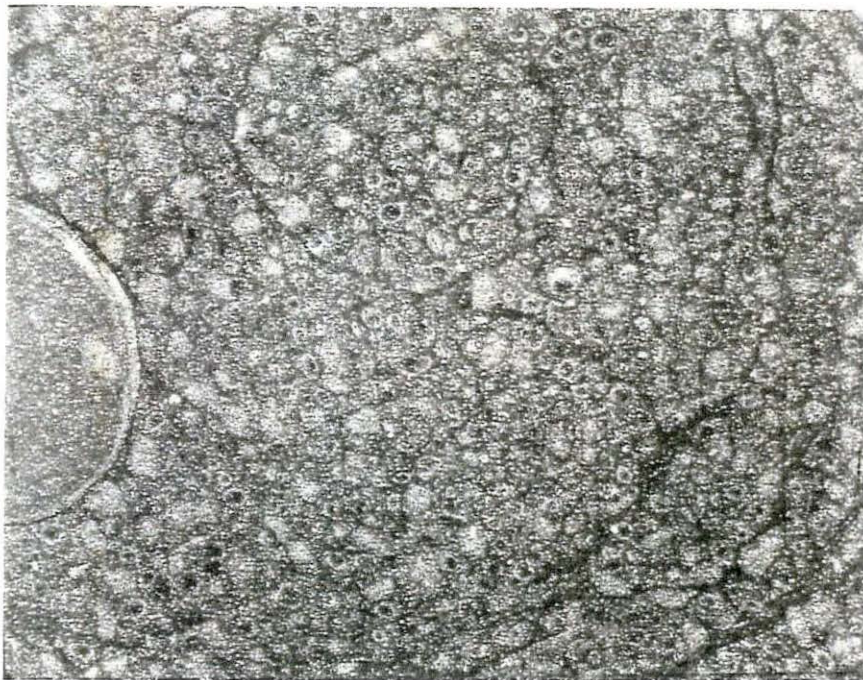
10  $\mu\text{m}$  

Figure 4.3: Backscattered electron image of one nerve strand of the middle section of animal #2 and of one nerve strand of the middle section of animal #14. There is more collagen and endoneurial matrix surrounding regenerated neural elements in animal #2 (no saline prefill) compared with that for the section from animal # 14 (saline prefill). The cuffs implanted with a saline prefill (animal #14) appear to exhibit better organization of the axons features of the middle region than the cuffs implanted with empty cuff lumen. (3A) Animal #2, 24 weeks post-implantation, Bodian Stain. (3B) Animal #14, 16 weeks post-implantation, Bodian Stain. Scale bar = 10  $\mu$ m



A

10  $\mu\text{m}$  



B


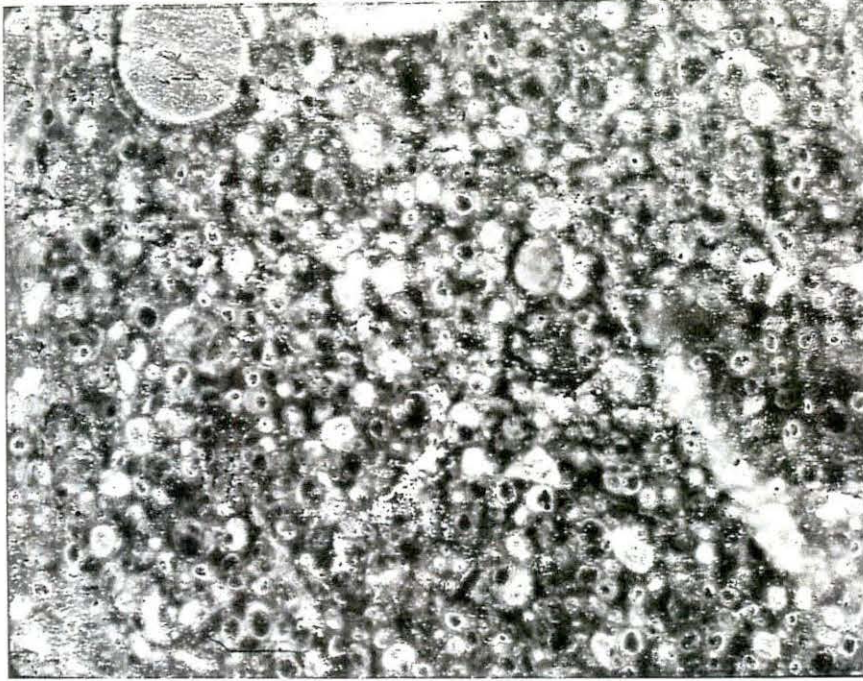

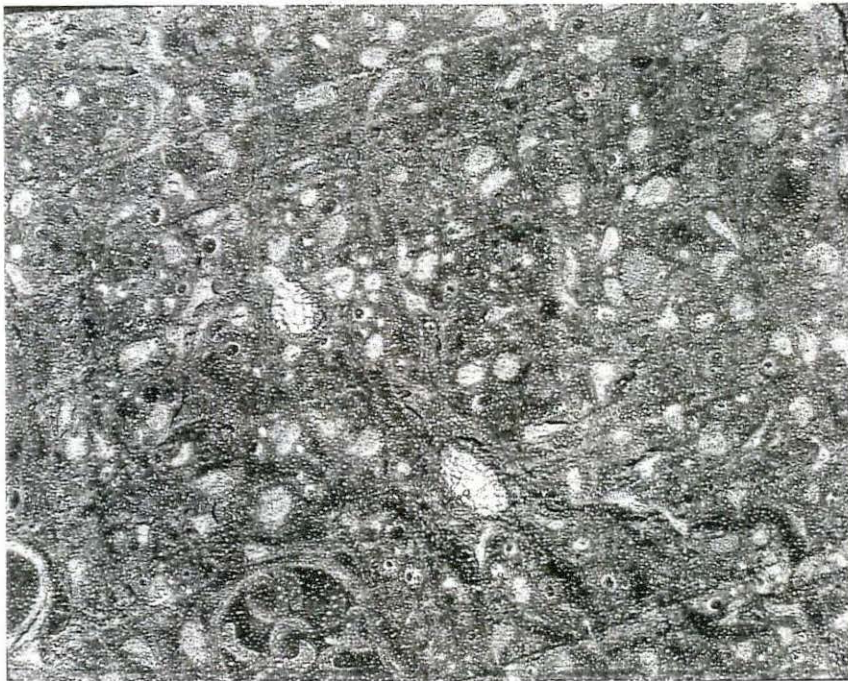
10  $\mu\text{m}$  

Figure 4.4: Backscattered electron image of one fascicle-like unit of the distal section of animal #2 and of the distal section of animal #14. (4A) Animal #2, distal section, 24 weeks post-implantation, no saline prefill, Bodian Stain. (4B) Animal #14, distal section, 16 weeks post-implantation, with saline prefill. Bodian Stain. Scale bar = 10  $\mu\text{m}$




A

10  $\mu\text{m}$  



B

10  $\mu\text{m}$  

organization (Figure 4.3B) of the axon features of the middle region than the cuffs implanted with empty cuff lumens (Figure 4.3A).

#### **4.1.1.3. Distal section**

Like the morphology seen for regenerated nerve strands in the middle section, every nerve bundle that crosses the gap and enters the distal stump maintains two zones: a central zone which includes neural elements and a peripheral zone which contains a connective tissue matrix (Figure 4.2C). The cuff specimens retrieved from saline prefill experiments show a clearly defined perineurial border between each regenerated fascicle or fascicle-like unit (16 week case) compared to a relatively poorly defined connective tissue perineurial border in specimens for which no saline prefill was used (24 weeks post-implantation period case). There are larger blood vessels and fascicular units in specimens implanted with saline in the lumens compared with those implanted with empty lumens (Figure 4.4A and B).

#### **4.1.2. Light microscope studies**

The patterns observed in light microscopy (LM) are similar to those results obtained from the backscattered electron image (BSE). In addition, it is as easy to identify axons in LM as it is in BSE images due to the Bodian's silver stain being specific to axons. However, BSE images have a superior contrast range compared to the light microscope pattern.

### **4.2. Fiber diameter frequency distribution**

These fiber diameter histograms are plotted as percentage of axons compared to diameter range (scaled to 0.5  $\mu\text{m}$  intervals; refer to Appendix). The diameter distribution for

certain proximal, middle and distal sections is plotted as a single diameter frequency distribution for either LM or SEM. In the SEM study, category I and category II plots represent uniformly stained axon features and non-uniformly stained axon features, respectively.

For the normal control animal, there is a broad, flat distribution covering the size range of 1.0  $\mu\text{m}$  to 11.0  $\mu\text{m}$  (LM result). In BSE cases, category I distributions indicate a broad diameter range from 1  $\mu\text{m}$  to 8.5  $\mu\text{m}$ , and category II distributions are somewhat broader (from 1.5  $\mu\text{m}$  to 9.5  $\mu\text{m}$ ). The frequency distribution of the combinations of axons from the two categories also occurs with a broad diameter range (between 1.0 and 9.5  $\mu\text{m}$ ).

#### **4.2.1. 8 weeks post-implantation (animal #34)**

In LM, the mode of the middle section peaks at 3.5  $\mu\text{m}$  but that of the distal section peaks at 4.0  $\mu\text{m}$ . SEM studies indicate that category I axons have axon distribution peak ranges of 3.0 to 5.5  $\mu\text{m}$  (proximal), 2.5 to 4.0  $\mu\text{m}$  (middle), and 3.0 to 4.5  $\mu\text{m}$  (distal). Category II axons of the middle and distal sections peak within a 1.5 to 3.0  $\mu\text{m}$  size range. About 90% of axon diameters of the proximal section are grouped within a size range of 1.5 to 3.5  $\mu\text{m}$  including a sharp peak at 2.0  $\mu\text{m}$ . Combined data for category I and II axons shifts the distribution toward somewhat larger diameter sizes.

#### **4.2.2. 12 weeks post-implantation (animal # 24)**

LM results show a sharp peak at 2.0  $\mu\text{m}$  in the proximal section. About 80% of the axon diameters of the middle section are found between 1.0 and 3.0  $\mu\text{m}$ . These are skewed to smaller sizes. In the distal section, the peak shifts toward larger sizes between 2.5 and 4.5  $\mu\text{m}$ .

SEM observations for category I axons indicate that over 80% of the proximal axons are grouped within a size range of 1.5 to 3.0  $\mu\text{m}$ ; for the middle section axons, the diameter is



from 1.0 to 3.5  $\mu\text{m}$  and contains over 80% of the axons examined for this section; and the distal distribution has a larger diameter range (2.0 to 6.0  $\mu\text{m}$ ), with about 90% of the axons occurring within in this range. For category II axons, over of 90% of the proximal distribution are grouped into a small diameter range from 1.0 to 3.0  $\mu\text{m}$  with over 85% of the middle section axons appearing within the same diameter range as for category I middle section axons. There is no category II axon count available for the distal section for this animal. This combination of category I and category II axons shows that 90% of the axons either in the proximal or in the middle section are sized between 1.0 and 3.0  $\mu\text{m}$ . The distal spectrum of total axons (SEM) is the same as that of the category I axons.

#### **4.2.3. 16 weeks post-implantation (animal # 14)**

LM results show that the proximal distribution peaks between 1.5 and 3.5  $\mu\text{m}$  and about 90% of the middle distribution are grouped between 1.0 and 3.5  $\mu\text{m}$ . For category I axons, the proximal distribution peaks between 1.5 and 4.0  $\mu\text{m}$ , with a mode at 3.0  $\mu\text{m}$ . In the middle section, about 90% of the axons are found to be between 1.0 and 4.0  $\mu\text{m}$ . The distal distribution is broad and ranges from 1.0 to 4.5  $\mu\text{m}$ . For the category II axons, the proximal axons usually have a size between 1.0 and 2.5  $\mu\text{m}$ . In the middle section, the principle distribution occurs between 1.0 and 2.0  $\mu\text{m}$ . Approximately 90% of the axons of the distal section group between the 1.0 and 2.5  $\mu\text{m}$  size range.

#### **4.2.4. 24 weeks post-implantation (animals #1, #2 and #3)**

In the LM case for animal 1, over 85% of the axons exhibit a diameter between 1.0  $\mu\text{m}$  and 3.5  $\mu\text{m}$  (proximal section), between 1.5  $\mu\text{m}$  and 2.0  $\mu\text{m}$  (middle section), and between 1.0  $\mu\text{m}$  to 4.0  $\mu\text{m}$  (distal section). For category I axons, about 80% of the proximal axon

diameters are grouped within the 1.5 $\mu\text{m}$  to 4.0  $\mu\text{m}$  range. The middle section axons have their mode at 3.0  $\mu\text{m}$ . The distal axons are primarily between 2.0 and 4.0  $\mu\text{m}$ . For category II axons, the data are more skewed with modes at 2.5  $\mu\text{m}$  (proximal), 1.5  $\mu\text{m}$  (middle) and 1.0  $\mu\text{m}$  (distal). Eighty percent of the diameters of the combination of category I and II axons are located between 1.0 and 3.0  $\mu\text{m}$  with a 2.0  $\mu\text{m}$  mode (proximal), between 1.5 and 4.0  $\mu\text{m}$  with a 2.0  $\mu\text{m}$  mode (middle), and between 2.0 and 4.0  $\mu\text{m}$  with a peak at 3.0  $\mu\text{m}$  (distal).

LM data for animal 2 are similar to those seen for animal 1. The most frequent (approximately 80%) sizes are within the 1.0 and 3.0  $\mu\text{m}$  range (proximal), 1.0 and 4.0  $\mu\text{m}$  range (middle), and 1.0 and 3.5  $\mu\text{m}$  range (distal). Category I axons exhibit their principle frequencies for the proximal, middle and distal sections between 1.5 and 3.5  $\mu\text{m}$ , between 1.0 to 4.0  $\mu\text{m}$ , and between 1.0 and 3.5  $\mu\text{m}$ , respectively. For category II axons, peaks occur at 2.0 (proximal), 2.0 (middle) and 1.5 (distal)  $\mu\text{m}$ . For the total axon diameter distribution (combination of category I and II axons), the spectra are similar to those of category II.

LM data for animal 3 show a sharp peak (40%; proximal) located at 2.0  $\mu\text{m}$ . The middle and distal distributions are grouped between 1.5  $\mu\text{m}$  and 3.5  $\mu\text{m}$  and between 1.0 and 2.5  $\mu\text{m}$ , respectively. In the frequency spectrum for category I axons, distributions have modes at 3.0 (proximal), 2.0 (middle), and 1.5  $\mu\text{m}$  (distal). Compared to category II axons, more frequencies group among the smaller diameter range, between 1.0 and 3.0  $\mu\text{m}$ , for all sections. For the total axonal diameter distribution, the proximal section has a mode at 3.0  $\mu\text{m}$ , the middle section has a platykurtic peak curve between 1.5 and 2.5  $\mu\text{m}$ , and the distal section has a 1.5  $\mu\text{m}$  mode.

### **4.3. Quantitative results**

The neuron quantitative results are displayed in Tables which follow. In Table 4.1 through Table 4.12, data listings mainly include the area examined, the total axon area,

percentage of area examined to the total related axon area, axon counts for area examined, axon counts per unit area ( $\#/\mu\text{m}^2$ ), mean axon diameter (with standard deviation) for area examined, and extrapolated axon counts based on total area. According to the methods of the studies and the uniformity of the staining, the tables are shown in the following order. LM results (Tables 4.1, 4.2, and 4.3), total axons results from SEM studies (Tables 4.4, 4.5, and 4.6), category I axon results from SEM (Tables 4.7, 4.8, and 4.9), and category II axon results from SEM (Tables 4.10, 4.11, and 4.12). For each group, the tables present information for proximal, middle, and distal locations. Because of the multiple lumen cuff design, the "number of strands" that occurred in the middle section and the results for each strand are also included in the appropriate table. One to seven fascicle-like units occurred in the distal section. This was determined in association with the one to seven strands that crossed the gap and entered the distal section. The individual fascicle-like unit series number does not correlate directly with position from the middle section data for these tabulations. On the other hand, the series number shown on the LM result tables is the same as that listed on the SEM result tables of the same section for comparison.

All axon mean diameters determined for the experimental animals (except the category I axon mean diameter of the proximal section of animal 34, 8 weeks implantation) are always smaller than that of the normal control animal. Axon counts per unit area obtained from examined area for an experimental animal usually indicate a larger density than that for the normal control animal. Axon counts per unit area of category I axons are usually higher than those of category II axons in the same area examined. Although strand-to-strand or fascicle-like unit to unit variations are indicated by comparisons, they are not significant. Extrapolated axon counts (based on total axon area) of each (available) section point out that the number in the proximal section is much higher than that of the middle section or the distal section. There are one to seven regenerated nerve strands in the middle section (repair site).

Table 4.13, Table 4.14, Table 4.15 and Table 4.16 list the percentage of the distribution of axons within  $\pm 1 \mu\text{m}$  of the mean diameter for axons of the LM, category I, category II and total axons counted in a BSE image. Over 60% of the axon frequency spectra group within  $\pm 1 \mu\text{m}$  of the mean diameter range seen for axons of these experimental animals. By contrast, the axon distribution percentage for the normal control animal is lower (45%).

Based on the equalized ellipse method, Table 4.17, Table 4.18, Table 4.19 and Table 4.20 show the major-to-minor axis ratios with standard deviations which are calculated for ratios of the major axis to the minor axis. The major axis is usually at least 1.4 times larger than the minor axis. Note that, the diameter ratio obtained from the normal animal is much higher than regenerated axons. In addition, there are differences between the equivalent circle diameter method and the equalized ellipse method. Based on the same samples, the diameter differences are 2% to 10% larger when calculated by the equalized ellipse method.

The comparisons are tested at significance level ( $\alpha$ ) 0.05. If the probability (P) of accepting the hypothesis (there is no difference between a pair of axon diameter means) is less than the  $\alpha$  chosen, the null hypothesis would be rejected. This is indicated by \*\*\* and the specific probability in the analysis appears in the table. Otherwise, a \* is indicated for accepting the hypothesis. Results are displayed in Tables 4.21 to 4.28. Table 4.21 shows the mean diameter comparisons obtained from LM and BSE images. In Table 4.22, the mean axon diameter for each area examined is significantly smaller than that of the normal control animal (LM). Then, Table 4.23 provides a way to compare mean axon diameters between different locations for the same animal (LM). Table 4.24 also indicates a significantly larger mean axonal diameter for the normal control animal than for the experimental animals (SEM). Similar results to that of Table 4.24 appear in Table 4.25 where mean diameter comparisons of the same category of axons can be made between repaired nerve and the normal control animal (SEM). Except for the normal control animal, Table 4.26 indicates that if mean axon diameter comparisons are made between the two categories in the same area examined, the mean

diameter of category I axons is always larger than that of category II axons. In Table 4.27, results are provided for mean diameter comparisons of the same category of axons but between different examined locations of the same animal (SEM). Data listings in Table 4.28 indicate that mean diameters in the proximal section show significantly larger diameters than those in strands in the middle sections of the same animal (SEM). In addition, there is also no significant difference in axon counts per unit area between salined prefill cases (16 weeks) and the non-saline prefill cases (24 weeks) for the same section. However, there are larger mean strand cross section areas shown at middle sections for saline prefill cases (16 weeks) compared to non-prefill cases (24 weeks).

**Table 4.1: Area examined, total area, percentage of area examined to total area, axon counts for area examined, axon counts per unit area, mean axon diameter, and extrapolated counts based on total area in the proximal section observed by LM**

Implant Period & Group	Animal Number	Area Examined ( $\mu\text{m}^2$ )	Total Area <sup>a</sup> ( $\mu\text{m}^2$ )	Area Examined Relative to Total Area (%)	Axon Counts for Area Examined (#)	Axon Counts Per Unit Area <sup>b</sup> ( $\# / \mu\text{m}^2$ )	Mean Axon Diameter for Area Examined & Standard Deviation ( $\mu\text{m}$ )	Extrapolated Axon Counts Based on Total Area (#)
24 Weeks								
Multiple Lumen	1	286000	713000	40%	7296	0.026	$2.5 \pm 1.3$	18240
24 Weeks								
Multiple Lumen	2	294000	1204000	24%	4800	0.016	$2.4 \pm 1.1$	20000
24 Weeks								
Multiple Lumen	3	295500	687000	43%	4020	0.014	$3.4 \pm 1.9$	9349
16 Weeks								
Multiple Lumen	14	276500	975000	28%	6020	0.022	$3.1 \pm 1.5$	21500
12 Weeks								
Multiple Lumen	24	186500	200000	93%	5230	0.028	$2.1 \pm 0.8$	5624
8 Weeks								
Multiple Lumen	34	-----	1146500	-----	-----	-----	-----	-----
16 Weeks <sup>c</sup>								
Normal Control	19	150000	165500	91%	1836	0.012	$4.4 \pm 2.1$	2018

a Total area is obtained from the total axon area of the proximal section.

b The axon counts per unit area are obtained from axon counts for area examined divided by the area examined.

c There is no surgery performed in the normal control animal but it was sacrificed for comparison with animals of the experiments; therefore, the proximal portion of nerve is considered the same as the middle portion of nerve and the data are taken from one fascicle of the single middle section.

**Table 4.2: Area examined, total area, percentage of area examined to total area, axon counts for area examined, axon counts per unit area, mean axon diameter, and extrapolated counts based on total area in the middle section observed by LM**

Implant Period & Group	Animal Number	Total Number of Strands Occurred in Section	Strand Series Number <sup>b</sup>	Area Examined ( $\mu\text{m}^2$ )	Total Area <sup>c</sup> ( $\mu\text{m}^2$ )	Area Examined Relative to Total Area (%)	Axon Counts for Area Examined (#)	Axon Counts Per Unit Area <sup>d</sup> ( $\# / \mu\text{m}^2$ )	Mean Axon Diameter for Area Examined & Standard Deviation ( $\mu\text{m}$ )	Extrapolated Axon Counts Based on Total Area (#)
24 Weeks										
Multiple Lumen	1	2	1	8500	17000	50%	202	0.024	$2.0 \pm 0.8$	404
24 Weeks										
Multiple Lumen	2	5 <sup>a</sup>	1	31500	37000	85%	304	0.010	$3.0 \pm 1.4$	358
			2	30000	30000	100%	407	0.014	----	407
			3	17500	17500	100%	337	0.019	----	337
24 Weeks										
Multiple Lumen	3	5	1	7500	7500	100%	208	0.028	----	208
			2	17500	19000	92%	588	0.034	$2.4 \pm 0.8$	639
			3	12000	12000	100%	137	0.011	----	137
16 Weeks										
Multiple Lumen	14	7	1	13500	13500	100%	435	0.032	----	435
			2	23000	23000	100%	271	0.012	----	271
			3	18500	18500	100%	432	0.023	----	432
			4	10500	10500	100%	303	0.029	----	303
			5	17500	18000	98%	866	0.049	$1.9 \pm 0.8$	892
			6	15000	15000	100%	374	0.025	----	374
			7	15000	15000	100%	393	0.026	----	393

- a There are five bridging strands inside and a sixth proximal strand extends half way across cuff.  
b Because some artifacts are on this portion of the sample, part of the strand information might not be available.  
c Total area is obtained from the total axon area of a strand examined in the section.  
d Axon counts per unit area are obtained from axon counts for the area examined divided by the area examined.

**Table 4.2: Continued**

Implant Period & Group	Animal Number	Total Number of Strands Occurred in Section	Strand Series Number <sup>b</sup>	Area Examined ( $\mu\text{m}^2$ )	Total Area <sup>c</sup> ( $\mu\text{m}^2$ )	Area Examined Relative to Total Area (%)	Axon Counts for Area Examined (#)	Axon Counts Per Unit Area <sup>d</sup> ( $\# / \mu\text{m}^2$ )	Mean Axon Diameter for Area Examined & Standard Deviation ( $\mu\text{m}$ )	Extrapolated Axon Counts Based on Total Area (#)
12 Weeks Multiple Lumen	24	7	1	33500	33500	100%	355	0.011		355
			2	20500	22000	91%	484	0.024	2.6 ± 1.3	532
			3	22000	22000	100%	115	0.005		115
			4	12000	12000	100%	250	0.021	----	250
			5	13500	13500	100%	63	0.005	----	63
			6	33500	33500	100%	180	0.005	----	180
			7	19000	19000	100%	266	0.014	----	266
8 Weeks Multiple Lumen	34	1	1	40000	41500	96%	632	0.016	3.6 ± 1.3	658
16 weeks Normal Control <sup>e</sup>	19	2 <sup>f</sup>	1	150000	165500	91%	1836	0.012	4.4 ± 2.1	2018

b Because some artifacts are on this portion of the sample, part of strand information might not be available.

c Total area is obtained from the total axon area of a strand examined in the section.

d Axon counts per unit area are obtained from axon counts for the area examined divided by the area examined.

e There is no surgery performed in the normal control animal, but it was sacrificed for comparison with animals of the experiments.

f There are two fascicles, but only one is studied.



**Table 4.3: Area examined, total area, percentage of area examined to total area, axon counts for area examined, axon counts per unit area, mean axon diameter, and extrapolated counts based on total area in the distal section observed by LM**

Implant Period & Group	Animal Number	Total Number of Strands Occurred in Middle	Total Number of Fascicle-like Unit in Distal	Fascicle-like Unit Series Number <sup>a</sup>	Area Examined ( $\mu\text{m}^2$ )	Total Area <sup>b</sup> ( $\mu\text{m}^2$ )	Area Examined Relative to Total Area (%)	Axon Counts for Area Examined (#)	Axon Counts Per Unit Area <sup>c</sup> ( $\# / \mu\text{m}^2$ )	Mean Axon Diameter for Area Examined & Standard Deviation ( $\mu\text{m}$ )	Extrapolated Axon Counts Based on Total Area (#)
24 Weeks											
Multiple Lumen	1	2	2	1	9000	9000	100%	137	0.015	----	137
				2	15000	19000	79%	241	0.016	$2.5 \pm 1.5$	305
24 Weeks											
Multiple Lumen	2	5	6	1	27000	27000	100%	292	0.011	----	292
				2	24000	24000	100%	71	0.003	----	71
				3	43000	43000	85%	728	0.020	$2.3 \pm 1.1$	856
				4	35000	35000	100%	179	0.005	----	179
				5	4000	4000	100%	78	0.020	----	78
6	24000	24000	100%	137	0.006	----	137				
24 Weeks											
Multiple Lumen	3	5	5	1	43000	43000	100%	312	0.007	----	312
				2	13000	13000	100%	70	0.005	----	70
				3	22000	22000	100%	510	0.023	----	510
				4	9000	9000	100%	69	0.008	----	69
5	29000	29000	100%	704	0.024	$2.0 \pm 0.9$	704				
16 Weeks											
Multiple Lumen	14	7		1	----	287000	----	----	----	----	----

- a The individual fascicle-like unit series number does not correlate directly from the middle position to the distal position.
- b Total area is obtained from the axon area of a fascicle-like unit examined in the distal section.
- c Axon counts per unit area are obtained from axon counts for the area examined divided by the area examined.

**Table 4.3: Continued**

Implant Period & Group	Animal Number	Total Number of Strands Occurred in Middle	Total Number of Fascicle-like Unit in Distal	Fascicle-like Unit Series Number <sup>a</sup>	Area Examined ( $\mu\text{m}^2$ )	Total Area <sup>b</sup> ( $\mu\text{m}^2$ )	Area Examined Relative to Total Area (%)	Axon Counts for Area Examined (#)	Axon Counts Per Unit Area <sup>c</sup> ( $\# / \mu\text{m}^2$ )	Mean Axon Diameter for Area Examined & Standard Deviation ( $\mu\text{m}$ )	Extrapolated Axon Counts Based on Total Area (#)
12 Weeks Multiple Lumen	24	7	7	1	25000	25000	100%	146	0.006	----	146
				2	10000	10000	100%	281	0.028	----	281
				3	27000	27000	100%	401	0.015	----	401
				4	31000	33000	93%	852	0.027	$3.7 \pm 1.5$	916
				5	33000	33000	100%	385	0.017	----	385
				6	43000	43000	100%	350	0.008	----	350
				7	32000	32000	100%	207	0.006	----	207
8 Weeks Multiple Lumen	34	1	2	1	36500	40000	91%	263	0.007	$3.9 \pm 1.5$	289
				2	35000	35000	100%	436	0.012	----	436
16 Weeks Normal Control <sup>d</sup>	19	2	2	1	150000	165500	91%	1836	0.012	$4.4 \pm 2.1$	2018

- a The individual fascicle-like unit series number does not correlate directly from the middle position to the distal position.
- b Total area is obtained from the the axon area of a fascicle-like unit examined in the distal section.
- c Axon counts per unit area are obtained from axon counts for the area examined divided by the area examined.
- d There is no surgery performed in the normal control animal but it was sacrificed for comparison with animals of the experiments; therefore, the distal portion of nerve is considered the same as the middle portion of nerve and the data are taken from one fascicle of the single middle section.

**Table 4.4: Area examined, total area, percentage of area examined to total area, axon counts for area examined, axon counts per unit area, mean axon diameter, and extrapolated counts based on total area in the proximal section observed by SEM**

Implant Period & Group	Animal Number	Area Examined ( $\mu\text{m}^2$ )	Total Area <sup>a</sup> ( $\mu\text{m}^2$ )	Area Examined Relative to Total Area (%)	Axon Counts for Area Examined (#)	Axon Counts Per Unit Area <sup>b</sup> ( $\# / \mu\text{m}^2$ )	Mean Axon Diameter for Area Examined & Standard Deviation ( $\mu\text{m}$ )	Extrapolated Axon Counts Based on Total Area (#)
24 Weeks								
Multiple Lumen	1	12500	713000	2%	200	0.016	3.0 ± 1.3	10000
24 Weeks								
Multiple Lumen	2	10000	1204000	1%	281	0.028	2.7 ± 1.2	28100
24 Weeks								
Multiple Lumen	3	9500	687000	1%	263	0.028	3.4 ± 1.9	26300
16 Weeks								
Multiple Lumen	14	10000	975000	1%	271	0.027	2.5 ± 1.1	6160
12 Weeks								
Multiple Lumen	24	10000	200000	5%	308	0.031	2.2 ± 0.9	12900
8 Weeks								
Multiple Lumen	34	10000	1146500	1%	129	0.013	4.0 ± 1.5	-----
16 Weeks <sup>c</sup>								
Normal Control	19	150000	165500	6%	124	0.012	4.2 ± 1.9	2067

- a Total area is obtained from the total axon area of the proximal section.
- b The axon counts per unit area are obtained from axon counts for the area examined divided by the area examined.
- c There is no surgery performed in the normal control animal but it was sacrificed for comparison with animals of the experiments; therefore, the proximal portion of nerve is considered the same as the middle portion of nerve and the data are taken from one fascicle of the single middle section.

**Table 4.5: Area examined, total area, percentage of area examined to total area, axon counts for area examined, axon counts per unit area, mean axon diameter, and extrapolated counts based on total area in the middle section observed by SEM**

Implant Period & Group	Animal Number	Total Number of Strands Occurred in Section	Strand Series Number <sup>b</sup>	Area Examined ( $\mu\text{m}^2$ )	Total Area <sup>c</sup> ( $\mu\text{m}^2$ )	Area Examined Relative to Total Area (%)	Axon Counts for Area Examined (#)	Axon Counts Per Unit Area <sup>d</sup> ( $\# / \mu\text{m}^2$ )	Mean Axon Diameter for Area Examined & Standard Deviation ( $\mu\text{m}$ )	Extrapolated Axon Counts Based on Total Area (#)
24 Weeks										
Multiple Lumen	1	2	1	6500	17000	38%	106	0.016	$2.3 \pm 1.1$	279
24 Weeks										
Multiple Lumen	2	5 <sup>a</sup>	1	9500	37000	26%	380	0.040	$2.4 \pm 1.0$	1462
24 Weeks										
Multiple Lumen	3	5	2	10000	19000	53%	290	0.029	$2.3 \pm 0.9$	553
16 Weeks										
Multiple Lumen	14	7	5	9500	18000	53%	372	0.039	$2.3 \pm 1.1$	702
12 Weeks										
Multiple Lumen	24	1	2	9500	22500	42%	299	0.031	$2.1 \pm 1.5$	712
8 Weeks										
Multiple Lumen	34	2	1	10000	41500	24%	331	0.033	$2.9 \pm 1.0$	1379
16 Weeks										
Normal Control <sup>e</sup>	19	2	1	10000	165500	6%	124	0.012	$4.2 \pm 1.9$	2067

a There are five bridging strands inside and a sixth proximal strand extends half way across cuff.

b The series number of this strand examined in SEM work corresponds to strand series number in LM work.

c Total area is obtained from the total axon area of a strand examined in the section.

d Axon counts per unit area are obtained from axon counts for the area examined divided by the area examined.

e There is no surgery performed in the normal control animal but it was sacrificed for comparison with animals of the experiments; there are two fascicles but only one is studied.

**Table 4.6: Area examined, total area, percentage of area examined to total area, axon counts for area examined, axon counts per unit area, mean axon diameter, and extrapolated axons counts based on total area in the distal section observed by SEM**

Implant Period & Group	Animal Number	Total Number of Strands Occurred in Middle	Total Number of Fascicle-like Unit in Distal	Fascicle-like Unit Series Number in LM <sup>a</sup>	Area Examined ( $\mu\text{m}^2$ )	Total Area <sup>b</sup> ( $\mu\text{m}^2$ )	Area Examined Relative to Total Area (%)	Axon Counts for Area Examined (#)	Axon Counts Per Unit Area <sup>c</sup> ( $\# / \mu\text{m}^2$ )	Mean Axon Diameter for Area Examined & Standard Deviation ( $\mu\text{m}$ )	Extrapolated Axon Counts Based on Total Area (#)
24 Weeks											
ML	1	2	2	2	10000	19000	53%	105	0.011	3.0 ± 1.1	198
24 Weeks											
ML	2	5	6	3	10000	43000	23%	352	0.035	2.2 ± 1.0	1530
24 Weeks											
ML	3	5	5	5	10000	29000	34%	310	0.031	2.1 ± 1.0	912
16 Weeks											
ML	14	7	1	----	9500	287000	3%	221	0.023	2.6 ± 1.8	7367
12 Weeks											
ML	24	7	7	4	10000	33500	30%	83	0.008	4.0 ± 1.6	277
8 Weeks											
ML	34	1	2	1	10000	40000	25%	224	0.022	3.1 ± 1.1	896
16 Weeks											
Control <sup>d</sup>	19	2	2	1	10000	165500	6%	124	0.012	4.2 ± 1.9	2067

ML Multiple-lumen studies.

- The individual fascicle-like unit series number does not correlate directly from the middle position to the distal position. In addition, the series number of this fascicle-like unit examined in SEM corresponds to the unit series number in LM.
- Total area is obtained from the axon area of a fascicle-like unit examined in the distal section.
- Axon counts per unit area are obtained from axon counts for the area examined divided by the area examined.
- There is no surgery performed in the normal control animal but it was sacrificed for comparison with animals of the experiments; therefore, the distal portion of nerve is considered the same as the middle portion of nerve and the data are taken from one fascicle of the single middle section.

**Table 4.7: Area examined, total area, percentage of area examined to total area, category I axon counts for area examined, category I axon counts per unit area, mean category I axon diameter, and extrapolated category I axon counts based on total area in the proximal section observed by SEM**

Implant Period & Group	Animal Number	Area Examined ( $\mu\text{m}^2$ )	Total Area <sup>a</sup> ( $\mu\text{m}^2$ )	Area Examined Relative to Total Area (%)	Axon Counts for Area Examined (#)	Axon Counts Per Unit Area <sup>b</sup> ( $\# / \mu\text{m}^2$ )	Mean Axon Diameter for Area Examined & Standard Deviation ( $\mu\text{m}$ )	Extrapolated Axon Counts Based on Total Area (#)
24 Weeks Multiple Lumen	1	12500	713000	2%	150	0.012	3.1 ± 1.3	7500
24 Weeks Multiple Lumen	2	10000	1204000	1%	180	0.018	2.8 ± 1.0	18000
24 Weeks Multiple Lumen	3	9500	687000	1%	105	0.011	3.5 ± 1.3	10500
16 Weeks Multiple Lumen	14	10000	975000	1%	156	0.016	2.9 ± 1.0	15600
12 Weeks Multiple Lumen	24	10000	200000	5%	143	0.014	2.3 ± 0.6	2860
8 Weeks Multiple Lumen	34	10000	1146500	1%	107	0.011	4.3 ± 1.4	10700
16 Weeks <sup>c</sup> Normal Control	19	150000	165500	6%	86	0.009	3.8 ± 1.7	1433

a Total area is obtained from the total axon area of the proximal section.

b The axon counts per unit area are obtained from axon counts for the area examined divided by the area examined.

c There is no surgery performed in the normal control animal but it was sacrificed for comparison with animals of the experiments; therefore, the proximal portion of nerve is considered the same as the middle portion of nerve and the data are taken from one fascicle of the single middle section.

**Table 4.8: Area examined, total area, percentage of area examined to total area, category I axon counts for area examined, category I axon counts per unit area, mean category I axon diameter, and extrapolated category I axon counts based on total area in the middle section observed by SEM**

Implant Period & Group	Animal Number	Total Number of Strands Occurred in Section	Strand Series Number <sup>b</sup>	Area Examined ( $\mu\text{m}^2$ )	Total Area <sup>c</sup> ( $\mu\text{m}^2$ )	Area Examined Relative to Total Area (%)	Axon Counts for Area Examined (#)	Axon Counts Per Unit Area <sup>d</sup> ( $\# / \mu\text{m}^2$ )	Mean Axon Diameter for Area Examined & Standard Deviation ( $\mu\text{m}$ )	Extrapolated Axon Counts Based on Total Area (#)
24 Weeks										
Multiple Lumen	1	2	1	6500	17000	38%	64	0.010	$2.6 \pm 1.2$	168
24 Weeks										
Multiple Lumen	2	5 <sup>a</sup>	1	9500	37000	26%	179	0.019	$2.5 \pm 1.1$	688
24 Weeks										
Multiple Lumen	3	5	2	10000	19000	53%	142	0.014	$2.5 \pm 1.0$	268
16 Weeks										
Multiple Lumen	14	7	5	9500	18000	53%	219	0.023	$2.6 \pm 1.1$	413
12 Weeks										
Multiple Lumen	24	1	2	9500	22500	42%	120	0.013	$2.3 \pm 1.1$	286
8 Weeks										
Multiple Lumen	34	2	1	10000	41500	24%	152	0.015	$3.2 \pm 1.0$	633
16 Weeks										
Normal Control <sup>e</sup>	19	2	1	10000	165500	6%	86	0.009	$3.8 \pm 1.7$	1433

- a There are five bridging strands inside and a sixth proximal strand extends half way across cuff.
- b The series number of this strand examined in SEM work corresponds to strand series number in LM work.
- c Total area is obtained from the total axon area of a strand examined in the section.
- d Axon counts per unit area are obtained from axon counts for the area examined divided by the area examined.
- e There is no surgery performed in the normal control animal but it was sacrificed for comparison with animals of the experiments; there are two fascicles but only one is studied.

**Table 4.9: Area examined, total area, percentage of area examined to total area, category I axon counts for area examined, category I axon counts per unit area, mean category I axon diameter, and extrapolated category I axons counts based on total area in the distal section observed by SEM**

Implant Period & Group	Animal Number	Total Number of Strands Occurred in Middle	Total Number of Fascicle-like Unit in Distal	Fascicle-like Unit Series Number in LM <sup>a</sup>	Area Examined ( $\mu\text{m}^2$ )	Total Area <sup>b</sup> ( $\mu\text{m}^2$ )	Area Examined Relative to Total Area (%)	Axon Counts for Area Examined (#)	Axon Counts Per Unit Area <sup>c</sup> ( $\# / \mu\text{m}^2$ )	Mean Axon Diameter for Area Examined & Standard Deviation ( $\mu\text{m}$ )	Extrapolated Axon Counts Based on Total Area (#)
24 Weeks											
ML	1	2	2	2	10000	19000	53%	87	0.009	3.1 ± 1.0	164
24 Weeks											
ML	2	5	6	3	10000	43000	23%	168	0.017	2.5 ± 1.1	730
24 Weeks											
ML	3	5	5	5	10000	29000	34%	188	0.019	2.3 ± 1.0	533
16 Weeks											
ML	14	7	1	----	9500	287000	3%	169	0.018	3.0 ± 1.9	5633
12 Weeks											
ML	24	7	7	4	10000	33500	30%	83	0.008	4.0 ± 1.6	277
8 Weeks											
ML	34	1	2	1	10000	40000	25%	156	0.016	3.4 ± 1.1	624
16 Weeks											
Control <sup>d</sup>	19	2	2	1	10000	165500	6%	86	0.009	3.8 ± 1.7	1433

ML Multiple-lumen studies.

- a The individual fascicle-like unit series number does not correlate directly from the middle position to the distal position. In addition, the series number of this fascicle-like unit examined in SEM corresponds to the unit series number in LM.
- b Total area is obtained from the axon area of a fascicle-like unit examined in the distal section.
- c Axon counts per unit area are obtained from axon counts for the area examined divided by the area examined.
- d There is no surgery performed in the normal control animal but it was sacrificed for comparison with animals of the experiments; therefore, the distal portion of nerve is considered the same as the middle portion of nerve and the data are taken from one fascicle of the single middle section.



**Table 4.10: Area examined, total area, percentage of area examined to total area, category II axon counts for area examined, category II axon counts per unit area, mean category II axon diameter, and extrapolated category II axon counts based on total area in the proximal section observed by SEM**

Implant Period & Group	Animal Number	Area Examined ( $\mu\text{m}^2$ )	Total Area <sup>a</sup> ( $\mu\text{m}^2$ )	Area Examined Relative to Total Area (%)	Axon Counts for Area Examined (#)	Axon Counts Per Unit Area <sup>b</sup> ( $\# / \mu\text{m}^2$ )	Mean Axon Diameter for Area Examined & Standard Deviation ( $\mu\text{m}$ )	Extrapolated Axon Counts Based on Total Area (#)
24 Weeks Multiple Lumen	1	12500	713000	2%	50	0.004	2.8 ± 1.2	2500
24 Weeks Multiple Lumen	2	10000	1204000	1%	101	0.010	2.5 ± 1.4	10100
24 Weeks Multiple Lumen	3	9500	687000	1%	158	0.017	3.3 ± 2.3	15800
16 Weeks Multiple Lumen	14	10000	975000	1%	115	0.012	2.1 ± 1.1	11500
12 Weeks Multiple Lumen	24	10000	200000	5%	165	0.017	2.1 ± 1.1	3300
8 Weeks Multiple Lumen	34	10000	1146500	1%	22	0.002	2.5 ± 0.9	2200
16 Weeks <sup>c</sup> Normal Control	19	150000	165500	6%	38	0.004	5.0 ± 2.1	633

a Total area is obtained from the total axon area of the proximal section.

b The axon counts per unit area are obtained from axon counts for the area examined divided by the area examined.

c There is no surgery performed in the normal control animal but it was sacrificed for comparison with animals of the experiments; therefore, the proximal portion of nerve is considered the same as the middle portion of nerve and the data are taken from one fascicle of the single middle section.

**Table 4.11: Area examined, total area, percentage of area examined to total area, category II axon counts for area examined, category II axon counts per unit area, mean category II axon diameter, and extrapolated category II axon counts based on total area in the middle section observed by SEM**

Implant Period & Group	Animal Number	Total Number of Strands Occurred in Section	Strand Series Number <sup>b</sup>	Area Examined ( $\mu\text{m}^2$ )	Total Area <sup>c</sup> ( $\mu\text{m}^2$ )	Area Examined Relative to Total Area (%)	Axon Counts for Area Examined (#)	Axon Counts Per Unit Area <sup>d</sup> ( $\# / \mu\text{m}^2$ )	Mean Axon Diameter for Area Examined & Standard Deviation ( $\mu\text{m}$ )	Extrapolated Axon Counts Based on Total Area (#)
24 Weeks										
Multiple Lumen	1	2	1	6500	17000	38%	42	0.006	$1.8 \pm 0.7$	111
24 Weeks										
Multiple Lumen	2	5 <sup>a</sup>	1	9500	37000	26%	201	0.021	$2.4 \pm 0.9$	773
24 Weeks										
Multiple Lumen	3	5	2	10000	19000	53%	148	0.015	$2.3 \pm 0.9$	279
16 Weeks										
Multiple Lumen	14	7	5	500	18000	53%	153	0.016	$1.8 \pm 1.0$	289
12 Weeks										
Multiple Lumen	24	1	2	9500	22500	42%	179	0.019	$1.9 \pm 1.7$	426
8 Weeks										
Multiple Lumen	34	2	1	10000	41500	24%	179	0.018	$2.7 \pm 1.0$	746
16 Weeks										
Normal Control <sup>e</sup>	19	2	1	10000	165500	6%	38	0.004	$5.0 \pm 2.1$	633

- a There are five bridging strands inside and a sixth proximal strand extends half way across cuff.
- b The series number of this strand examined in SEM work corresponds to strand series number in LM work.
- c Total area is obtained from the total axon area of a strand examined in the section.
- d Axon counts per unit area are obtained from axon counts for the area examined divided by the area examined.
- e There is no surgery performed in the normal control animal but it was sacrificed for comparison with animals of the experiments; there are two fascicles but only one is studied.

**Table 4.12: Area examined, total area, percentage of area examined to total area, category II axon counts for area examined, category II axon counts per unit area, mean category II axon diameter, and extrapolated category II axons counts based on total area in the distal section observed by SEM**

Implant Period & Group	Animal Number	Total Number of Strands Occurred in Middle	Total Number of Fascicle-like Unit in Distal	Fascicle-like Unit Series Number in LM <sup>a</sup>	Area Examined ( $\mu\text{m}^2$ )	Total Area <sup>b</sup> ( $\mu\text{m}^2$ )	Area Examined Relative to Total Area (%)	Axon Counts for Area Examined (#)	Axon Counts Per Unit Area <sup>c</sup> ( $\# / \mu\text{m}^2$ )	Mean Axon Diameter for Area Examined & Standard Deviation ( $\mu\text{m}$ )	Extrapolated Axon Counts Based on Total Area (#)
24 Weeks											
ML	1	2	2	2	10000	19000	53%	18	0.002	2.3 ± 1.3	34
24 Weeks											
ML	2	5	6	3	10000	43000	23%	184	0.018	2.0 ± 0.9	800
24 Weeks											
ML	3	5	5	5	10000	29000	34%	122	0.012	2.1 ± 1.0	359
16 Weeks											
ML	14	7	1	---	9500	287000	3%	52	0.006	1.4 ± 0.5	1733
12 Weeks											
ML	24	7	7	4	10000	33500	30%	0	0	0	0
8 Weeks											
ML	34	1	2	1	10000	40000	25%	68	0.007	2.5 ± 1.0	272
16 Weeks											
Control <sup>d</sup>	19	2	2	1	10000	165500	6%	633	0.004	5.0 ± 2.1	633

ML Multiple-lumen studies.

- a The individual fascicle-like unit series number does not correlate directly from the middle position to the distal position. In addition, the series number of this fascicle-like unit examined in SEM corresponds to the unit series number in LM.
- b Total area is obtained from the axon area of a fascicle-like unit examined in the distal section.
- c Axon counts per unit area are obtained from axon counts for the area examined divided by the area examined.
- d There is no surgery performed in the normal control animal but it was sacrificed for comparison with animals of the experiments; therefore, the distal portion of nerve is considered the same as the middle portion of nerve and the data are taken from one fascicle of the single middle section.

**Table 4.13: Percentage of axons within  $\pm 1 \mu\text{m}$  of the mean axon diameter (LM)**

Implant Periods, Type of Repair & Animal Numbers	Nerve Section	Percentage of Axons in the Frequency Distribution Within $\pm 1 \mu\text{m}$ of the Mean Diameter										
		Scale ( $\mu\text{m}$ )										
		1	1.5	2	2.5	3	3.5	4	4.5	5	5.5	6
24 Weeks, ML #1  #2  #3	Proximal				71							
	Middle			94								
	Distal				87							
	Proximal				77							
	Middle					62						
	Distal				73							
	Proximal						49					
	Middle				87							
	Distal			89								
16 Weeks, ML #34	Proximal					65						
	Middle			93								
	Distal <sup>a</sup>											
12 Weeks, ML #24	Proximal			95								
	Middle				74							
	Distal						63					
8 Weeks, ML #34	Proximal <sup>a</sup>											
	Middle						68					
	Distal							62				
16 Weeks, NC #19	Middle								45			

a The data are not available.

ML The specimen is taken from the multiple-lumen cuff nerve repair.

NC The specimen is taken from the normal control animal.

**Table 4.14: Percentage of axons within  $\pm 1 \mu\text{m}$  of the mean axon diameter for category I axons (SEM)**

Implant Periods, Type of Repair & Animal Numbers	Nerve Section	Percentage of Axons in the Frequency Distribution Within $\pm 1 \mu\text{m}$ of the Mean Diameter										
		Scale ( $\mu\text{m}$ )										
		1	1.5	2	2.5	3	3.5	4	4.5	5	5.5	6
24 Weeks, ML #1 #2 #3	Proximal					71						
	Middle				77							
	Distal					87						
	Proximal					76						
	Middle				69							
	Distal				75							
	Proximal						74					
	Middle				84							
	Distal				80							
16 Weeks, ML #14	Proximal					78						
	Middle				76							
	Distal					62						
12 Weeks, ML #24	Proximal				97							
	Middle				70							
	Distal							60				
8 Weeks, ML #34	Proximal								59			
	Middle					87						
	Distal						73					
16 Weeks, NC #19	Middle							48				

ML The specimen is taken the from multiple-lumen cuff nerve repair.

NC The specimen is taken from the normal control animal.

**Table 4.15: Percentage of axons within  $\pm 1 \mu\text{m}$  of the mean diameter for category II axons (SEM)**

Implant Periods, Type of Repair & Animal Numbers	Nerve Section	Percentage of Axons in the Frequency Distribution Within $\pm 1 \mu\text{m}$ of the Mean Diameter										
		Scale ( $\mu\text{m}$ )										
		1	1.5	2	2.5	3	3.5	4	4.5	5	5.5	6
24 Weeks, ML #1  #2  #3	Proximal				78							
	Middle			95								
	Distal				50							
	Proximal				82							
	Middle				88							
	Distal			93								
	Proximal						57					
	Middle			91								
	Distal			93								
16 Weeks, ML #14	Proximal			90								
	Middle			95								
	Distal			100								
12 Weeks, ML #24	Proximal			93								
	Middle			98								
	Distal <sup>a</sup>											
8 Weeks, ML #34	Proximal				96							
	Middle				79							
	Distal				84							
16 Weeks, NC #19	Middle								42			

a There are no category II axon data available for this section.

ML The specimen is taken from the multiple-lumen cuff nerve repair.

NC The specimen is taken from the normal control animal.

**Table 4.16: Percentage of axons within  $\pm 1 \mu\text{m}$  of mean diameter for all axons (Category I plus Category II; SEM)**

Implant Periods, Type of Repair & Animal Numbers	Nerve Section	Percentage of Axons in the Frequency Distribution Within $\pm 1 \mu\text{m}$ of the Mean Diameter										
		Scale ( $\mu\text{m}$ )										
		1	1.5	2	2.5	3	3.5	4	4.5	5	5.5	6
24 Weeks, ML #1	Proximal					58						
	Middle				76							
	Distal					82						
#2	Proximal				80							
	Middle				79							
	Distal			85								
#3	Proximal							73				
	Middle				85							
	Distal			85								
16 Weeks, ML #14	Proximal				79							
	Middle				75							
	Distal				65							
12 Weeks, ML #24	Proximal			95								
	Middle			90								
	Distal							60				
8 Weeks, ML #34	Proximal							53				
	Middle					80						
	Distal					71						
16 Weeks, NC #19	Middle							49				

ML The specimen is taken from the multiple-lumen cuff nerve repair.  
 NC The specimen is taken from the normal control animal.

**Table 4.17: Diameter ratios and predicted differences of measurements for total axons (LM)**

Implant Periods & Type of Repair	Animal Number	Diameter Ratio $\pm$ Standard Deviation <sup>a</sup>			Diameter Differences Between Methods <sup>b</sup> (%)		
		P	M	D	P	M	D
<b>24 Weeks</b>							
Multiple Lumen	1	2.0 $\pm$ 1.0	1.8 $\pm$ 0.6	2.1 $\pm$ 1.2	7 (+)	4 (+)	6 (+)
	2	2.0 $\pm$ 1.5	2.0 $\pm$ 1.3	1.8 $\pm$ 1.0	6 (+)	3 (+)	5 (+)
	3	1.8 $\pm$ 0.8	1.5 $\pm$ 0.5	1.4 $\pm$ 0.4	4 (+)	3 (+)	5 (+)
<b>16 Weeks</b>							
Multiple Lumen	14	1.8 $\pm$ 0.9	1.6 $\pm$ 0.6	N/A <sup>d</sup>	5 (+)	3 (+)	N/A <sup>d</sup>
<b>12 Weeks</b>							
Multiple Lumen	24	2.1 $\pm$ 1.2	1.8 $\pm$ 0.7	2.5 $\pm$ 1.3	7 (+)	4 (+)	9 (+)
<b>8 Weeks</b>							
Multiple Lumen	34	N/A <sup>d</sup>	1.7 $\pm$ 0.8	2.0 $\pm$ 1.7	N/A <sup>d</sup>	4 (+)	6 (+)
<b>16 Weeks <sup>c</sup></b>							
Normal Control	19	————	2.7 $\pm$ 1.7	————	——	10 (+)	——

(+) There is a larger mean axon diameter in the present study compared to Daniel's study.

a Diameter ratio = Major Axis  $\div$  Minor Axis.

b Diameter difference between equalized ellipse and equivalent circle methods  
 $= 100\% \times \{ 1 - ( \text{Major Axis} \times \text{Minor Axis} )^{0.5} \div [ 0.5 \times ( \text{Major Axis} + \text{Minor Axis} ) ] \}$   
Diameter obtained from the equalized ellipse method:  $0.5 \times ( \text{Major Axis} + \text{Minor Axis} )$   
Diameter obtained from the equivalent circle method:  $( \text{Major Axis} \times \text{Minor Axis} )^{0.5}$

c The data base is only for the middle section axons.

d The data are not available.

P The data are obtained from the **proximal** section.

M The data are obtained from area examined of the observed cable of the **middle** section.

D The data are obtained from area examined of the observed fascicle-like unit of the **distal** section.



**Table 4.18: Diameter ratios and predicted differences of measurements for category I axons (SEM)**

Implant Periods & Type of Repair	Animal Number	Diameter Ratio $\pm$ Standard Deviation <sup>a</sup>			Diameter Differences Between Methods <sup>b</sup> (%)		
		P	M	D	P	M	D
<b>24 Weeks</b>							
Multiple Lumen	1	2.0 $\pm$ 0.9	1.8 $\pm$ 0.8	1.9 $\pm$ 0.8	6 (+)	5 (+)	5 (+)
	2	2.0 $\pm$ 0.9	2.0 $\pm$ 1.1	1.6 $\pm$ 0.6	6 (+)	6 (+)	3 (+)
	3	1.5 $\pm$ 0.6	1.6 $\pm$ 0.3	1.6 $\pm$ 0.7	2 (+)	3 (+)	4 (+)
<b>16 Weeks</b>							
Multiple Lumen	14	1.6 $\pm$ 0.6	1.6 $\pm$ 0.6	1.8 $\pm$ 0.8	3 (+)	3 (+)	4 (+)
<b>12 Weeks</b>							
Multiple Lumen	24	1.5 $\pm$ 0.4	1.7 $\pm$ 0.6	2.0 $\pm$ 0.8	3 (+)	4 (+)	6 (+)
<b>8 Weeks</b>							
Multiple Lumen	34	1.7 $\pm$ 0.7	1.7 $\pm$ 0.7	1.7 $\pm$ 0.9	4 (+)	4 (+)	4 (+)
<b>16 Weeks <sup>c</sup></b>							
Normal Control	19	————	2.6 $\pm$ 1.7	————	————	9 (+)	————

(+) There is a larger mean axon diameter in the present study compared to Daniel's study.

a Diameter ratio = Major Axis  $\div$  Minor Axis.

b Diameter difference between equalized ellipse and equivalent circle methods

$$= 100\% \times \{ 1 - ( \text{Major Axis} \times \text{Minor Axis} )^{0.5} \div [ 0.5 \times ( \text{Major Axis} + \text{Minor Axis} ) ] \}$$

Diameter obtained from the equalized ellipse method:  $0.5 \times ( \text{Major Axis} + \text{Minor Axis} )$

Diameter obtained from the equivalent circle method:  $( \text{Major Axis} \times \text{Minor Axis} )^{0.5}$

c The data base is for the middle section axons.

P The data are obtained from the **proximal** section.

M The data are obtained from area examined of the observed cable of the **middle** section.

D The data are obtained from area examined of the observed fascicle-like unit of the **distal** section.

**Table 4.19: Diameter ratios and predicted differences of measurements for category II axons (SEM)**

Implant Periods & Type of Repair	Animal Number	Diameter Ratio $\pm$ Standard Deviation <sup>a</sup>			Diameter Differences Between Methods <sup>b</sup> (%)		
		P	M	D	P	M	D
<b>24 Weeks</b>							
Multiple Lumen	1	1.7 $\pm$ 0.7	1.4 $\pm$ 0.4	1.9 $\pm$ 0.9	4 (+)	2 (+)	5 (+)
	2	1.7 $\pm$ 0.7	1.6 $\pm$ 1.0	1.5 $\pm$ 0.5	4 (+)	3 (+)	3 (+)
	3	1.5 $\pm$ 0.6	1.4 $\pm$ 0.3	1.5 $\pm$ 0.4	2 (+)	4 (+)	2 (+)
<b>16 Weeks</b>							
Multiple Lumen	14	1.5 $\pm$ 0.4	1.5 $\pm$ 0.5	1.7 $\pm$ 0.7	2 (+)	3 (+)	3 (+)
<b>12 Weeks</b>							
Multiple Lumen	24	1.6 $\pm$ 0.7	1.9 $\pm$ 0.8	2.0 $\pm$ 0.8	3 (+)	6 (+)	6 (+)
<b>8 Weeks</b>							
Multiple Lumen	34	1.5 $\pm$ 0.5	1.5 $\pm$ 0.5	1.6 $\pm$ 0.6	3 (+)	3 (+)	3 (+)
<b>16 Weeks <sup>c</sup></b>							
Normal Control	19	————	2.4 $\pm$ 1.5	————	——	9 (+)	——

(+) There is a larger mean axon diameter in the present study compared to Daniel's study.

a Diameter ratio = Major Axis  $\div$  Minor Axis.

b Diameter difference between equalized ellipse and equivalent circle methods

$$= 100\% \times \{ 1 - (\text{Major Axis} \times \text{Minor Axis})^{0.5} \div [ 0.5 \times (\text{Major Axis} + \text{Minor Axis}) ] \}$$

Diameter obtained from the equalized ellipse method:  $0.5 \times (\text{Major Axis} + \text{Minor Axis})$

Diameter obtained from the equivalent circle method:  $(\text{Major Axis} \times \text{Minor Axis})^{0.5}$

c The data base is for the middle section axons.

P The data are obtained from the **proximal** section.

M The data are obtained from area examined of the observed cable of the **middle** section.

D The data are obtained from area examined of the observed fascicle-like unit of the **distal** section.

**Table 4.20: Diameter ratios and predicted differences of measurements for total axons (SEM)**

Implant Periods & Type of Repair	Animal Number	Diameter Ratio $\pm$ Standard Deviation <sup>a</sup>			Diameter Differences Between Methods <sup>b</sup> (%)		
		P	M	D	P	M	D
24 Weeks							
Multiple Lumen	1	2.0 $\pm$ 0.9	1.6 $\pm$ 0.7	1.9 $\pm$ 0.8	6 (+)	4 (+)	5 (+)
	2	1.8 $\pm$ 1.0	1.8 $\pm$ 1.0	1.5 $\pm$ 0.5	5 (+)	4 (+)	3 (+)
	3	1.5 $\pm$ 0.6	1.5 $\pm$ 0.5	1.6 $\pm$ 0.6	2 (+)	2 (+)	3 (+)
16 Weeks							
Multiple Lumen	14	1.5 $\pm$ 0.5	1.6 $\pm$ 0.6	1.7 $\pm$ 0.7	3 (+)	3 (+)	4 (+)
12 Weeks							
Multiple Lumen	24	1.6 $\pm$ 0.7	1.8 $\pm$ 0.7	2.0 $\pm$ 0.8	3 (+)	5 (+)	6 (+)
8 Weeks							
Multiple Lumen	34	1.5 $\pm$ 0.6	1.5 $\pm$ 0.4	1.7 $\pm$ 0.8	3 (+)	3 (+)	4 (+)
16 Weeks <sup>c</sup>							
Normal Control	19	————	2.6 $\pm$ 1.7	————	——	9 (+)	——

(+) There is a larger mean axon diameter in the present study compared to Daniel's study.

a Diameter ratio = Major Axis  $\div$  Minor Axis.

b Diameter difference between equalized ellipse and equivalent circle methods  
 $= 100\% \times \{ 1 - ( \text{Major Axis} \times \text{Minor Axis} )^{0.5} \div [ 0.5 \times ( \text{Major Axis} + \text{Minor Axis} ) ] \}$   
 Diameter obtained from the equalized ellipse method:  $0.5 \times ( \text{Major Axis} + \text{Minor Axis} )$   
 Diameter obtained from the equivalent circle method:  $( \text{Major Axis} \times \text{Minor Axis} )^{0.5}$

c The data base is for the middle section axons.

P The data are obtained from the **proximal** section.

M The data are obtained from area examined of the observed cable of the **middle** section.

D The data are obtained from area examined of the observed fascicle-like unit of the **distal** section.

**Table 4.21: Mean axon diameter comparisons between LM and SEM studies in the same nerve section**

Animal Number	Type of Repair	Periods	Section Comparisons	Significance
1	Mutiple-Lumen	24 Weeks Implantation	P	*** (p<0.0001) (-)
			M	*** (p<0.0014) (-)
			D	*** (p<0.0021) (-)
2	Mutiple-Lumen	24 Weeks Implantation	P	*** (p<0.0002) (-)
			M	*** (p<0.0001) (+)
			D	*
3	Mutiple-Lumen	24 Weeks Implantation	P	*
			M	*
			D	*
14	Mutiple-Lumen	16 Weeks Implantation	P	*** (p<0.0001) (+)
			M	*** (p<0.0001) (-)
			D	N/A <sup>a</sup>
24	Mutiple-Lumen	12 Weeks Implantation	P	*
			M	*** (p<0.0001) (+)
			D	*
34	Mutiple-Lumen	8 Weeks Implantation	P	N/A <sup>a</sup>
			M	*** (p<0.0001) (+)
			D	*** (p<0.0001) (+)
19	Normal Control	16 Weeks <sup>b</sup>	M	*

P The data are obtained from the **proximal** section.

M The data are obtained from area examined of the observed cable in the **middle** section.

D The data are obtained from area examined of the observed fascicle-like unit in the **distal** section.

\*\*\* Comparison is significant at  $\alpha$  value of the 0.05 level.

\* Comparison is not significant at  $\alpha$  value of the 0.05 level.

(+) There is a larger mean axon diameter in LM.

(-) There is a larger mean axon diameter in SEM.

a The data are not available due to unsatisfactory sample preparation.

b The normal control animal (no surgery during the 16 week period) was sacrificed for comparison with animals of the experiments.

**Table 4.22: Mean axon diameter comparisons between repaired nerve sections and normal control (LM)**

Animal Number	Type of Repair	Implantation Periods	Section Comparisons <sup>a</sup>	Significance
1	Multiple-Lumen	24 Weeks	P	*** (p<0.0001) (+)
			M	*** (p<0.0001) (+)
			D	*** (p<0.0001) (+)
2	Multiple-Lumen	24 Weeks	P	*** (p<0.0001) (+)
			M	*** (p<0.0001) (+)
			D	*** (p<0.0001) (+)
3	Multiple-Lumen	24 Weeks	P	*** (p<0.0001) (+)
			M	*** (p<0.0001) (+)
			D	*** (p<0.0001) (+)
14	Multiple-Lumen	16 Weeks	P	*** (p<0.0001) (+)
			M	*** (p<0.0001) (+)
			D	N/A <sup>b</sup>
24	Multiple-Lumen	12 Weeks	P	*** (p<0.0001) (+)
			M	*** (p<0.0001) (+)
			D	*** (p<0.0001) (+)
34	Multiple-Lumen	8 Weeks	P	N/A <sup>b</sup>
			M	*** (p<0.0001) (+)
			D	*** (p<0.0001) (+)

P The data are obtained from the **proximal** section.

M The data are obtained from area examined of the observed strand in the **middle** section.

D The data are obtained from area examined of the observed fascicle-like unit in the **distal** section.

\*\*\* Comparison is significant at  $\alpha$  value of the 0.05 level.

(+) There is a larger mean axon diameter in normal control.

a The mean diameter of the section is compared to that of the normal control.

b The data are not available due to unsatisfactory sample preparation.

**Table 4.23: Mean axon diameter comparisons between nerve sections in the same animal (LM)**

Animal Number	Type of Repair	Implant Periods	Section Comparisons	Significance
1	Multiple-Lumen	24 Weeks	P, M	*** (p<0.0001) (+)
			P, D	*
			M, D	*** (p<0.0001) (-)
2	Multiple-Lumen	24 Weeks	P, M	*** (p<0.0001) (-)
			P, D	*
			M, D	*** (p<0.0001) (+)
3	Multiple-Lumen	24 Weeks	P, M	*** (p<0.001) (+)
			P, D	*** (p<0.001) (+)
			M, D	*** (p<0.001) (+)
14	Multiple-Lumen	16 Weeks	P, M	*** (p<0.0001) (+)
			P, D	N/A <sup>a</sup>
			M, D	N/A <sup>a</sup>
24	Multiple-Lumen	12 Weeks	P, M	*** (p<0.0001) (-)
			P, D	*** (p<0.0001) (-)
			M, D	*** (p<0.0001) (-)
34	Multiple-Lumen	8 Weeks	P, M	N/A <sup>a</sup>
			P, D	N/A <sup>a</sup>
			M, D	*** (p<0.0001) (-)

P The data are obtained from the **proximal** section.

M The data are obtained from area examined of the observed strand in the **middle** section.

D The data are obtained from area examined of the observed fascicle-like unit in the **distal** section.

\*\*\* Comparison is significant at  $\alpha$  value of the 0.05 level.

\* Comparison is not significant at  $\alpha$  value of the 0.05 level.

(+) There is a larger mean axon diameter in the first nerve section.

(-) There is a larger mean axon diameter in the second nerve section.

a The data are not available due to unsatisfactory sample preparation.

**Table 4.24: Mean axon diameter comparisons between repaired nerve sections and normal control (SEM)**

Animal Number	Type of Repair	Implant Periods	Section Comparisons <sup>a</sup>	Significance
1	Multiple-Lumen	24 Weeks	P	*** (p<0.0001) (+)
			M	*** (p<0.0001) (+)
			D	*** (p<0.0001) (+)
2	Multiple-Lumen	24 Weeks	P	*** (p<0.0001) (+)
			M	*** (p<0.0001) (+)
			D	*** (p<0.0001) (+)
3	Multiple-Lumen	24 Weeks	P	*** (p<0.0001) (+)
			M	*** (p<0.0001) (+)
			D	*** (p<0.0001) (+)
14	Multiple-Lumen	16 Weeks	P	*** (p<0.0001) (+)
			M	*** (p<0.0001) (+)
			D	*** (p<0.0001) (+)
24	Multiple-Lumen	12 Weeks	P	*** (p<0.0001) (+)
			M	*** (p<0.0001) (+)
			D	*
34	Multiple-Lumen	8 Weeks	P	*
			M	*** (p<0.0001) (+)
			D	*** (p<0.0001) (+)

P The data are obtained from the **proximal** section.

M The data are obtained from area examined of the observed strand in the **middle** section.

D The data are obtained from area examined of the observed fascicle-like unit in the **distal** section.

\*\*\* Comparison is significant at  $\alpha$  value of the 0.05 level.

\* Comparison is not significant at  $\alpha$  value of the 0.05 level.

(+) There is a larger mean axon diameter in normal control.

<sup>a</sup> The data of the section are compared with that of the normal control.

**Table 4.25: Mean diameter comparisons of the same category axons between repaired nerve sections and normal control (SEM)**

Animal Number	Type of Repair	Implant Periods	Nerve Sections <sup>a</sup>	Axon Comparisons	Significance
1	Multiple-Lumen	24 Weeks	P	C	*** (p<0.0002) (+)
			P	PA	*** (p<0.0001) (+)
			M	C	*** (p<0.0001) (+)
			M	PA	*** (p<0.0001) (+)
			D	C	*** (p<0.0008) (+)
			D	PA	*** (p<0.0001) (+)
2	Multiple-Lumen	24 Weeks	P	C	*** (p<0.0001) (+)
			P	PA	*** (p<0.0001) (+)
			M	C	*** (p<0.0001) (+)
			M	PA	*** (p<0.0001) (+)
			D	C	*** (p<0.0001) (+)
			D	PA	*** (p<0.0001) (+)
3	Multiple-Lumen	24 Weeks	P	C	*
			P	PA	*** (p<0.0001) (+)
			M	C	*** (p<0.0001) (+)
			M	PA	*** (p<0.0001) (+)
			D	C	*** (p<0.0001) (+)
			D	PA	*** (p<0.0001) (+)

P The data are obtained from the **proximal** section.

M The data are obtained from area examined of the observed strand in the **middle** section.

D The data are obtained from area examined of the observed fascicle-like unit in the **distal** section.

C The data are obtained from **uniformly stained** (category I) axons.

PA The data are obtained from **non-uniformly stained** (category II) axons.

\*\*\* Comparison is significant at  $\alpha$  value of the 0.05 level.

\* Comparison is not significant at  $\alpha$  value of the 0.05 level.

a The mean diameter of the nerve section is compared with that of the normal control.

(+) There is a larger mean axon diameter in normal control.

(-) There is a smaller mean axon diameter in normal control.



**Table 4.25: Continued**

Animal Number	Type of Repair	Implant Periods	Nerve Section <sup>a</sup>	Axon Comparisons	Significance
14	Multiple-Lumen	16 Weeks	P	C	*** (p<0.0001) (+)
			P	PA	*** (p<0.0001) (+)
			M	C	*** (p<0.0001) (+)
			M	PA	*** (p<0.0001) (+)
			D	C	*** (p<0.0008) (+)
			D	PA	*** (p<0.0001) (+)
24	Multiple-Lumen	12 Weeks	P	C	*** (p<0.0001) (+)
			P	PA	*** (p<0.0001) (+)
			M	C	*** (p<0.0001) (+)
			M	PA	*** (p<0.0001) (+)
			D	C	*
			D	PA	*** (p<0.0001) (+)
34	Multiple-Lumen	8 Weeks	P	C	*** (p<0.0445) (-)
			P	PA	*** (p<0.0001) (+)
			M	C	*** (p<0.0001) (+)
			M	PA	*** (p<0.0001) (+)
			D	C	*** (p<0.0147) (+)
			D	PA	*** (p<0.0001) (+)

P The data are obtained from the **proximal** section.

M The data are obtained from area examined of the observed strand in the **middle** section.

D The data are obtained from area examined of the observed fascicle-like unit in the **distal** section.

C The data are obtained from **uniformly stained** (category I) axons.

PA The data are obtained from **non-uniformly stained** (category II) axons.

\*\*\* Comparison is significant at  $\alpha$  value of the 0.05 level.

\* Comparison is not significant at  $\alpha$  value of the 0.05 level.

(+) There is a larger mean axon diameter in normal control.

(-) There is a smaller mean axon diameter in normal control.

**Table 4.26: Diameter comparisons between category I and category II stained axons in the same nerve section (SEM)**

Animal Number	Type of Repair	Periods	Nerve Section	Significance
1	Multiple-Lumen	24 Weeks Implantation	P	*
			M	*** (p<0.0001) (-)
			D	*** (p<0.0001) (-)
2	Multiple-Lumen	24 Weeks Implantation	P	*
			M	*
			D	*** (p<0.0001) (-)
3	Multiple-Lumen	24 Weeks Implantation	P	*
			M	*** (p<0.0005) (-)
			D	*
14	Multiple-Lumen	16 Weeks Implantation	P	*** (p<0.0001) (-)
			M	*** (p<0.0001) (-)
			D	*** (p<0.0001) (-)
24	Multiple-Lumen	12 Weeks Implantation	P	*
			M	*** (p<0.0474) (-)
			D	*** (p<0.0001) (-)
34	Multiple-Lumen	8 Weeks Implantation	P	*** (p<0.0001) (-)
			M	*** (p<0.0001) (-)
			D	*** (p<0.0001) (-)
19	Normal Control	16 Weeks <sup>a</sup>	M	*** (p<0.0001) (+)

P The data are obtained from the **proximal** section.

M The data are obtained from area examined of the observed strand in the **middle** section.

D The data are obtained from area examined of the observed fascicle-like unit in the **distal** section.

\*\*\* Comparison is significant at  $\alpha$  value of the 0.05 level.

\* Comparison is not significant at  $\alpha$  value of the 0.05 level.

(-) There is a larger mean axon diameter in category I (uniformly stained) axons.

(+) There is a larger mean axon diameter in category II (non-uniformly stained) axons.

a The normal control animal (no surgery during the 16 week period) was sacrificed for comparison with animals of the experiments.

**Table 4.27: Mean diameter comparisons of the same category of axons in different nerve sections (SEM)**

Animal Number	Type of Repair	Implant Periods	Section Comparisons	Axon Type	Significance
1	Multiple-Lumen	24 Weeks	P, M	C	*** (p<0.0182) (+)
			P, M	PA	*** (p<0.0001) (+)
			P, D	C	*
			P, D	PA	*
			M, D	C	*** (p<0.0182) (-)
			M, D	PA	*
2	Multiple-Lumen	24 Weeks	P, M	C	*
			P, M	PA	*
			P, D	C	*** (p<0.0179) (+)
			P, D	PA	*** (p<0.0001) (+)
			M, D	C	*
			M, D	PA	*** (p<0.0001) (+)
3	Multiple-Lumen	24 Weeks	P, M	C	*** (p<0.0001) (+)
			P, M	PA	*** (p<0.0001) (+)
			P, D	C	*** (p<0.0001) (+)
			P, D	PA	*** (p<0.0001) (+)
			M, D	C	*
			M, D	PA	*

P The data are obtained from the **proximal** section.

M The data are obtained from area examined of the observed strand in the **middle** section.

D The data are obtained from area examined of the observed fascicle-like unit in the **distal** section.

C The data are obtained from **uniformly stained** (category I) axons.

PA The data are obtained from **non-uniformly stained** (category II) axons.

\*\*\* Comparison is significant at  $\alpha$  value of the 0.05 level.

\* Comparison is not significant at  $\alpha$  value of the 0.05 level.

(+) There is a larger mean axon diameters in the first nerve section.

(-) There is a larger mean axon diameters in the second nerve section.

**Table 4.27: Continued**

Animal Number	Type of Repair	Implant Periods	Nerve Section	Axon Comparisons	Significance
14	Multiple-Lumen	16 Weeks	P, M	C	*
			P, M	PA	*** (p<0.0001) (+)
			P, D	C	*
			P, D	PA	*** (p<0.0001) (+)
			M, D	C	*** (p<0.0173) (-)
			M, D	PA	*** (p<0.0001) (+)
24	Multiple-Lumen	12 Weeks	P, M	C	*
			P, M	PA	*
			P, D	C	*** (p<0.0001) (-)
			P, D	PA	*** (p<0.0001) (+)
			M, D	C	*** (p<0.0001) (-)
			M, D	PA	*** (p<0.0001) (+)
34	Multiple-Lumen	8 Weeks	P, M	C	*** (p<0.0001) (+)
			P, M	PA	*
			P, D	C	*** (p<0.0001) (+)
			P, D	PA	*
			M, D	C	*
			M, D	PA	*

P The data are obtained from the **proximal** section.

M The data are obtained from area examined of the observed strand in the **middle** section.

D The data are obtained from area examined of the observed fascicle-like unit in the **distal** section.

C The data are obtained from **uniformly stained** (category I) axons.

PA The data are obtained from **non-uniformly stained** (category II) axons.

\*\*\* Comparison is significant at  $\alpha$  value of the 0.05 level.

\* Comparison is not significant at  $\alpha$  value of the 0.05 level.

(+) There is a larger mean axon diameters in the first nerve section.

(-) There is a larger mean axon diameters in the second nerve section.

**Table 4.28: Mean diameter comparisons of total stained axons between nerve sections in the same animal (SEM)**

Animal Number	Type of Repair	Implant Periods	Section Comparisons	Significance
1	Multiple-Lumen	24 Weeks	P, M	*** (p<0.0001) (+)
			P, D	*
			M, D	*** (p<0.0001) (-)
2	Multiple-Lumen	24 Weeks	P, M	*** (p<0.0001) (+)
			P, D	*** (p<0.0001) (+)
			M, D	*** (p<0.0001) (+)
3	Multiple-Lumen	24 Weeks	P, M	*** (p<0.0001) (+)
			P, D	*** (p<0.0001) (+)
			M, D	*
14	Multiple-Lumen	16 Weeks	P, M	*** (p<0.0036) (+)
			P, D	*
			M, D	*** (p<0.0036) (-)
24	Multiple-Lumen	12 Weeks	P, M	*
			P, D	*** (p<0.0001) (-)
			M, D	*** (p<0.0001) (-)
34	Multiple-Lumen	8 Weeks	P, M	*** (p<0.0001) (+)
			P, D	*** (p<0.0001) (+)
			M, D	*

P The data are obtained from the **proximal** section.

M The data are obtained from area examined of the observed strand in the **middle** section.

D The data are obtained from area examined of the observed fascicle-like unit in the **distal** section.

\*\*\* Comparison is significant at  $\alpha$  value of the 0.05 level.

\* Comparison is not significant at  $\alpha$  value of the 0.05 level.

(+) There is a larger mean axon diameter in the first nerve section.

(-) There is a larger mean axon diameter in the second nerve section.

## 5. DISCUSSION

The goal of the nerve cuff application is to re-establish physical continuity of the impaired nervous tissue. The results of the backscattered electron image and light micrographs indicate that the multiple lumen nerve cuff indeed serves as a conduit for a regenerating nerve as based on the presence of Bodian's silver stained axons seen in the proximal, middle (the repair site), and distal sections. The pattern of the middle section is determined by the arrangement of the openings of the multiple lumen cuff. This pattern carries over to the distal section as the axons maintain circular fascicle-like patterns in the distal stumps. The two-zone reorganization seen is similar to single-lumen cases observed by Jenq and Coggeshall (1986), Lundborg et al. (1982a), Madison et al. (1988), Seckel et al. (1984), Williams and Varon (1985), and Williams et al. (1983, 1984). To supply the nutrition required by Schwann cells during nerve regeneration, a large number of blood capillaries appear in each of the two zones (Jenq and Coggeshall, 1986; Seckel et al., 1984). The middle section axons of each lumen merge into one large central axon matrix where perineurial connective tissue confines neuron elements within mini-fascicles. Similar phenomena are also reported for single lumen cases by Jenq and Coggeshall (1986), Lundborg et al. (1981), and Mathur et al. (1983) and for a surgical repair by Orgel and Huser (1980).

BSE images present atomic number contrast which clearly reveals the Bodian stained axon features as some investigators suggested (Taylor et al., 1984; Ushiki and Fujita, 1986; Von Langsdorff et al., 1990). In addition, Bodian silver stain has a high and specific affinity for neurofilament proteins. Because of the higher resolution available in the scanning electron microscope compared with the light microscope, these stained axons can be further subdivided into two staining categories. In addition to the apparent non-uniformity of the staining, some cross sections provide evidence of artifacts caused by the sectioning of the nerve.

The fiber diameter frequency distribution displayed a much broader axon diameter range in the control animal compared to those for the experiments. This is also seen by Fields and Ellisman (1986b) and Rosen et al. (1983, 1992) for single lumen examples. Multiple-lumen cuff experiments exhibit size frequencies for the axons which are skewed toward the larger diameter ranges. Even with increasing time, the fiber diameter spectra show that over 60% of the axon diameters are grouped into a narrow diameter range within  $\pm 1 \mu\text{m}$  of mean diameter.

As also reported by Fields and Ellisman (1986b), Henry et al. (1985), Le Beau et al. (1988b) and Rosen et al. (1983, 1989) for single lumen cases, it was found that the mean diameters of the regenerated axons in multiple lumen cases never reach those of a normal control. Although the regenerated axons do not pack as tightly as the normal controls do, their smaller axon diameter without regenerated myelin or with thinner regenerated myelin might result in the higher axon counts per unit area. In most cases, axon counts per unit area of the category I axons are higher than that of those category II axons in the same area probably due to better staining uniformity.

Because the proximal section still maintains its continuity with the trophic center of the neuron, the extrapolated number of axon counts in the proximal section are the highest among the three sections (proximal, middle, and distal). Other sources of influence on relative numbers of axons include branching, compressive forces associated with the tube, and the relative time of the implantation. Therefore, the comparison results of the extrapolated number of axons between the middle section and distal section might be mixed. Similarly, these factors are probably present in the axon counts per unit area data. Even though all of the multiple lumen tubes of a cuff are in the same implantation condition, strand-to-strand or fascicle-like unit-to-unit variations are seen.

Williams et al. (1984) reported that four stages of the regeneration are critical for success: (1) the chamber must fill with fluid; (2) a fibrin matrix must form; (3) non-neuronal

cells must populate and replace the matrix; and (4) the cells must possess properties supportive of axonal elongation. In addition, Lundborg et al. (1982c) proved that the fluids exuding from nerve stumps and collected in *in vivo* chambers contain trophic factors. Thus, if saline solution is present at the beginning of the implantation, this would allow immediate diffusion of the stump exudates and therefore provide an environment for a more uniform initial fibrin gel formation as part of the formative stages leading to the bridging of the gap by a strand. However, the amounts of fibrin and related trophic substances contributed to a chamber are finite. The initial dilution imposed by saline prefilling of a relatively large chamber would exceed the acceptable limits for an effective progression of the regeneration. Transected nerves repaired by using multiple-lumen cuffs with relatively small chamber prefilled with saline solution regenerate with better organization, with more nerve strands regenerating through repair sites, and with a rich vascularization occurring at a shorter post-implantation period (16 weeks) than those without saline prefilling (24 weeks). The regenerated blood vessels appear to be larger than those seen in the normal nerve sections (also reported by Jenq and Coggeshall (1986)) for single lumen cases. They are of vital importance for preserving Schwann cells.

The diameter axis ratios results are larger than 1.0. This indicates that the shape of most axons of the cross section studied are not circular. Smaller diameter ratios obtained from regenerated axons compared with those obtained from the normal animal also indicate that the shape of regenerated axons still does not recover to that shape of the normal control animal axons. There is less than a 10% diameter difference obtained between the equivalent circle diameter method and the equalized ellipse figure based on the same area. This estimation agrees with Duncan's work (1934).



## 6. CONCLUSION

The microstructural results show that this multiple-lumen silicone rubber cuff has potential. The pattern of regenerated nerve strands indicates that their orientation and organization are determined by the arrangement of the opening of the multiple lumens in the middle section.

Even with increasing time, the mean diameters of regenerated axons in multiple-lumen cases do not recover to that seen for a normal control animal. In addition, the regenerated axon diameter spectra are grouped to smaller diameter ranges and are skewed toward a larger diameter range.

BSE images display atomic number contrast which clearly reveals the axon features stained with Bodian's silver stain. With higher resolution, SEM provides some advantages for interpretation of nerve regeneration due to the relatively higher level of magnification compared with LM. The difference between those results obtained from LM and those obtained from SEM suggests that more axons need to be examined in the same section for comparisons. This may be a disadvantage because of higher costs of SEM characterization work.

The intrachamber environment can be modified by saline prefilling. In this regard, different time periods of study might provide additional useful information about the development of regenerating nerves. With the multiple-lumen design, different neurotrophic stimulus agents might be copolymerized with or injected into the individual lumens of the ML cuff to enhance nerve regeneration. Also, this study shows strand or fascicle-like unit variance within an individual animal.

## BIBLIOGRAPHY

- Aebischer, P., V. Guénard, S. R. Winn, R. F. Valentini, and P. M. Galletti. 1988. Blind-ended semipermeable guidance channels support peripheral nerve regeneration in the absence of a distal nerve stump. *Brain Research* 454: 179-187.
- Aebischer, P., V. Guénard, and S. Brace. 1989a. Peripheral nerve regeneration through blind-ended semipermeable guidance channels: Effect of the molecular weight cutoff. *J. of Neuroscience* 9 (10): 3590-3595.
- Aebischer, P., A. N. Salessiotis, and S. R. Winn. 1989b. Basic fibroblast growth factor released from synthetic guidance channels facilitates peripheral nerve regeneration across long nerve gaps. *J. of Neuroscience Research* 23: 282-289.
- Aguayo, A. J., R. P. Bunge, I. D. Duncan, P. M. Wood, and G. M. Bray. 1979. Rat Schwann cells, cultured in vitro, can ensheath axons regenerating in mouse nerve. *Neurology* 29:589.
- Allt, G. 1976. Pathology of the peripheral nerve. Pages 666-739. in D. N. Landon, editor. *The Peripheral Nerve*. John Willey & Sons, Inc., New York.
- Bassett, C. A. L., J. B. Campbell, and J. Husby. 1959. Peripheral nerve and spinal cord regeneration : Factors leading to success of a tubulation technique employing Millipore. *Experimental Neurology* 1: 386-406.
- Braley, S. 1970. The chemistry and properties of the medical-grade silicones. *J. of Macromolecular Science-Chemistry* A4(3): 529-544.
- Chiu, D. T. W., I. Janecka, T. J. Krizek, M. Wolff, and R. E. Lovelace. 1982. Autogenous vein graft as a conduit for nerve regeneration. *Surgery* 91(2): 226-233.
- Chiu, D. T. W., R. E. Lovelace, L. T. Yu, M. Wolff, S. Stengel, L. Middleton, I. P. Janecka, and T. J. Krizek. 1988. Comparative electrophysiologic evaluation of nerve grafts and autogenous vein grafts as nerve conduits: An experimental study. *J. of Reconstructive Microsurgery* 4(4): 303-309.
- Cuadros, C. L. and C. E. Granatir. 1987. Nerve regeneration through a synthetic microporous tube (expanded polytetrafluoroethylene): Experimental study in the sciatic nerve of the rat. *Microsurgery* 8: 41-46.

- Daniel, J. M. K. 1991. Reorganization and orientation of peripheral nerve fibers regenerating through a multiple-lumen silicone rubber cuff: An experimental study using the sciatic nerve of rats. Doctoral dissertation, Iowa State University, Ames, IA. 152 pages.
- Daniel, R. K. and J. K. Terzis. 1977. Structure and function of the peripheral nerve. Page 299. in *Reconstructive Microsurgery*. Little, Brown and Company, Boston.
- Duncan, D. 1934. A relation between axone diameter and myelination determined by measurement of myelinated spinal root fibers. *J. of Comparative Neurology* 60: 437-471.
- Ducker, T. B. and G. J. Hayes. 1968. Experimental improvements in the use of silastic cuff for peripheral nerve repair. *J. Neurosurgery* 28: 582-587.
- Espejo, F. and J. Alvarez. 1986. Microtubules and calibers in normal and regenerating axons of the sural nerve of the rat. *J. of Comparative Neurology* 250: 65-72.
- Fields, R. D. and M. H. Ellisman. 1986a. Axons regenerated through silicone tube splices I. Conduction properties. *Experimental Neurology* 92: 48-60.
- Fields, R. D. and M. H. Ellisman. 1986b. Axons regenerated through silicone tube splices II. Functional morphology. *Experimental Neurology* 92: 61-74.
- Gartner, L. P. and J. L. Hiatt. 1987. Nervous tissue. Pages 96-112. in *Atlas of Histology*. Williams & Wilkins, Baltimore.
- Gibson, K. L. and J. K. Daniloff. 1989. Comparison of sciatic nerve regeneration through silicone tubes and nerve allografts. *Microsurgery* 10: 126-129.
- Henry, E. W., T. H. Chiu, E. Nyilas, T. M. Brushart, P. Dikkes, and R. L. Sidman. 1985. Nerve regeneration through biodegradable polyester tubes. *Experimental Neurology* 90: 652-676.
- Ide, C., K. Tohyama, R. Yokota, T. Nitatori, and S. Onodera. 1983. Schwann cell basal lamina and nerve regeneration. *Brain Research* 288: 61-75.
- Jenq, C. B. and R. E. Coggeshall. 1985. Numbers of regenerating axons in parent and tributary peripheral nerves in the rat. *Brain Research* 326: 27-40.

- Jenq, C. B. and R. E. Coggeshall. 1986. The effects of an autologous transplant on patterns of regeneration in rat sciatic nerve. *Brain Research* 364: 45-56.
- Junqueira, L. C. and J. Carneiro. 1983. Nerve tissue. Pages 180 and 189. in *Basic Histology*. Forth edition. Lange Medical Publications, Los Altos, CA.
- Katz, M. J. and L. F. Watson. 1985. Intensifier for Bodian staining of tissue sections and cell cultures. *Stain Technology* 60(2): 81-87.
- Kiernan, J. A. 1981. Neurohistological techniques. Pages 256-279. in *Histological & Histochemical Methods : Theory and practice*. First edition. Pergamon Press, New York.
- Kline, D. G. 1988. Comparative electrophysiologic evaluation of nerve grafts and autogenous vein grafts as nerve conduits: An experimental study. *J. of Reconstructive Microsurgery* 4(4): 311-312.
- Kumagai, K., T. Ushiki, K. Tohyama, M. Arakawa, and C. Ide. 1990. Regenerating axons and their growth cones observed by scanning electron microscopy. *J. Electron Microscopy* 39: 108-114.
- Le Beau, J. M., M. LaCorbiere, H. C. Powell, M. H. Ellisman, and D. Schubert. 1988a. Extracellular fluid conditioned during peripheral nerve regeneration stimulates Schwann cell adhesion, migration and proliferation. *Brain Research* 459: 93-104.
- Le Beau, J. M., M. H. Ellisman, and H. C. Powell. 1988b. Ultrastructural and morphometric analysis of long-term peripheral nerve regeneration through silicone tubes. *J. of Neurocytology* 17: 161-172.
- Low, F. N. 1976. The perineurium and connective tissue of peripheral nerve. Pages 159-187. in D. N. Landon, editor. *The Peripheral Nerve*. John Wiley and Sons, Inc., New York.
- Lundborg, G., L. B. Dahlin, N. Danielsen, R. H., Gelberman, F. M. Longo, H. C. Powell, and S. Varon. 1982a. Nerve regeneration in silicone chambers: Influence of gap length and of distal stump components. *Experimental Neurology* 76: 361-375.
- Lundborg, G., R. H. Gelberman, F. M. Longo, H. C. Powell, and S. Varon. 1982b. In vivo regeneration of cut nerves encased in silicone tubes. Growth across a six-millimeter gap. *J. of Neuropathology and Experimental Neurology* 41: 412-422.

- Lundborg, G., F. M. Longo, and S. Varon. 1982c. Nerve regeneration model and trophic factors in vivo. *Brain Research* 232: 157-161.
- Lundborg, G., L. B. Dahlin, N. P. Danielsen, H. A. Hansson, and K. Larsson. 1981. Reorganization and orientation of regenerating nerve fibers, perineurium, and epineurium in preformed mesothelial tubes- An experimental study on the sciatic nerve of rats. *J. of Neuroscience Research* 6: 265-281.
- Madison, R., C. Da Silva, P. Dikkes, T. Chiu, and R. L. Sidman. 1985. Increased rate of peripheral nerve regeneration using bioresorbable nerve guides and laminin-containing gel. *Experimental Neurology* 88: 767-772.
- Madison, R. D., C. Da Silva, and P. Dikkes. 1988. Entubulation repair with protein additives increases the maximum nerve gap distance successfully bridged with tubular prostheses. *Brain Research* 447: 325-334.
- Madison, R. D., C. Da Silva, P. Dikkes, R. L. Sidman, and T. H. Chiu. 1987. Peripheral nerve regeneration with entubulation repair: Comparison of biodegradable nerve guides versus polyethylene tubes and the effects of a laminin-containing gel. *Experimental Neurology* 95: 378-390.
- Marshall, D. M., M. Grosser, M. C. Stephanides, R. D. Keeley, and J. M. Rosen. 1989. Sutureless nerve repair at the fascicular level using a nerve coupler. *J. of Rehabilitation Research and Development* 26(3): 63-76.
- Mathur, A., J. C. Merrell, R. C. Russell, and E. G. Zook. 1983. A scanning electron microscopy evaluation of peripheral nerve regeneration. *Scanning Electron Microscopy* II: 975-981.
- McQuarrie, I. G. 1983. Role of the axonal cytoskeleton in the regenerating nervous system. Pages 51-88. in F. J. Seil, editor. *Nerve, Organ, and Tissue Regeneration: Research Perspectives*. Academic Press, New York.
- Molander, H., O. Engkvist, J. Hägglund, Y. Olsson, and E. Torebjörk. 1983. Nerve repair using a polyglactin tube and nerve graft: An experimental study in the rabbit. *Biomaterials* 4: 276-280.
- Müller, H., L. R. Williams, and S. Varon. 1987. Nerve regeneration chamber: evaluation of exogenous agents applied by multiple injections. *Brain Research* 413: 320-326.

- Orgel, M. G. and J. W. Huser. 1980. A comparison of light and scanning electron microscopy in nerve regeneration studies. *Plastic and Reconstructive Surgery* 65(5): 628-634.
- Park, J. B. 1984. Polymeric implant materials. Pages 265-303. in *Biomaterials Science and Engineering*. Plenum Press, New York.
- Phillips, L. L., L. Autilio-Gambetti, and R. J. Lasek. 1983. Bodian's silver method reveals molecular variation in the evolution of neurofilament proteins. *Brain Research* 278: 219-223.
- Politis, M. J., K. Ederle, and P. S. Spencer. 1982. Tropism in nerve regeneration in vivo. Attraction of regenerating axons by diffusible factors derived from cells in distal nerve stumps of transected peripheral nerves. *Brain Research* 253: 1-12.
- Rosen, J. M., E. N. Kaplan, D. L. Jewett, and J. R. Daniels. 1979. Fascicular sutureless and suture repair of the peripheral nerves. A comparison study in laboratory animals. *Orthopaedic Review* 8(4): 85-92.
- Rosen, J. M., V. R. Hentz, and E. N. Kaplan. 1983. Fascicular tubulization: A cellular approach to peripheral nerve repair. *Annals of Plastic Surgery* 11(5): 397-411.
- Rosen, J. M., H. N. Pham, G. Abraham, L. Harold, and V. R. Hentz. 1989. Artificial nerve graft compared to autograft in a rat model. *J. of Rehabilitation Research and Development* 26 (1): 1-14.
- Rosen, J. M., J. A. Padilla, K. D. Nguyen, J. Siedman, and H. N. Pham. 1992. Artificial nerve graft using glycolide trimethylene carbonate as a nerve conduit filled with collagen compared to sutured autograft in a rat model. *J. of Rehabilitation Research and Development* 29(2): 1-12.
- Satou, T., S. Nishida, S. Hiruma, K. Tanji, M. Takahashi, S. Fujita, Y. Mizuhara, F. Akai, and S. Hashimoto. 1986. A morphological study on the effects of collagen gel matrix on regeneration of severed rat sciatic nerve in silicone tubes. *Acta Pathologica Japonica* 36(2): 199-208.
- Schlaepfer, W. W. and S. Micko. 1978a. Chemical and structural changes of neurofilaments in transected rat sciatic nerve. *J. of Cell Biology* 78: 369-378.
- Schlaepfer, W. W. and L. A. Freeman. 1978b. Neurofilament proteins of rat peripheral nerve and spinal cord. *J. of Cell Biology* 78: 653-662.

- Seckel, B. R., T. H. Chiu, E. Nyilas, and R. L. Sidman. 1984. Nerve regeneration through synthetic biodegradable nerve guides: Regulation by the target organ. *Plastic and Reconstructive Surgery* 74(2): 173-181.
- Shine, H. D., P. G. Harcourt, and R. L. Sidman. 1985. Cultured peripheral nervous system cells support peripheral nerve regeneration through tubes in the absence of distal nerve stump. *J. of Neuroscience Research* 14: 393-401.
- Suematsu, N., Y. Atsuta, and T. Hirayama. 1988. Vein graft for repair of peripheral nerve gap. *J. of Reconstructive Microsurgery* 4(4): 313-318.
- Swaim, S. F. 1987. Peripheral nerve surgery. Pages 493-512. in J. E. Oliver, Jr., B. F. Hoerlein, and I. G. Mayhew, eds. *Veterinary Neurology*. W. B. Saunders Company, Philadelphia.
- Taylor, J. S. H., J. W. Fawcett, and L. Hirst. 1984. The use of backscattered electrons to examine selectively stained nerve fibers in the scanning electron microscope. *Stain Technology* 59(6): 335-341.
- Tohyama, K. and K. Kumagai. 1992. Backscattered electron imaging by scanning electron microscopy of regenerating peripheral nerve axons immunostained with antineurofilament antibody. *J. of Electron Microscopy* 41: 397-401.
- Ushiki, T. and T. Fujita. 1986. Backscattered electron imaging. Its application to biological specimens stained with heavy metals. *Archivum Histologicum Japonicum* 49(1): 139-154.
- Uzman, B. G. and G. M. Villegas. 1983a. Peripheral nerve regeneration through semipermeable tubes. Pages 111-153. in F. J. Seil, editor. *Nerve, Organ, and Tissue Regeneration: Research Perspectives*. Academic Press, New York.
- Uzman, B. G. and G. M. Villegas. 1983b. Mouse sciatic nerve regeneration through semipermeable tubes: A quantitative model. *J. of Neuroscience Research* 9: 325-338.
- Vale, R. D., G. Banker, and Z. W. Hall. 1992. The neuronal cytoskeleton. Pages 247-280. in Z. W. Hall, editor. *An Introduction to Molecular Neurobiology*. Sinauer Associates, Inc., Publishers, Sunderland, MA.
- Valentini, R. F., P. Aebischer, S. R. Winn, and P. M. Galletti. 1987. Collagen- and laminin-containing gels impede peripheral nerve regeneration through semipermeable nerve guidance channels. *Experimental Neurology* 98: 350-356.

- Vejsada, R., J. Palecek, P. Hnik, and T. Soukup. 1985. Postnatal development of conduction velocity and fibre size in the rat tibial nerve. *International J. of Developmental Neuroscience* 3(5): 583-595.
- Von Langsdorff, D., S. S. Ali and F. Nürnberger. 1990. An improved silver staining technique as an alternative nuclear or combined nuclear nerve-fiber impregnation for comparative light-, secondary and backscattered electron scanning microscopy. *J. of Neuroscience Methods* 35: 3-8.
- Williams, L. R., N. Danielsen, H. Müller, and S. Varon. 1987. Exogenous matrix precursors promote functional nerve regeneration across a 15-mm gap within a silicone chamber in the rat. *J. of Comparative Neurology* 264: 284-290.
- Williams, L. R., F. M. Longo, H. C. Powell, G. Lundborg, and S. Varon. 1983. Spatial-temporal progress of peripheral nerve regeneration within a silicone chamber: Parameters for a bioassay. *J. of Comparative Neurology* 218: 460-470.
- Williams, L. R., H. C. Powell, G. Lundborg, and S. Varon. 1984. Competence of nerve tissue as distal insert promoting nerve regeneration in a silicone chamber. *Brain Research* 293: 201-211.
- Williams, L. R. and S. Varon. 1985. Modification of fibrin matrix formation in situ enhances nerve regeneration in silicone chambers. *J. of Comparative Neurology* 231: 209-220.
- Yannas, I. V., A. Chang, H. Loree, S. Perutz, C. Krarup, and T. V. Norregaard. 1989. Regeneration of peripheral nerves in controlled polymeric environments. *Transactions of the Society for Biomaterials* (15th Annual Meeting), page 119.
- Young, B. L., P. Begovac, D. G. Stuart, and G. E. Goslow, Jr. 1984. An effective sleeving technique in nerve repair. *J. of Neuroscience Methods* 10: 51-58.
- Yoshii, S., T. Yamamuro, S. Ito, and M. Hayashi. 1987. In vivo guidance of regenerating nerve by laminin-coated filaments. *Experimental Neurology* 96: 469-473.



## ACKNOWLEDGMENTS

This thesis is dedicated to my parents, my brother, and my sister. Without their sustained support and understanding encouragement, I would not have come this far.

I wish to express my deep appreciation to Dr. Raymond T. Greer, my major professor, for his great patience, encouragement, and guidance through my graduate study.

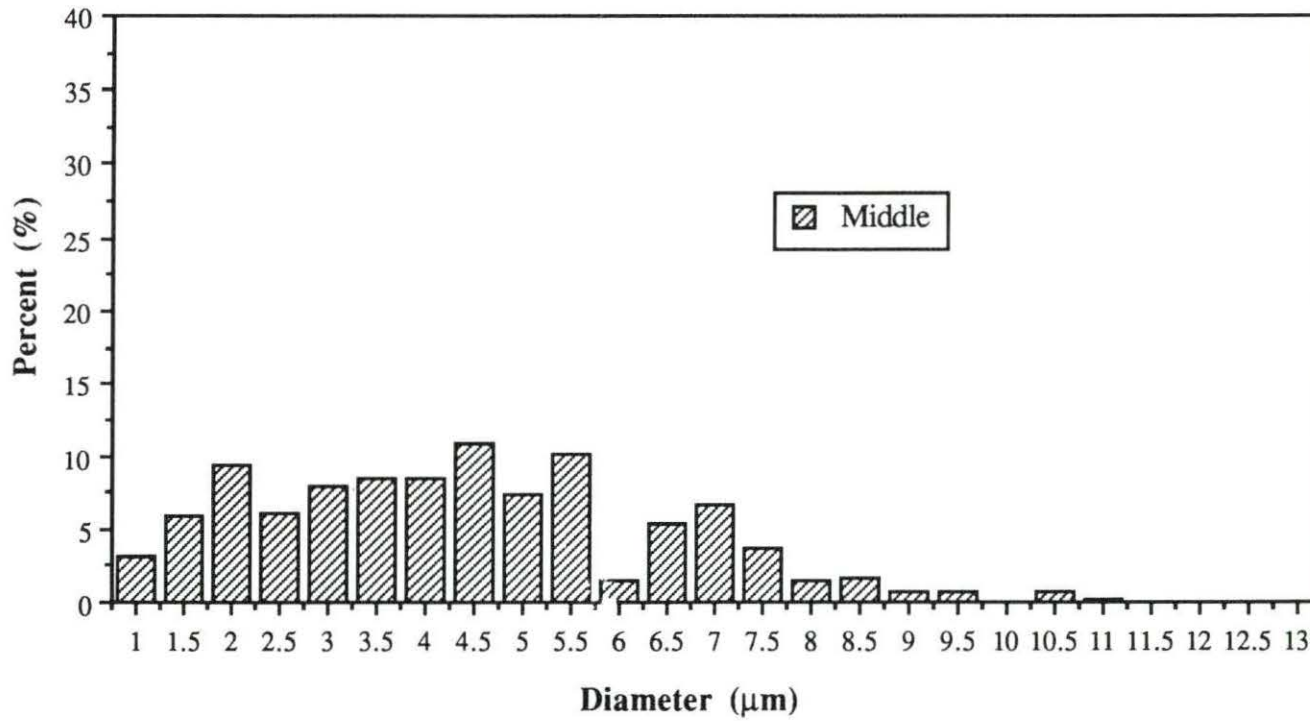
I would also like to sincerely thank Dr. Mary Helen Greer and Dr. Frederick Hembrough for serving as members of my committee.

I have a special appreciation for the assistance provided by James M. Fosse and Jerry L. Amenson.

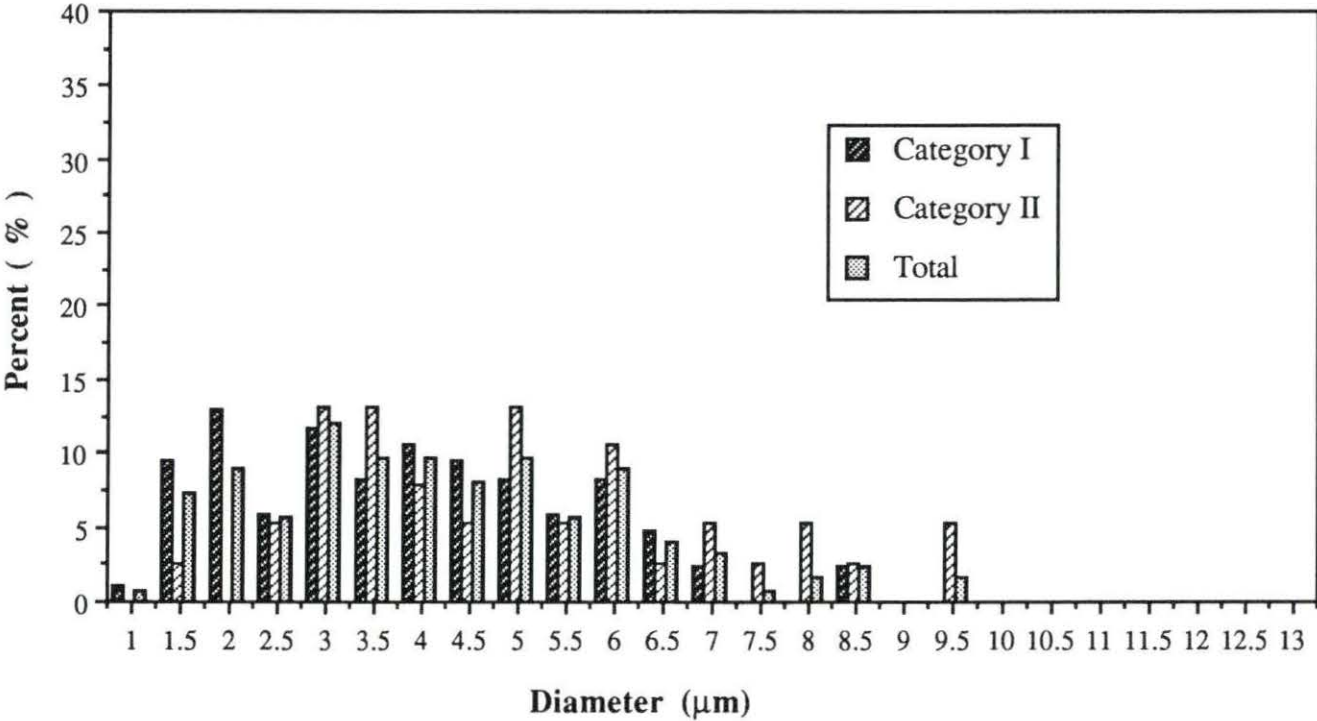
Finally, I would also like to express my appreciation to my friends whose help I received during my years at Iowa State University.

**APPENDIX: FIBER DIAMETER HISTOGRAMS**

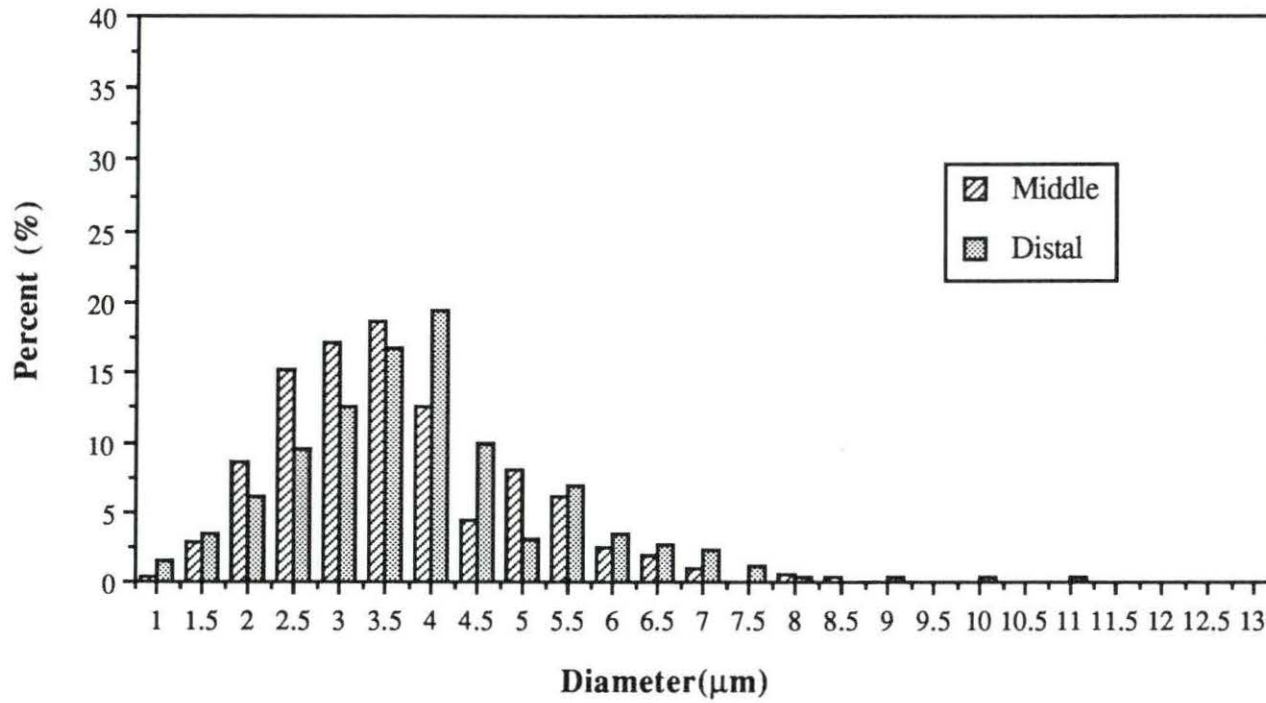
**Axon Diameter Distribution  
Animal # 19 (LM)  
16 Weeks, Normal Control**



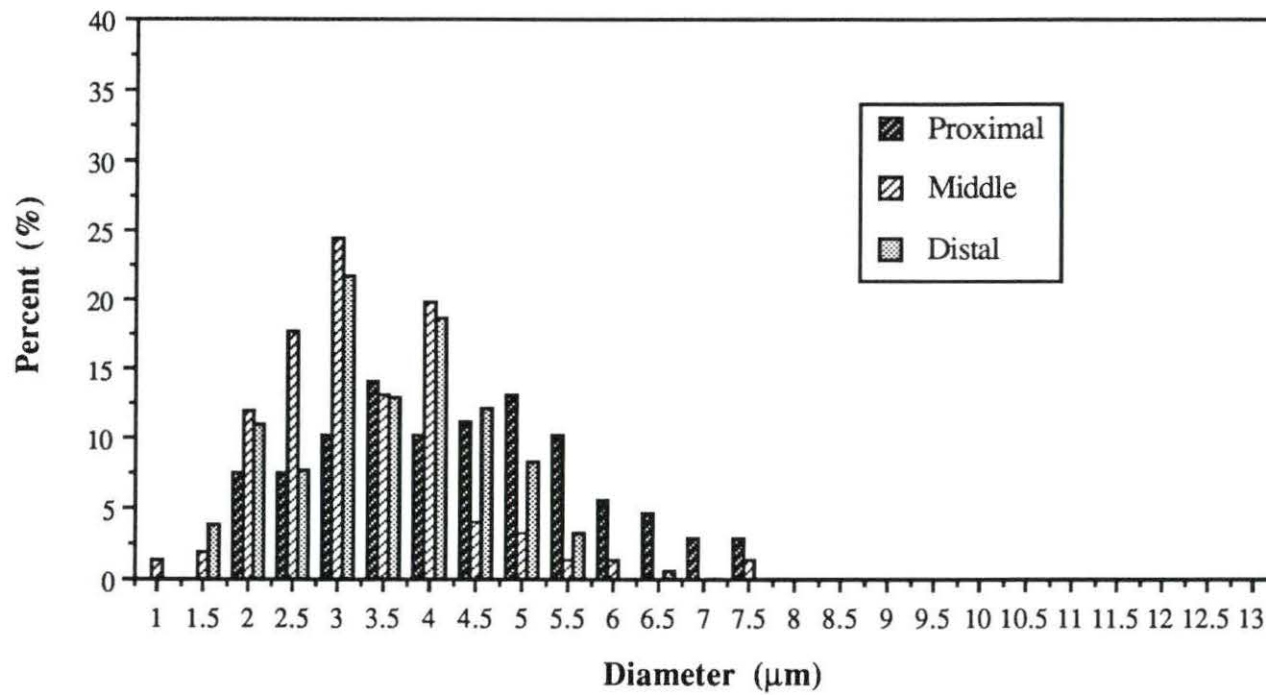
**Axon Diameter Distribution  
Animal #19 (BSE)  
16 Weeks, Normal Control**



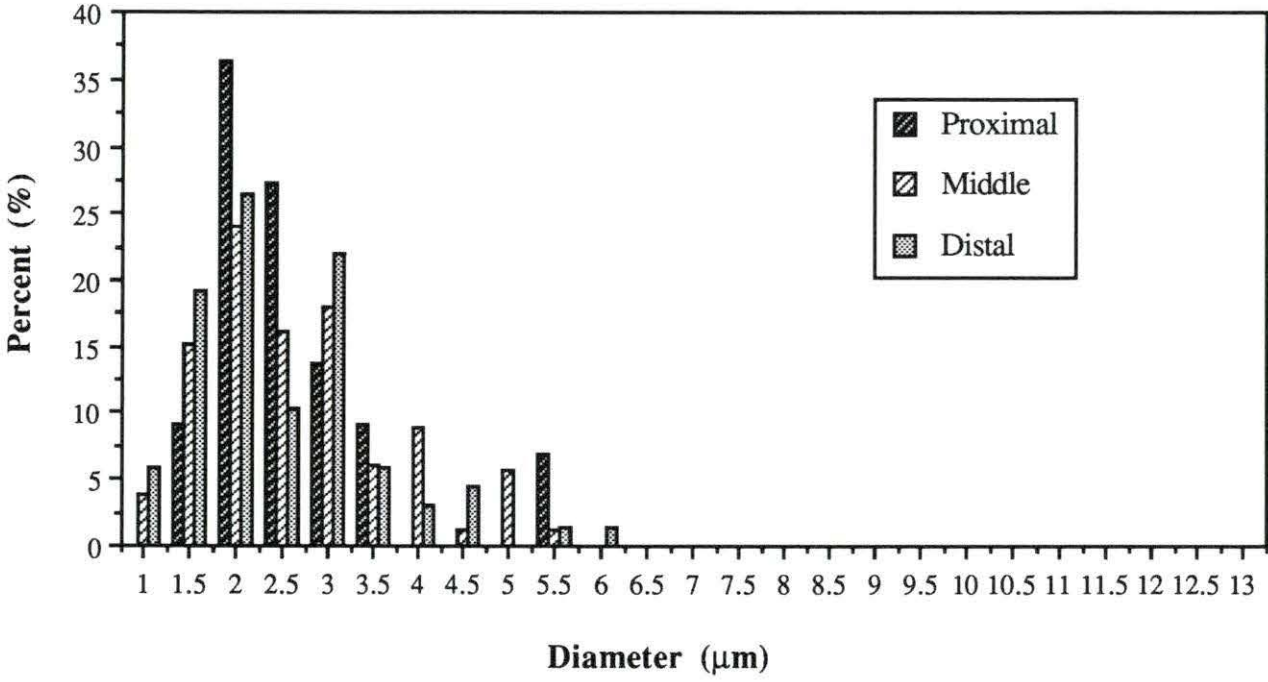
**Axon Diameter Distribution  
Animals #34 (LM)  
8 Weeks, Multiple-Lumen Cuff**



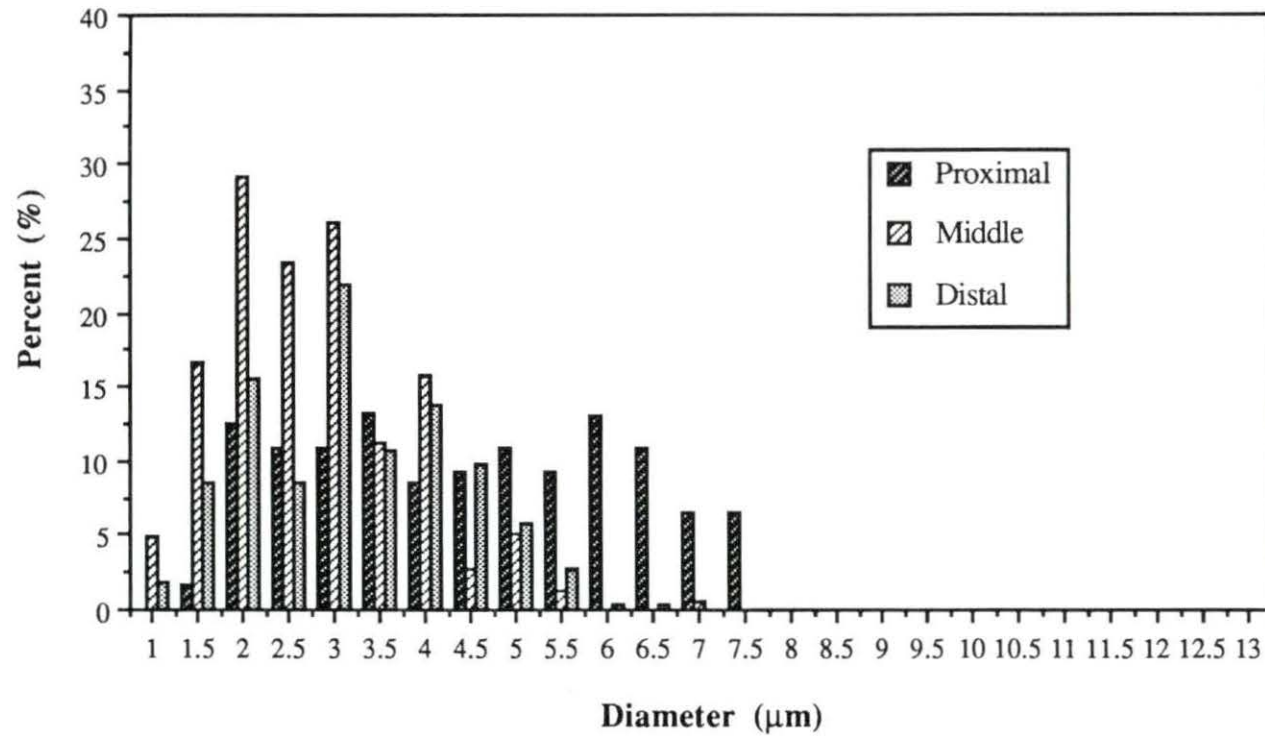
**Category I Axon  
Diameter Distribution  
Animal # 34 (BSE)  
8 Weeks, Multiple-Lumen Cuff**



**Category II Axon  
Diameter Distribution  
Animal #34 (BSE)  
8 Weeks, Multiple-Lumen Cuff**

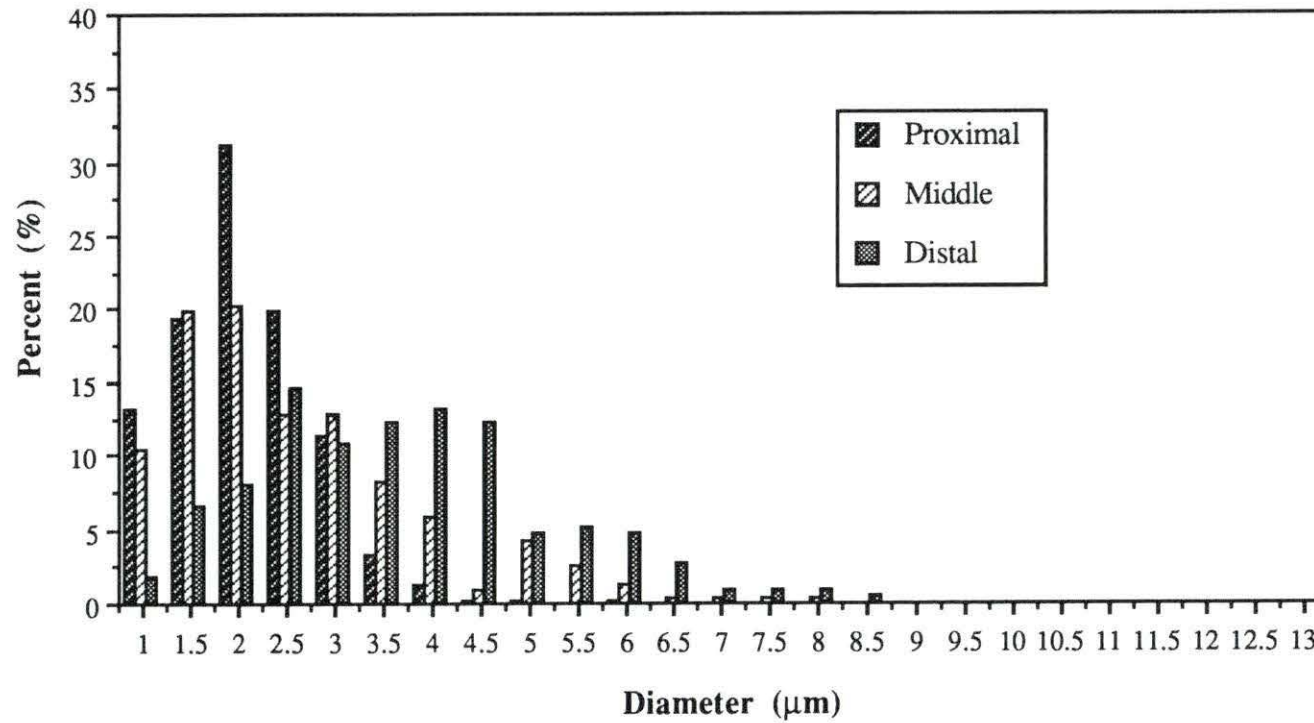


**Total Axon Diameter Distribution  
Animal # 34 (BSE)  
8 Weeks, Multiple-Lumen Cuff**

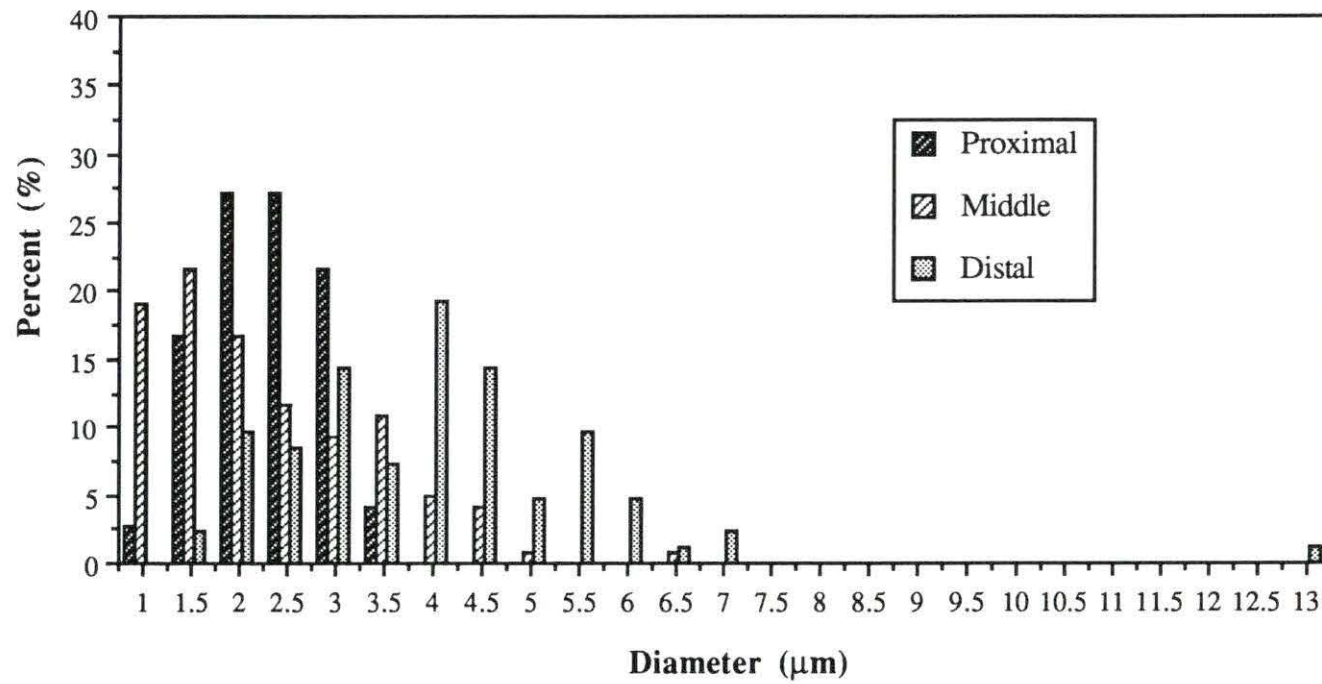




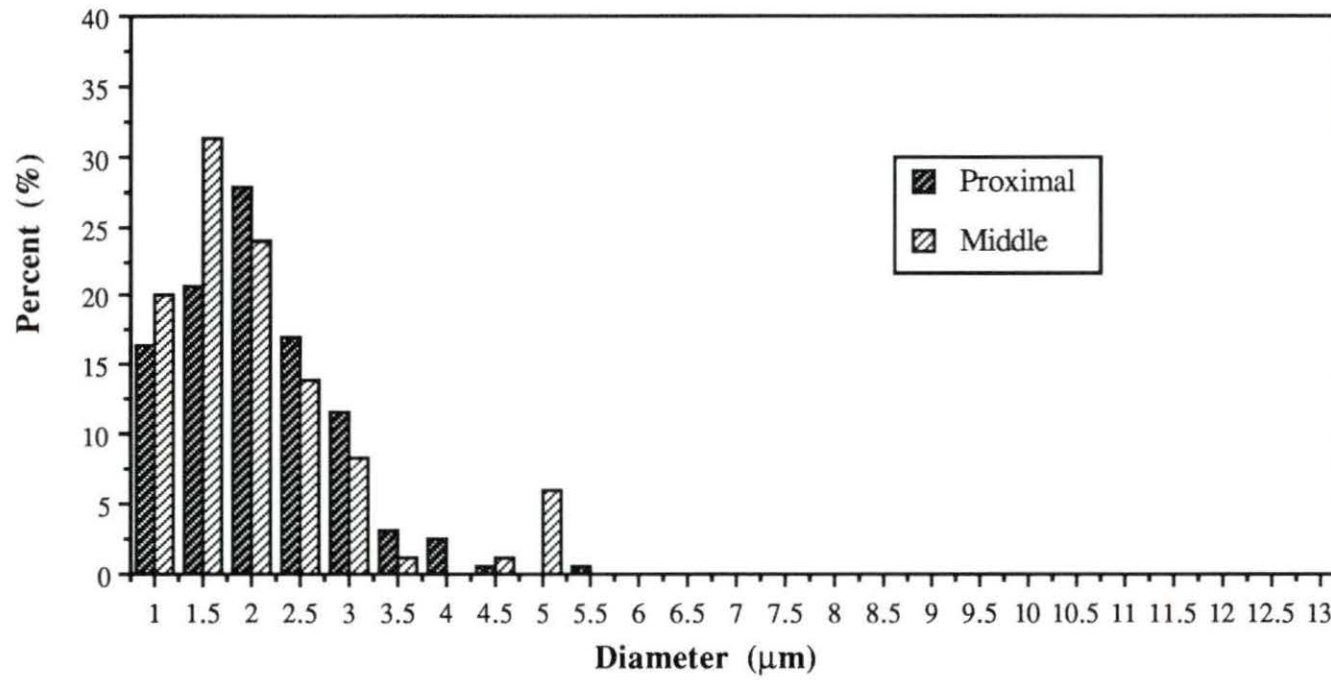
**Axon Diameter Distribution  
Animal # 24 (LM)  
12 Weeks, Multiple-Lumen Cuff**



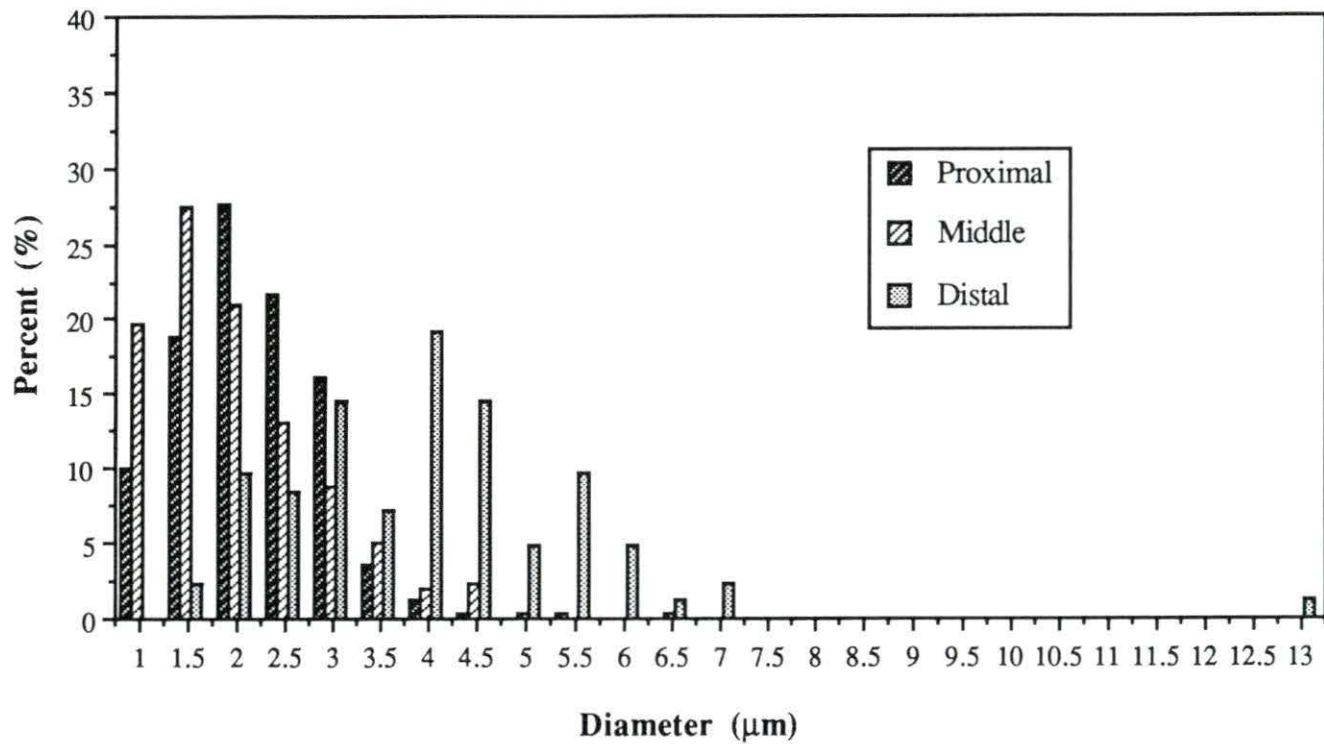
**Category I Axon  
Diameter Distribution  
Animal # 24 (BSE)  
12 Weeks, Multiple-Lumen Cuff**



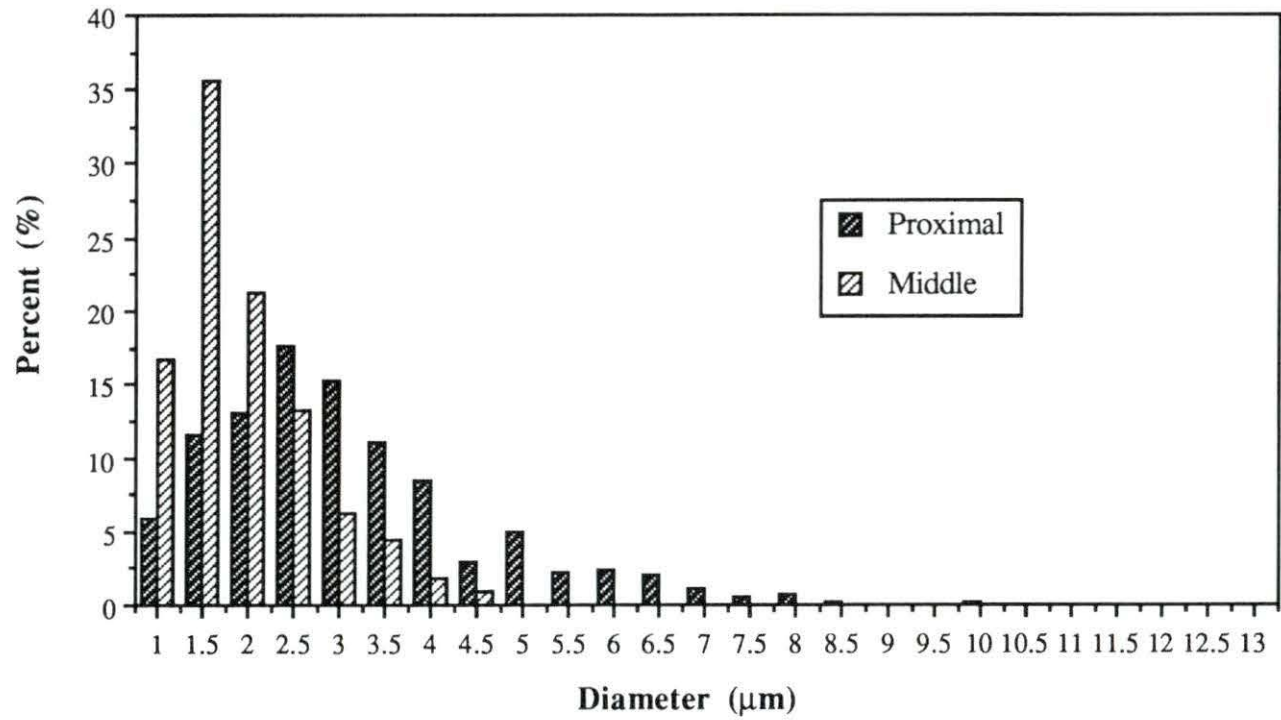
Category II Axon  
Diameter Distribution  
Animal # 24 (BSE)  
12 Weeks, Multiple-Lumen Cuff



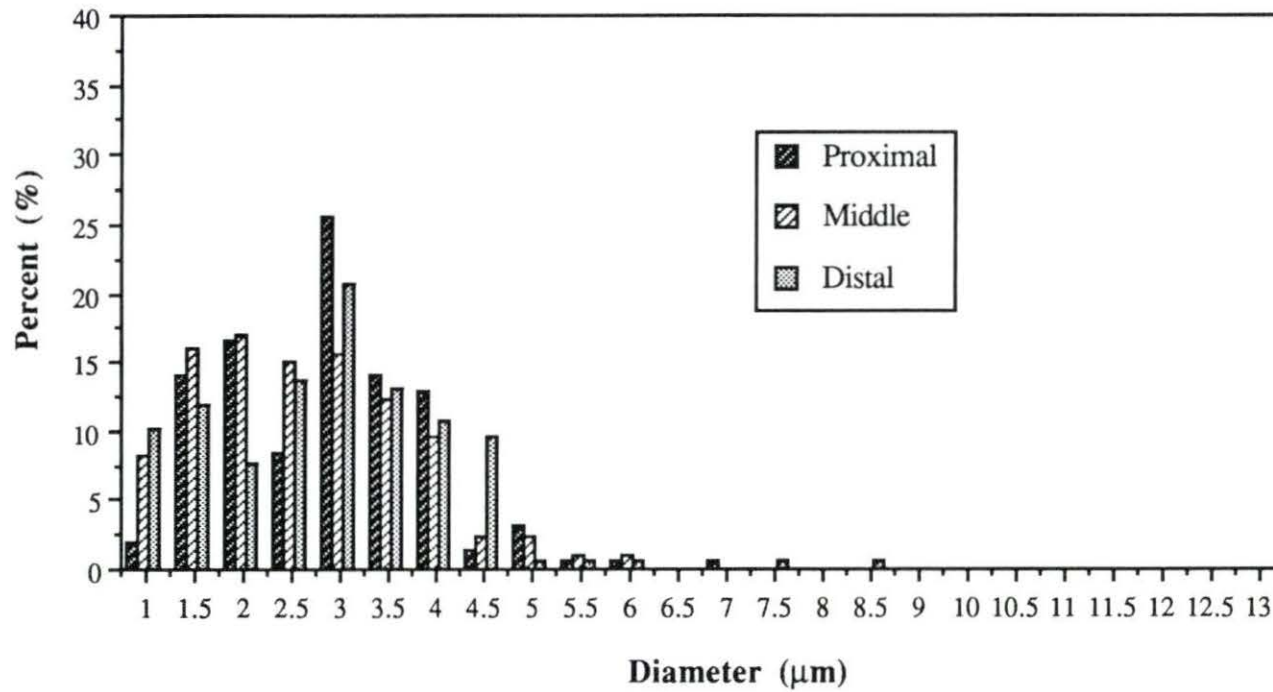
**Total Axon Diameter Distribution  
Animal # 24 (BSE)  
12 Weeks, Multiple-Lumen cuff**



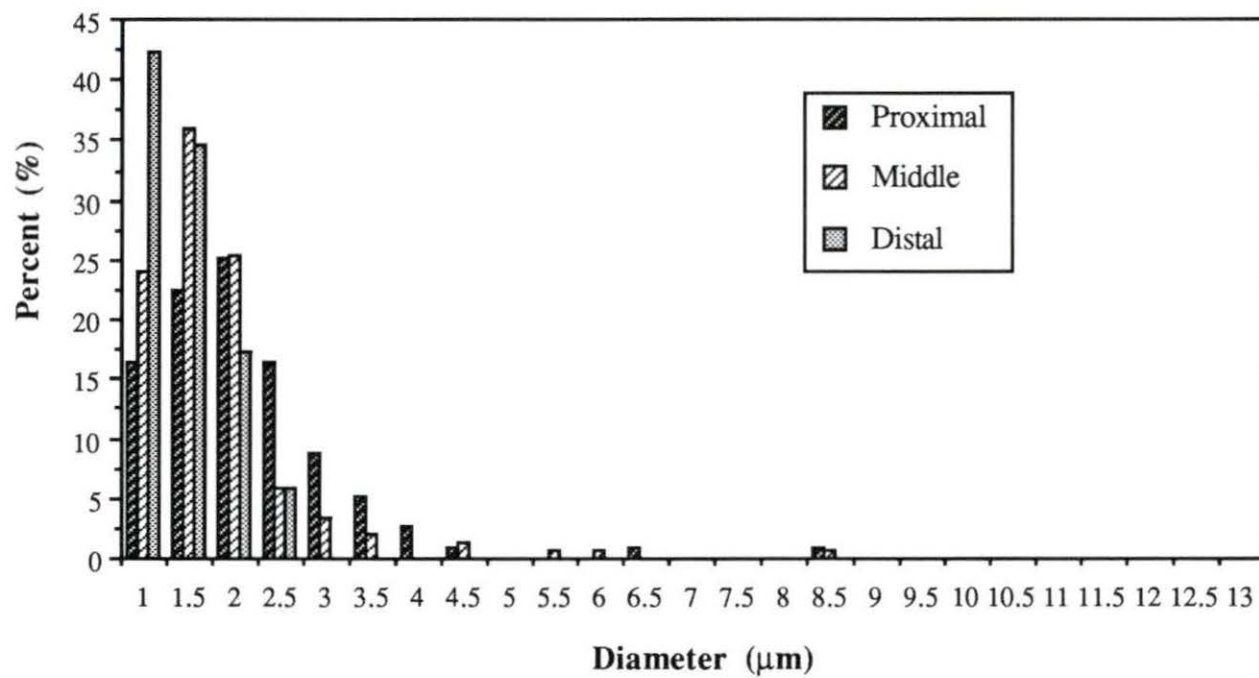
**Axon Diameter Distribution  
Animal # 14 (LM)  
16 Weeks, Multiple-Lumen Cuff**



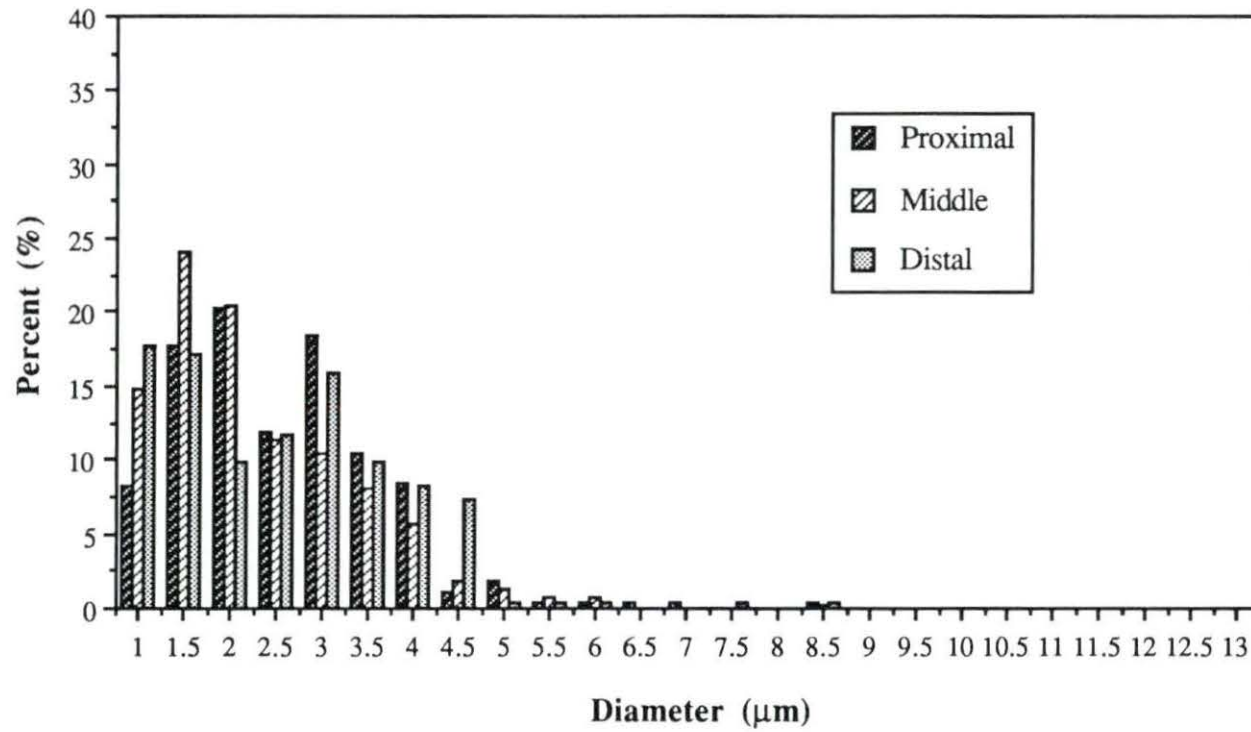
**Category I Axon  
Diameter Distribution  
Animal # 14 (BSE)  
16 Weeks, Multiple-Lumen Cuff**



**Category II Axon  
Diameter Distribution  
Animal # 14 (BSE)  
16 Weeks, Multiple-Lumen Cuff**

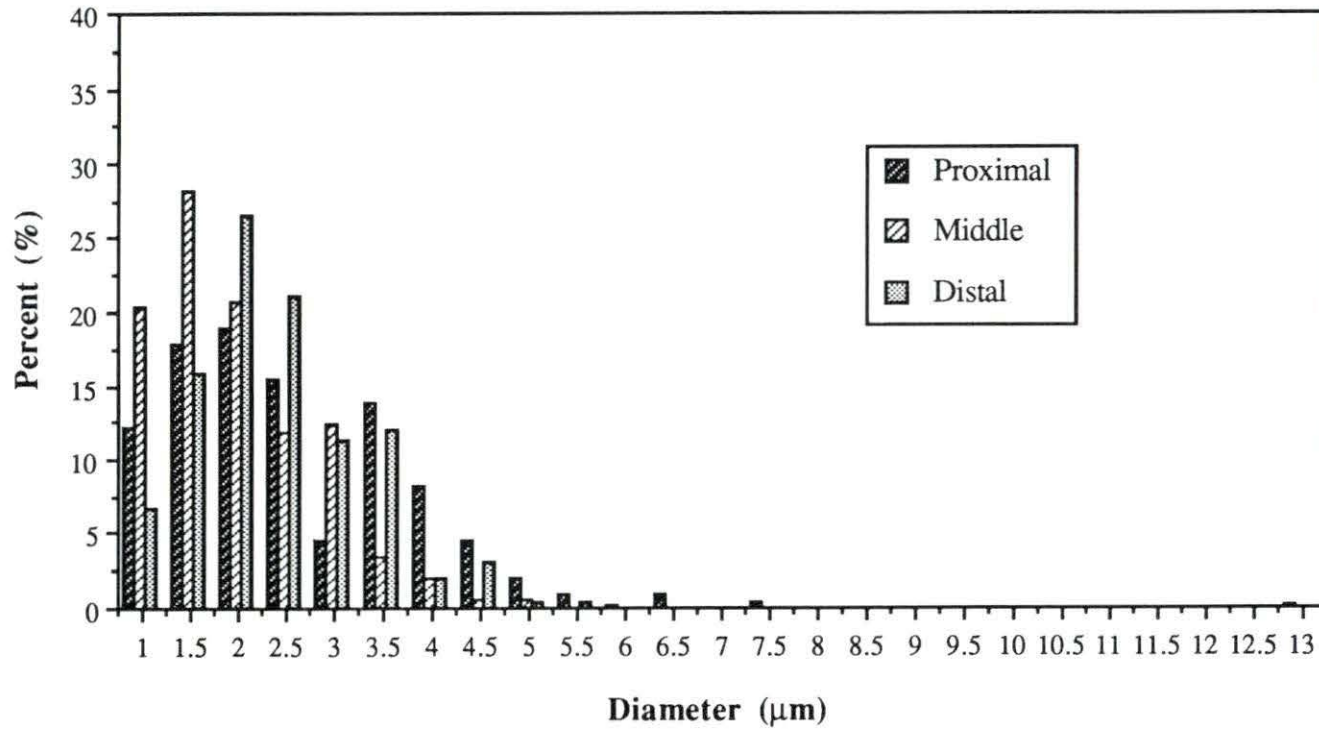


**Total Axon Diameter Distribution  
Animal # 14 (BSE)  
16 Weeks, Multiple-Lumen Cuff**

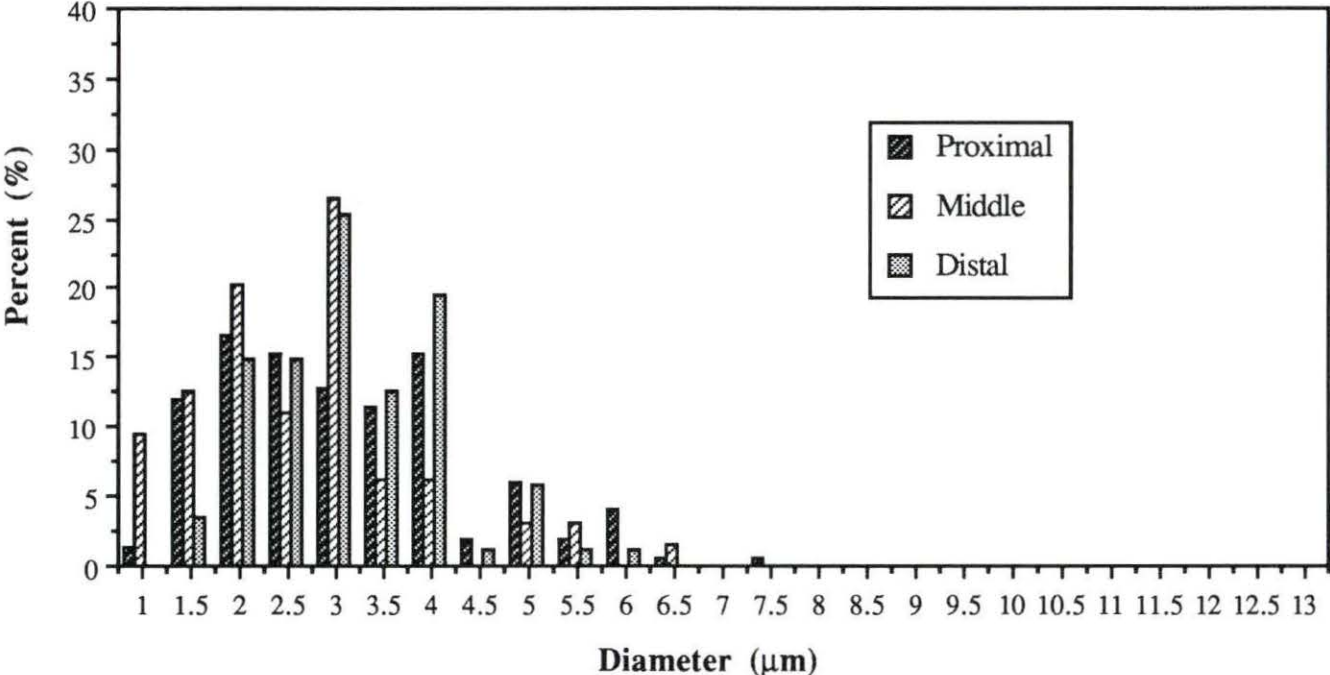




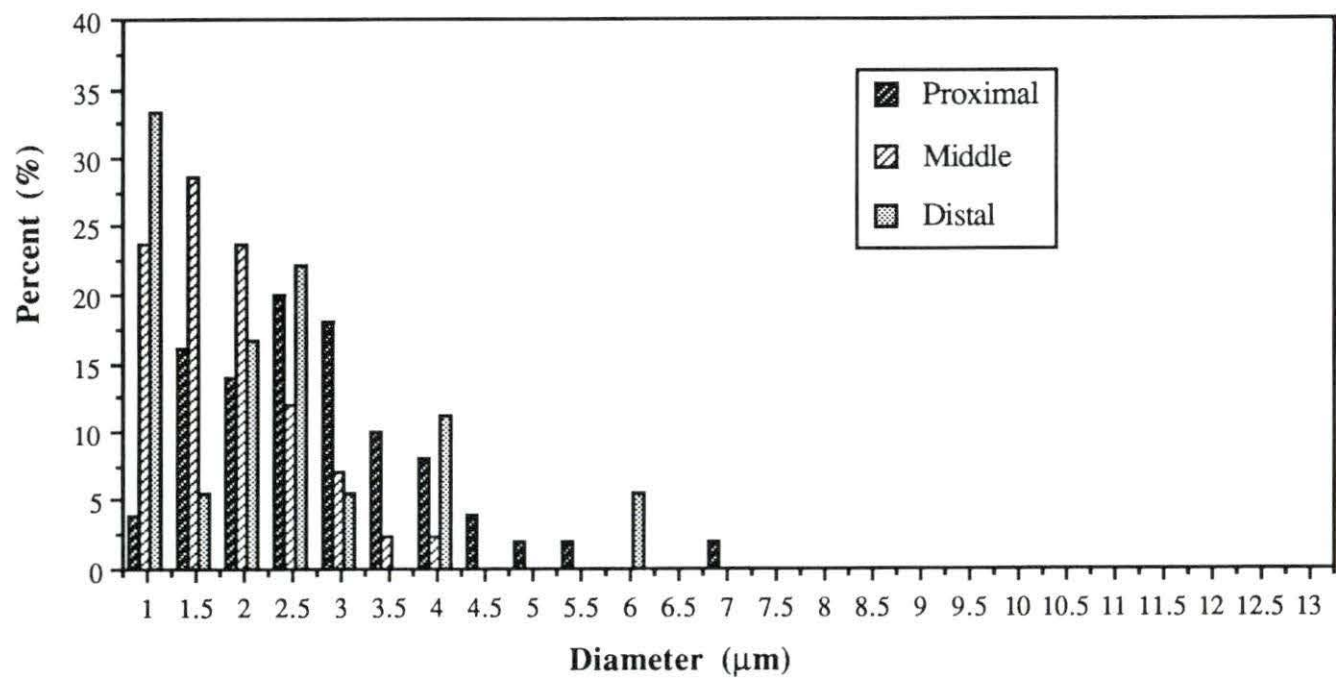
**Axon Diameter Distribution**  
**Animal # 1 (LM)**  
**24 Weeks, Multiple-Lumen Cuff**



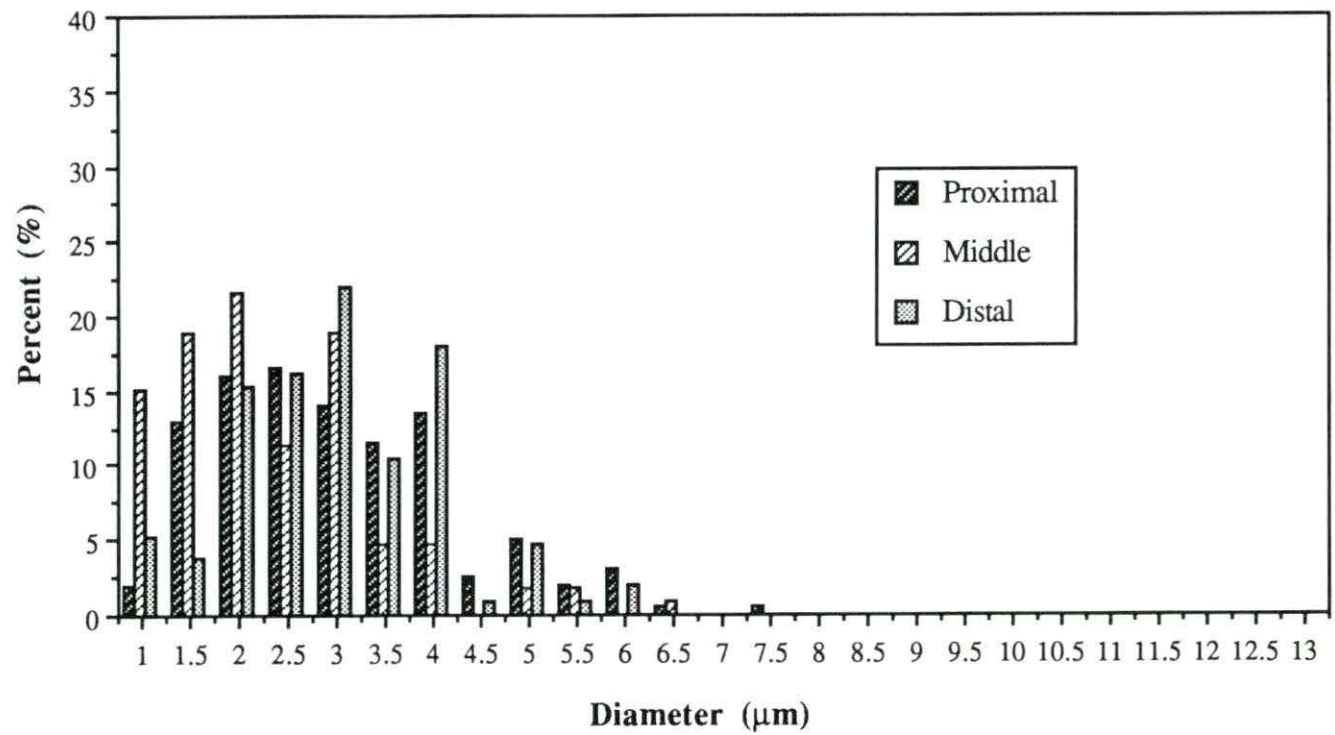
**Category I Axon  
Diameter Distribution  
Animal # 1 (BSE)  
24 Weeks, Multiple-Lumen Cuff**



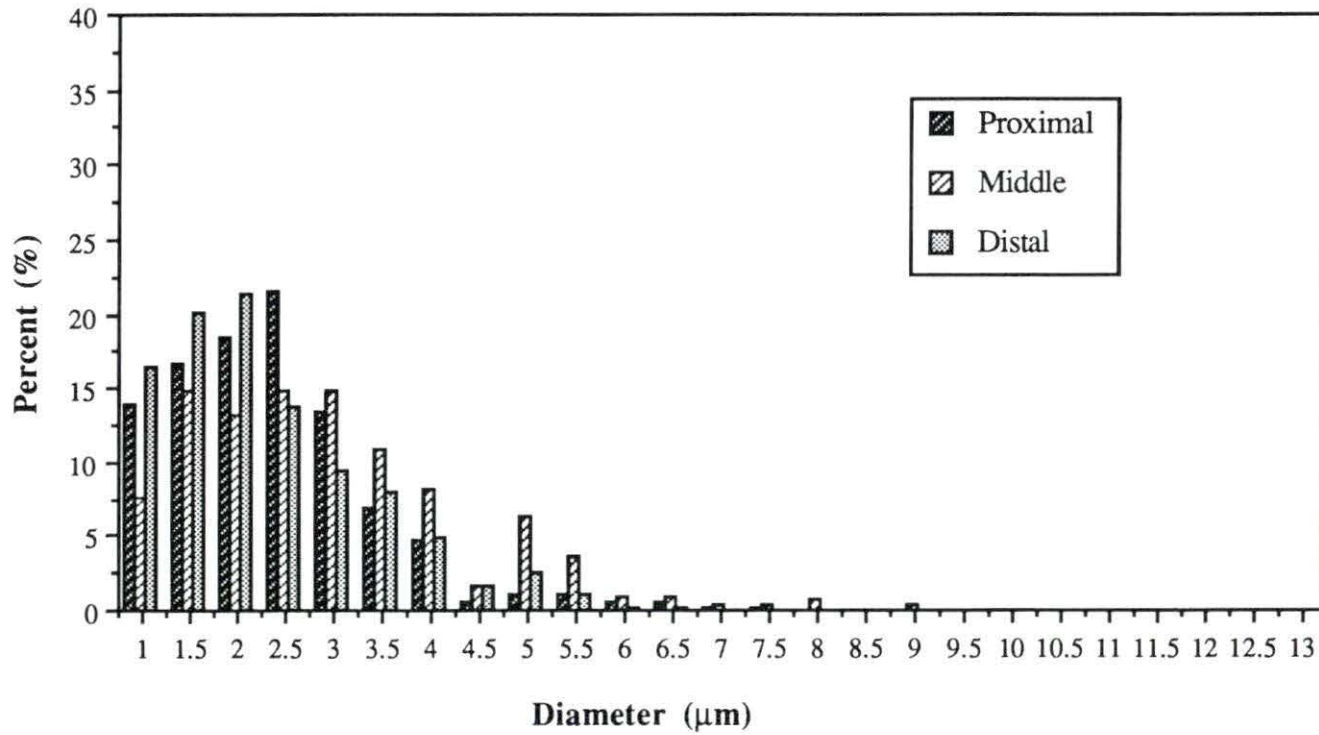
**Category II Axon  
Diameter Distribution  
Animal # 1 (BSE)  
24 Weeks, Multiple-Lumen Cuff**



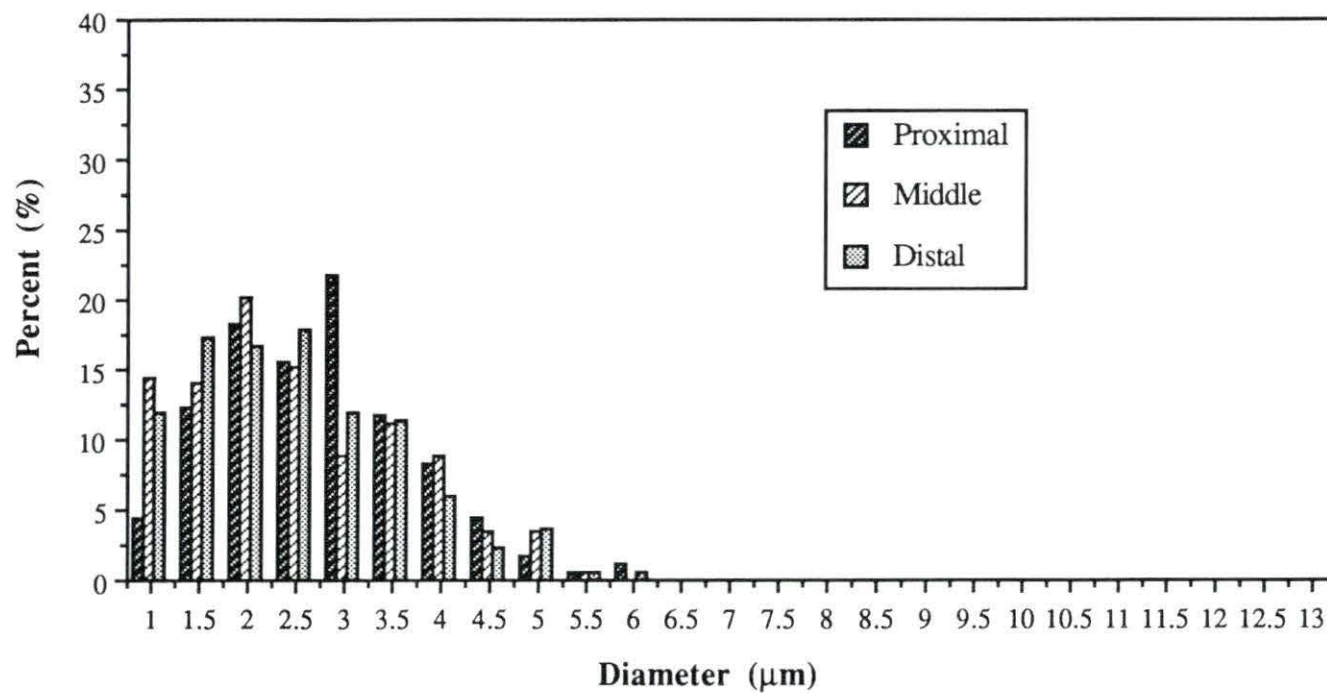
**Total Axon Diameter Distribution  
Animal # 1 (BSE)  
24 Weeks, Multiple-Lumen Cuff**



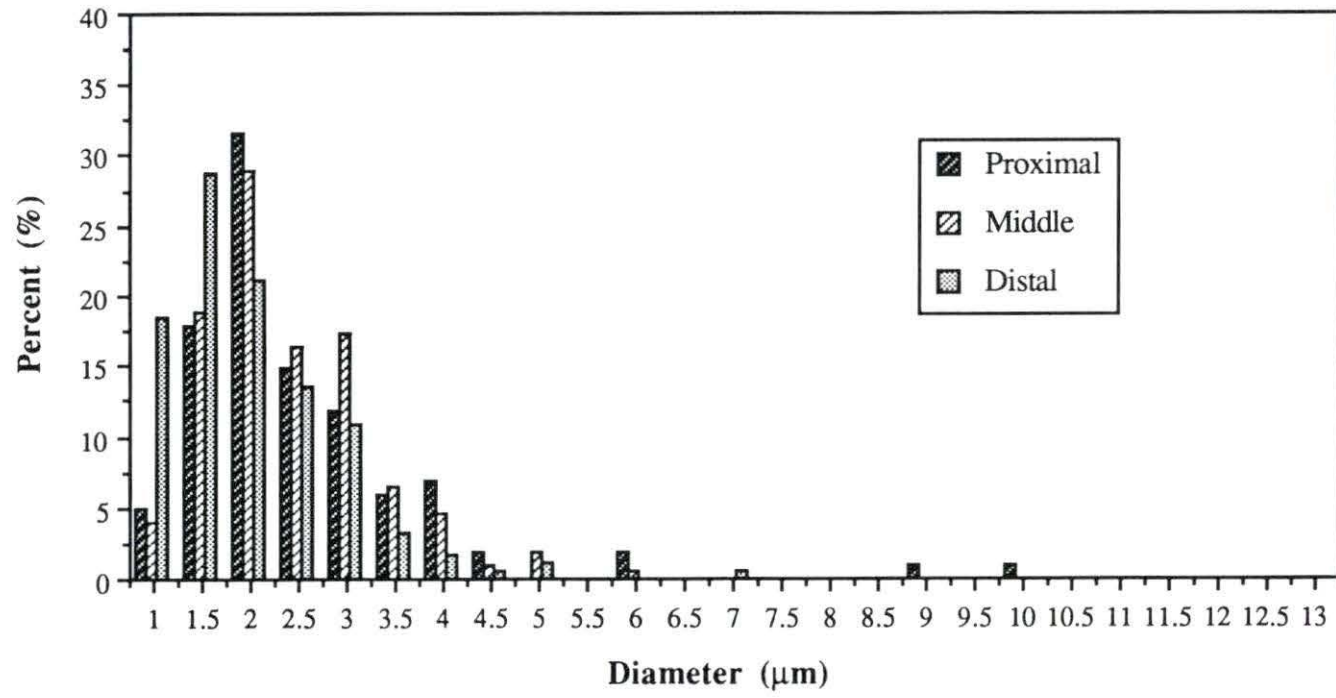
**Axon Diameter Distribution**  
**Animal # 2 (LM)**  
**24 Weeks, Multiple-Lumen Cuff**



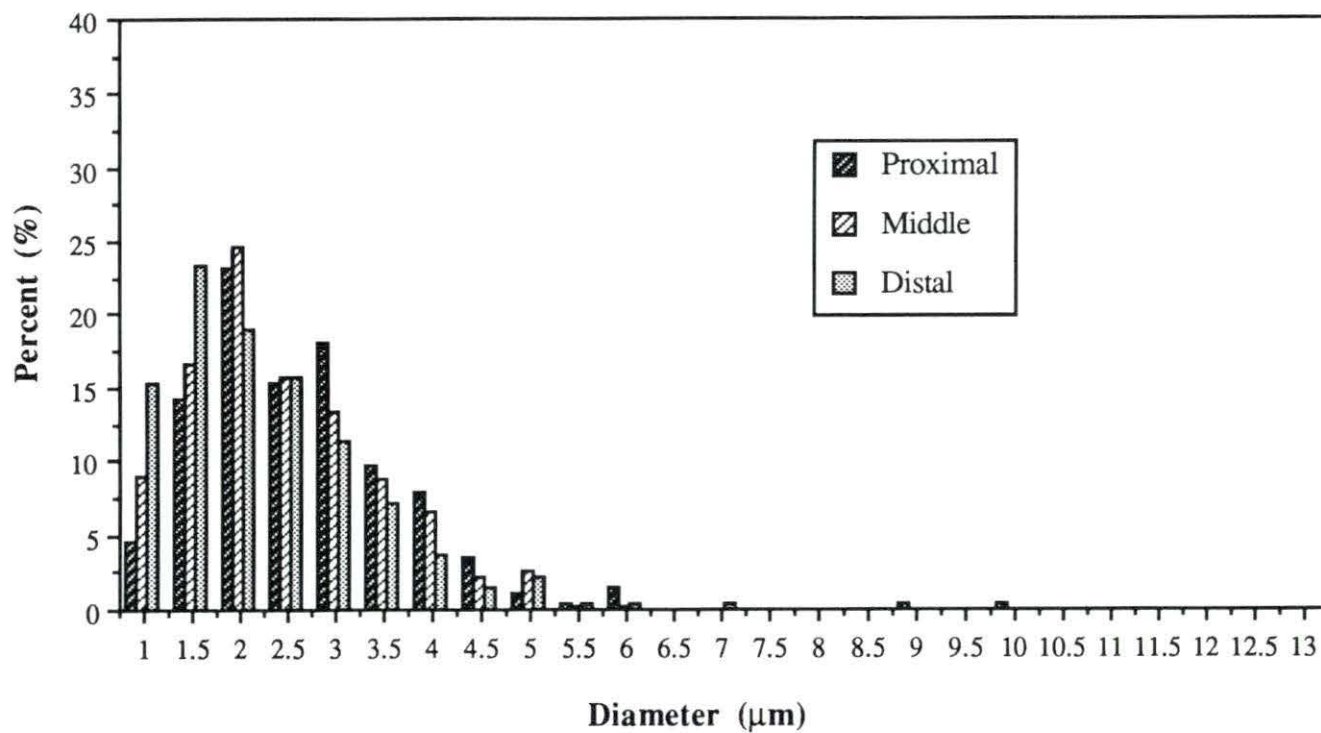
**Category I Axon  
Diameter Distribution  
Animal # 2 (BSE)  
24 Weeks, Multiple-Lumen Cuff**



**Category II Axon  
Diameter Distribution  
Animal # 2 (BSE)  
24 Weeks, Multiple-Lumen Cuff**

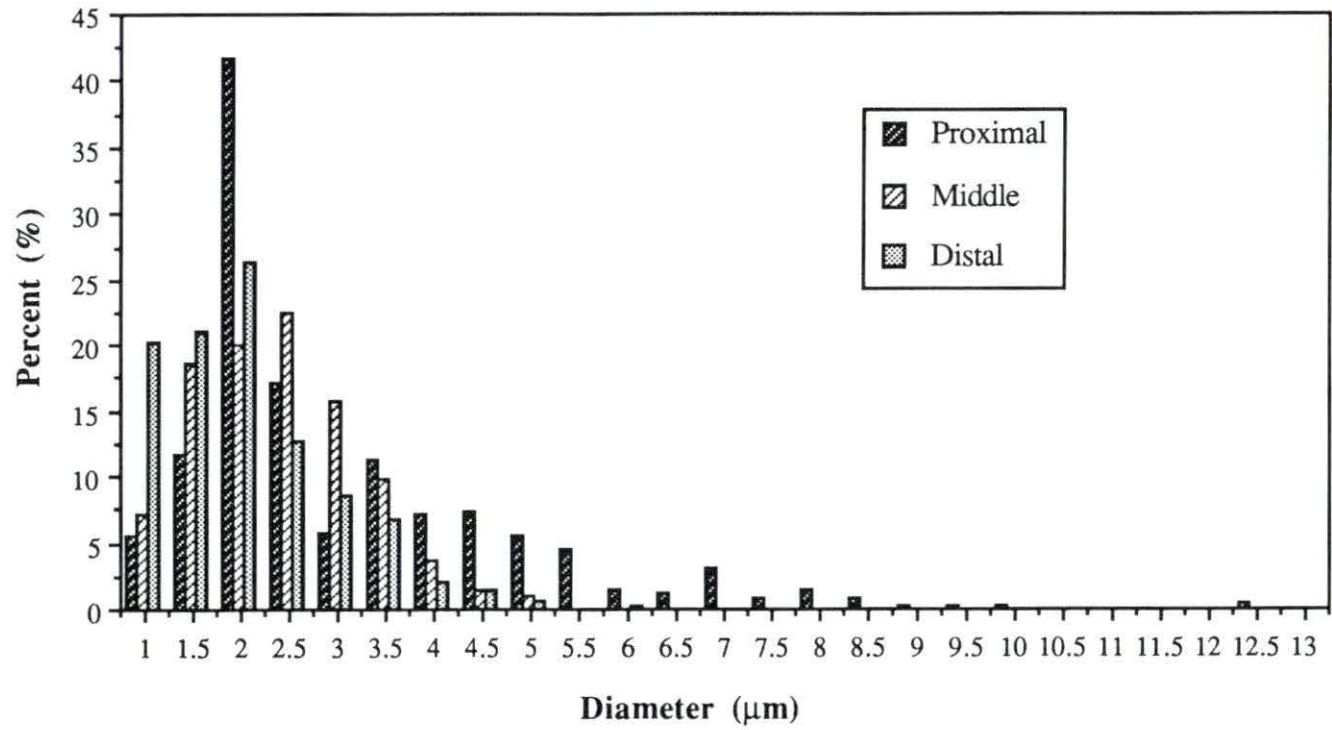


**Total Axon Diameter Distribution  
Animal # 2 (BSE)  
24 Weeks, Multiple-Lumen Cuff**

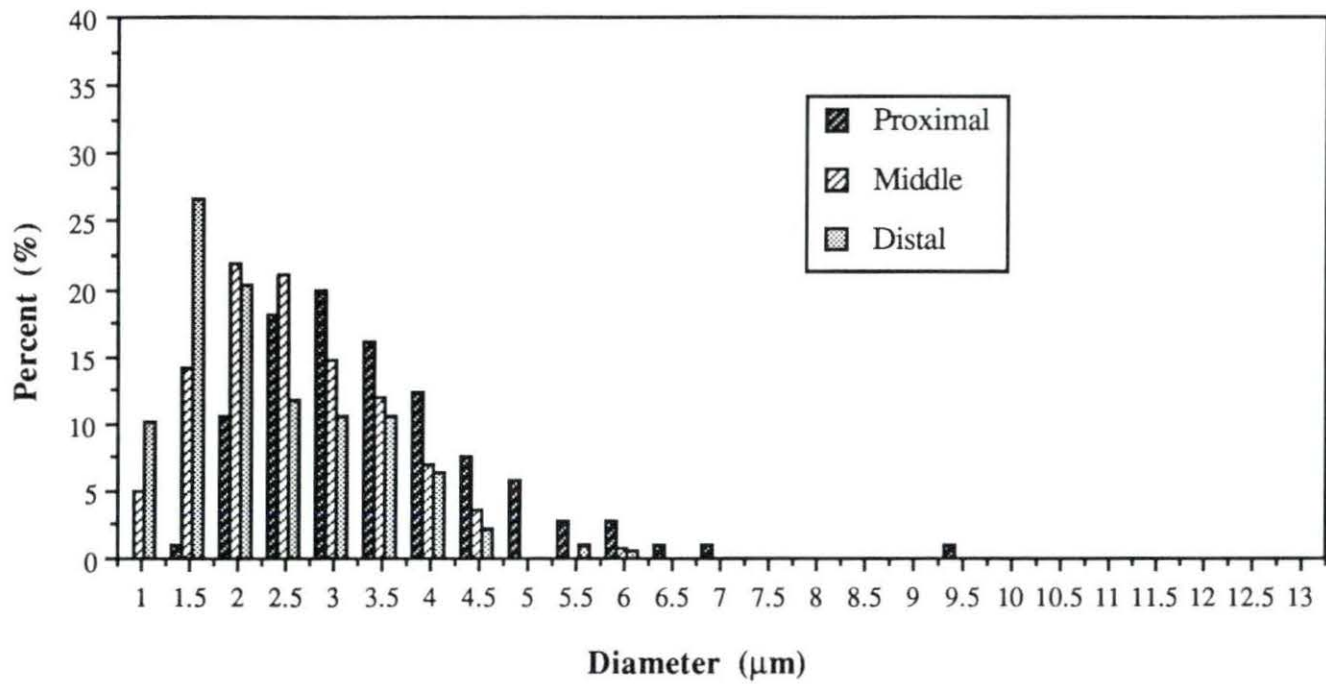




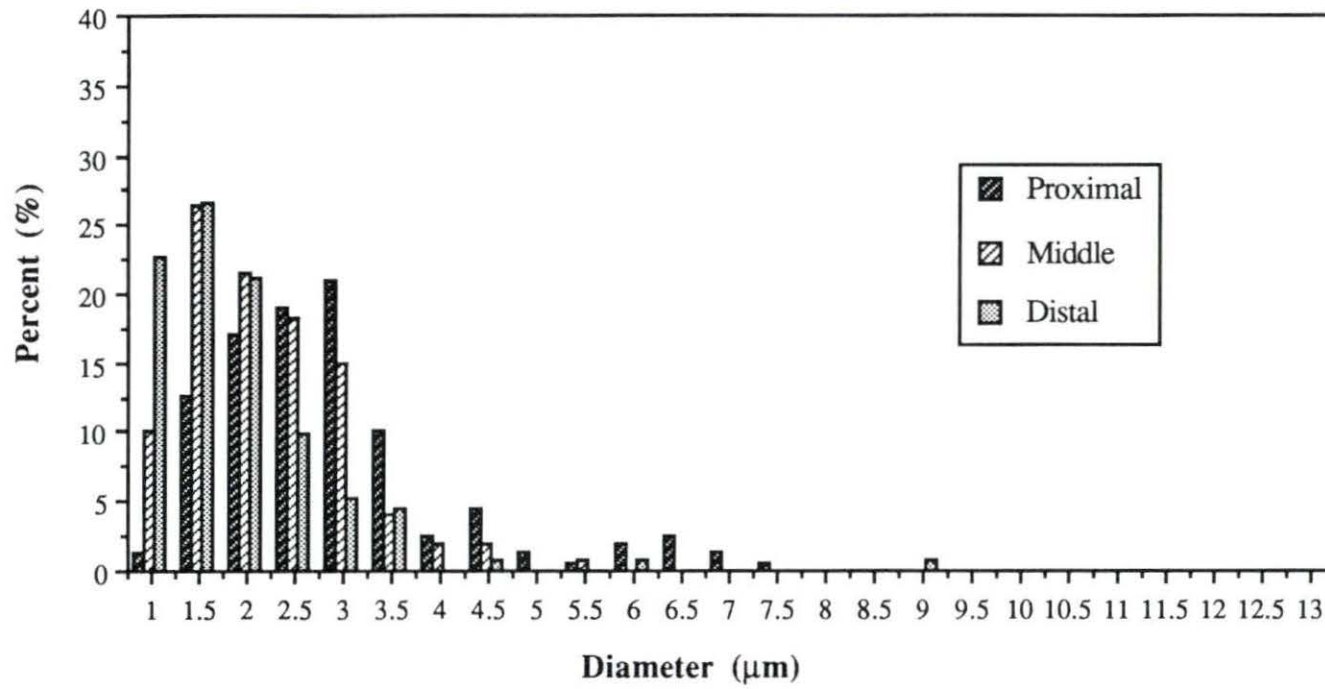
Axon Diameter Distribution  
Animal # 3 (LM)  
24 Weeks, Multiple-Lumen Cuff



**Category I Axon  
Diameter Distribution  
Animal # 3 (BSE)  
24 Weeks, Multiple-Lumen Cuff**



**Category II Axon  
Diameter Distribution  
Animal # 3 (BSE)  
24 Weeks, Multiple-Lumen Cuff**



**Total Axon Diameter Distribution  
Animal # 3 (BSE)  
24 Weeks, Multiple-Lumen Cuff**

